A-P-T RESEARCH, INC.
an employee-owned company

# 2024 ATF Perforating Gun Test Series to Support Quantitative Risk Assessment

Prepared for:
2025 International Explosives Safety Summit and Exposition (IESSE)
Held January 20 to 23, 2026
IN Phoenix, Arizona

Prepared by:
A-P-T Research, Inc.
4950 Research Dr.
Huntsville, AL 35805
Phone: 256.327.4015
Fax: 256.837.7786
www.apt-research.com
January 20, 2026
T-26-00101

Lead Authors:
John Tatom
Jake Romano

Contributors:
Laura Murray

A product of:


4950 Research Drive
Huntsville, AL 35805
USA
+1-256-327-3373
www.apt-research.com

# TABLE OF CONTENTS

## LIST OF FIGURES

## LIST OF TABLES

# APPENDICES

# ACRONYMS

| | |
|---|---|
| APT | A-P-T Research, Inc. |
| ATF | Bureau of Alcohol, Tobacco, Firearms & Explosives |
| JPG | Jet Perforating Gun |
| ATD | American Table of Distances |
| IMESAFR | Institute of Makers of Explosives Safety Analysis for Risk |
| QRA | Quantitative Risk Assessment |
| NEW | Net Explosive Weight |
| SPF | Shots per Foot |
| IME | Institute of Makers of Explosives |
| RAM | R.A. McClure, Inc. |
| GPS | Global Positioning System |
| RISI | Teledyne RISI Inc. |
| EBW | Exploding Bridgewire |

# 1.0 Background

The Bureau of Alcohol, Tobacco, Firearms and Explosives (ATF) is the governmental organization that regulates the storage of commercial explosives in the United States, including the storage of jet perforating guns (JPGs). ATF regulates storage safety based on the American Table of Distances (ATD) [1]; however, they do accept variances based on quantitative risk assessments (QRA) using the Institute of Makers of Explosive Safety Assessment for Risk (IMESAFR©) tool [2]. IMESAFR has a JPG model, however the model is not based on JPG test data. Therefore, in 2024 ATF sponsored a series of JPG tests with the goal of collecting test data that could be used to enhance IMESAFR in its ability to conduct QRA, including modeling fragmentation and blast hazards from JPGs. By enhancing IMESAFR's ability to model these factors, the risk in operations utilizing JPGs can be better predicted and managed, potentially leading to safer scenarios.

To ensure that accurate test results were acquired from this test series, it was important to ensure that the JPGs were tested in realistic configurations, representative of scenarios in which an accidental detonation of a JPG may occur. The storage of these guns has been previously authorized per ATF Ruling 2010-7, which relates to *Title 18 U.S.C. 842 (j): Storage of explosives*, and also under both *27 CFR 555.22: Alternate methods or procedures* and *27 CFR 555.205 Movement of explosive materials*. More detail is provided in Appendix A.

The primary objectives of these tests, in order of priority, were to characterize the following parameters upon forced initiation of the JPG(s) in each of the emplacement conditions:

1. Range, bearing, and mass of the fragments produced by the JPG body
2. Pressure as a function of distance
3. Velocity of fragments

## 1.1 WHAT IS A JET PERFORATING GUN?

JPGs are specialized tools that are used in the oil and gas industry to assist in well completion. Each JPG contains a series of conical shaped charges (perforators) which, when detonated, produce a hypervelocity jet that punches through the gun itself, the wellbore casing, and the geologic formation, allowing oil or gas to flow up the well. Given that these tools are meant to be used in deep wellbores, they are normally designed to operate in the high-pressure-fluid environments that exist within oil and gas wells. While some JPGs are designed to function at atmospheric pressures, the goal of this test series was to observe how JPGs designed to function in high-pressure environments behave if they are detonated in atmospheric pressure. When utilized in standard operations, the gun body is engineered to remain in one piece; however, considering that the JPGs selected for testing were not rated for open air operations, it was not unreasonable to expect that the guns' bodies may rupture upon detonation. Figure 1 is a

schematic provided by the Institute of Makers of Explosives (IME) depicting the type of system that was utilized for this test series and some of the typical JPG components [3].

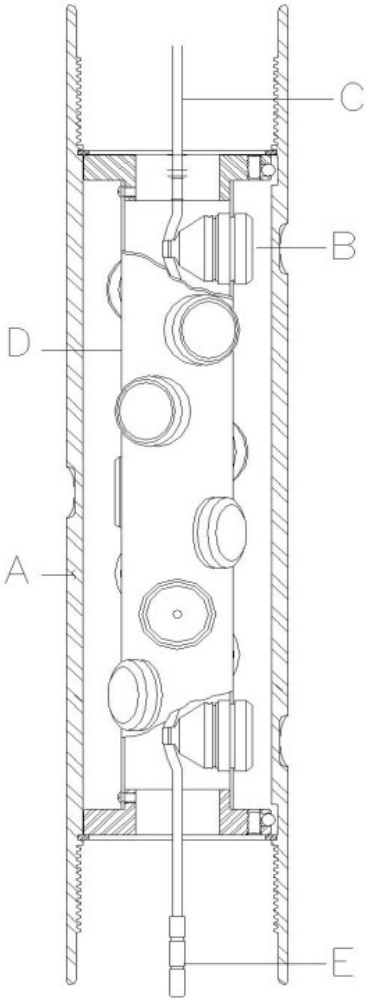


**Gun System Components**

| Label | Component | Comments |
|---|---|---|
| A | Gun body | |
| B | Perforator | |
| C | Detonating Cord | |
| D | Carrier Tube | |
| E | Explosive Transfer Device (explosive)<br>or Detcord End Seal (non-explosive) | Optional<br>Optional |
| F | Lead Wire | Optional<br>(not shown) |

**Figure 1: JPG Schematic**

While Figure 1 depicts most of the components of the JPGs that were tested in this test series there are two components that are not shown. The first additional component is the bulkhead that was installed on one of the JPGs that was tested. In normal operations, this bulkhead is used to isolate the firing system from wellbore fluids and helps to maintain the structural integrity of the JPG. The second component not shown in the schematic is the connecting sub which was present on all the JPGs that were tested. The connecting sub, or sub, allows for stacking or connecting multiple JPG sections, however, it should be noted that none of the guns tested in this series were connected to one another. These additional components are shown in Figure 2.

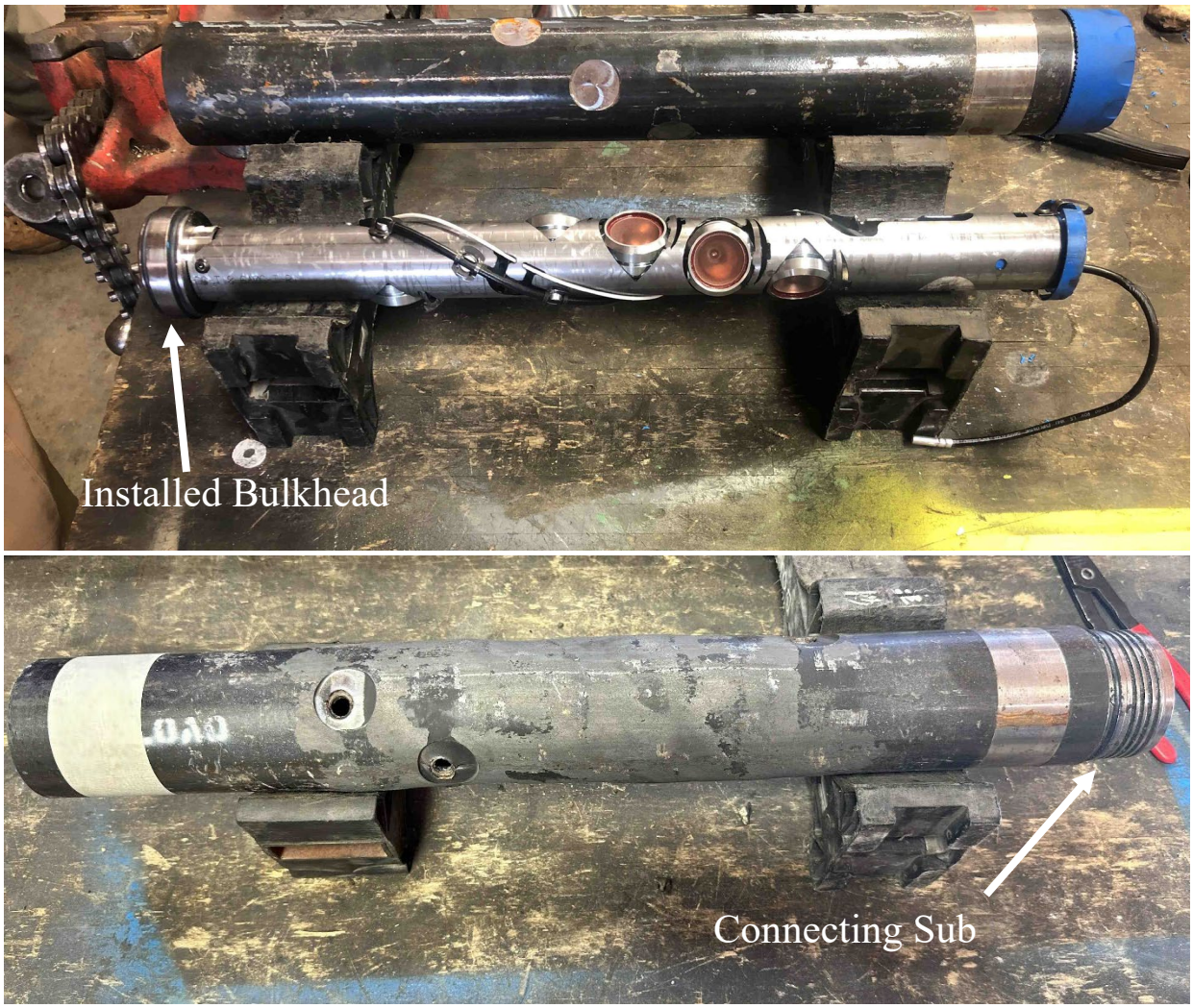


**Figure 2: Additional JPG Components**

## 1.2 MODEL BACKGROUND

While IMESAFR does already have a model for JPGs, it must be noted that this was based on data extrapolated from a model of a larger surrogate explosive article. The size of the surrogate item was chosen because at the time of IMESAFR's original release, about 20 years ago, JPGs were typically larger than they are today. Therefore, it was unknown exactly how accurate the current model would be in comparison to the results of this test series. One area that it was believed the current model would be inaccurate was the number of fragments generated by the item detonating. This is because IMESAFR scales the amount of fragmentation according to the ratio of charge weights between the original, surrogate item and the item being modeled. While the surrogate item was larger than all of the items tested in this series, the scaling in IMESAFR would reduce the number of fragments being modeled (based on the ratio of the actual charge weight per item to the modeled charge weight per item), so it was unknown if the program would

overpredict or underpredict the number of fragments generated. More details on the comparison of the current model and the test results are provided in Section 4.3.

The key parameters that were needed to update the existing model are the fragment mass distribution and fragment position (range and azimuth); hence they were listed as the highest priority. The pressure measurements were a secondary concern for this test series and were primarily to confirm that the tests went as expected. This is because IMESAFR uses the Kingery-Bulmash hemispherical TNT equations to calculate pressure and impulse, so drastic differences between the calculated and the actual pressure measurements were not expected. That being said, it was anticipated that the way pressure is modeled for JPGs in IMESAFR does need to be updated to reflect the asymmetric blast wave that JPGs create. The fragment velocity was the lowest concern since, while it may be a modeling term, IMESAFR does not need exact values if the fragment pattern (range and azimuth) was obtained from the test.

## 1.3 TEST BACKGROUND

To most effectively enhance IMESAFR, the desired empirical test data must be determined by numerous different tests utilizing different JPGs and configurations. By testing a variety of different configurations and JPGs, a wider selection of data becomes available, and it also provides a better understanding of how different parameters could affect the model. Some of the different parameters that should be tested include: gun size (outer diameter and total length), the phasing angle (i.e., if the gun has a helix configuration or the openings are in a straight line), the total number of charges, the NEW per charge, the shots-per-foot (SPF), the orientation of the gun (vertical or horizontal), the height of the gun when it detonates, and the number of guns.

Based on the available time and funding, ATF decided that testing the full matrix of parameters was too extensive for the first test series, and therefore a more attainable series of eight tests was planned that aligned with the timeline and budget. It was planned that this test series would be performed with a focus on the following parameters: phasing angle, number of charges, and number of items. Each test in this series was done with guns of the same size and phasing, but one of the three other parameters would be changed in each test. It should be noted that the JPG size, charge size, and SPF selected for this test series were based on what was most commonly used for the US land market. Based on this plan, the JPGs would have all their charges initiated simultaneously, resulting in a possible worst-case scenario. The preliminary strawman test matrix (as created in 2024) outlining the proposed parameters of each test is shown in Table 1.

Table 1: Preliminary 2024 Strawman Test Matrix

| Test | Diameter | Phasing Angle | # of Charges | # of Items | Orientation | Initiation |
|---|---|---|---|---|---|---|
| **Test 1** | 3.125 in | Line | 3 | Single | Vertical | Field |
| **Test 2** | 3.125 in | Line | 3 | Multi | Vertical | Field |
| **Test 3** | 3.125 in | Line | 6 | Single | Vertical | Field |
| **Test 4** | 3.125 in | Line | 6 | Multi | Vertical | Field |
| **Test 5** | 3.125 in | Helix | 3 | Single | Vertical | Field |
| **Test 6** | 3.125 in | Helix | 3 | Multi | Vertical | Field |
| **Test 7** | 3.125 in | Helix | 6 | Single | Vertical | Field |
| **Test 8** | 3.125 in | Helix | 6 | Multi | Vertical | Field |

# 2.0 Pre-Test

## 2.1 RANGE REQUIREMENTS

Before any further planning for this test series could be done, a list of general range requirements that must be met for data collection and safety had to be established. It was possible that no range could meet these requirements or was available. If this was the case, then the requirements may have needed to be adjusted to fit the available range(s), or another testing plan may have needed to be considered.

Requirements included:

- The range was generally clear of any excessive vegetation and debris.
- The test area had no elevation changes greater than 20 ft above or below ground zero.
- The test area was not within line of sight of any overhead power lines, water towers, or other vertical structures that could be impacted by test article fragments.
- The range did not have any non-test-related underground pipe, conduit, or cabling of any kind within 200 ft of the detonation site.
- The range was able to secure the test area from foot and vehicular traffic.

## 2.2 PLANNING

This test series was initially intended to be conducted as a series of field tests, with fragment recovery efforts following each test, covering the matrix outlined in Table 1. However, due to the limited time between the initial planning phase and the testing timeframe, the team was doubtful that a site that was both suitable for fragment recovery efforts and met the general range requirements outlined in Section 2.1 could be secured.

In order to continue with testing, the team considered pursuing a series of “arena” tests, as fragment recovery efforts would not be required. In an arena test, a series of fiberboard collection bundles surround ground zero and “catch” the fragments. Upon completion of the test,

the fragments are then recovered to determine the mass distribution [4]. Additionally, after the test, the bundles are then analyzed to determine the trajectory of each fragment and how far it penetrates, which allows for estimates of initial launch angles (horizontal and vertical) and fragment velocity to be made. Using these estimates, a prediction of the fragment map (i.e., the range and bearing of each fragment) could be made. While this was not the preferred method for this test series, it was an approach considered given the time, funding, and range space limitations involved.

Upon further discussion, it was determined that arena testing would not be a cost-effective way to complete this test series due to the number (and associated cost) of collection bundles that would be required. Therefore, it was decided to pursue the field tests once again. Fortunately, at this point in the planning process, Company A[1] graciously offered not only to host the tests at their corporate testing site in Texas but also some JPGs for the tests. However, to perform the test series at their facility, it would have to be limited to certain tests that Company A would be comfortable with. It was ultimately decided to pursue this option further and have personnel from ATF, APT, and IME visit the site to see if the Company A facility was suitable.

## 2.3 SITE SELECTION

Upon visiting the facility and specific range that Company A was offering, it was determined that their facility was capable of meeting the outlined general requirements and was able to accommodate the desired timeframe for testing. However, before a final choice could be made concerning the suitability of the site, some site-specific limitations had to be considered, most notably the fact that the potential site had limited space for a full 360° debris recovery. After consulting with Company A about this issue, they provided some estimates concerning the max throw range and azimuthal spread based on their experience. Specifically, Company A estimated that the vast majority of the debris from a JPG detonation would be limited to a 45° cone off each end of the gun, thus suggesting there was no need for a 360° recovery effort. Company A also expected the maximum throw range for the fragments to be limited to 1,000 ft and predicted something on the order of a few hundred fragments in total. Based on these estimates, it was decided the Company A facility in Texas would be suitable for the performance of this test series, although the originally envisioned test matrix would have to be revised.

## 2.4 TEST MATRIX

### 2.4.1 Revised Plan

As stated in Section 2.2, with Company A's facility selected as the test series location, the testing needed to be limited to tests they were comfortable with. Therefore, a new test plan and matrix had to be devised to replace the one outlined in Table 1. This new testing plan was developed

[1] For the sake of confidentiality, the companies that donated perforating guns for this test series are referred to as Companies A, B, C, and D throughout the entirety of this paper.

with subject matter expert input provided by Company A, which served as the basis for the initial estimates for max throw, azimuthal spread, and number of fragments. In addition to Company A, all of IME's oil and gas members were consulted and provided information that helped to guide the gun size selection and experimental setup. To determine what other tests would be possible at the Company A facility, it was decided to break down the test series into two phases. Phase 1 consisted of only one test, and one calibration shot utilizing JPGs from Company A. These guns had six charges per gun, arranged in a helix configuration with 60° phasing, and had a bulkhead installed. This first phase of testing provided a better idea of what other tests could be performed at the Company A site in Phase 2 to complete the test series. Upon reviewing the results of Test 1, which are outlined in Section 3.1.2, it was determined that if the search area was decreased, then another four tests could be performed in Phase 2; Company A also agreed to the testing of JPGs from other manufacturers, as long as calibration shots were conducted in advance. Therefore, Phase 2 planning also included tests with JPGs from Company B and Company C. Like in the Phase 1 test, the Phase 2 tests were all planned to be done with six charges per gun, arranged in a helix configuration with 60° phasing; however, in Phase 2, only the Company A guns would have had a bulkhead installed. Furthermore, this new plan did not include any tests in which the guns were vertically oriented, since at the time that this initial plan was put together Company A was not fully comfortable with the potential results (specifically the maximum range of fragments) of vertically oriented tests. Finally, this series primarily consisted of single item tests in horizontal configurations, but one test would have been a multi-gun configuration. The details of the revised plan for the test series are provided in Table 2.

**Table 2: Revised Test Matrix**

| Test | JPG | Diameter | Length | Initiation Height | Number of Items | Orientation | NEW per Charge | Total Weight (Gun + Charges) |
|---|---|---|---|---|---|---|---|---|
| **Test 1** | Company A | 3.125 in | 23 in | 1 ft | Single | Horizontal | 21.5 g | 10,117 g |
| **Test 2** | Company C | 3.125 in | 24.5 in | 1 ft | Single | Horizontal | 21.5 g | 13,416 g |
| **Test 3** | Company B | 3.125 in | 21 in | 1 ft | Single | Horizontal | 21.5 g | 9,448 g |
| **Test 4** | Company A | 3.125 in | 23 in | 3 ft | Single | Horizontal | 21.5 g | 10,117 g |
| **Test 5** | Company A | 3.125 in | 23 in | Gun on Pallet | Multiple (6) | Horizontal | 21.5 g | 60,702 g |

### 2.4.2 Final Plan

Prior to the start of the Phase 2 tests, it was initially predicted that a total of four tests would be completed in a two-week time frame. Initially, it was believed that it would take two days to complete the fragment collection for each test. However, following the completion of Test 2, it was found that fragment collection for a single item test could be completed in a single day, given the smaller search area. Therefore, the revised test matrix (as shown in Table 2) for this

test series had to be updated. The new final plan now called for a total of eight tests to be performed, including the two tests that had already been conducted. It was planned that, in addition to the JPGs from the manufacturers listed in the previous plan, another JPG would be acquired from a fourth manufacturer, Company D. As in the previous plan, it was planned that these tests would all be done with six charges per gun, in a helix configuration with 60° phasing. In this new plan, the Company A gun in Test 3 had its bulkhead removed. Additionally, this new plan called for the inclusion of a test with one gun in the vertical orientation, the performance of which was dependent on Company A's approval after observing how several other tests performed. Lastly, it was also decided that the multi-gun test would now be performed with Company B guns rather than Company A guns. The details of this final plan for the test series are provided in Table 3.

**Table 3: Final Test Matrix**

| Test | JPG | Diameter | Length | Initiation Height | Number of Items | Orientation | NEW per Charge | Total Weight (Gun + Charges) |
|---|---|---|---|---|---|---|---|---|
| **Test 1** | Company A | 3.125 in | 23 in | 1 ft | Single | Horizontal | 21.5 g | 10,117 g |
| **Test 2** | Company B | 3.125 in | 21 in | 1 ft | Single | Horizontal | 21.5 g | 9,448 g |
| **Test 3** | Company A | 3.125 in | 23 in | 1 ft | Single | Horizontal | 21.5 g | 9,639 g |
| **Test 4** | Company C | 3.125 in | 24.5 in | 1 ft | Single | Horizontal | 21.5 g | 13,416 g |
| **Test 5** | Company B | 3.125 in | 21 in | 3 ft | Single | Horizontal | 21.5 g | 9,502 g |
| **Test 6** | Company D | 3.125 in | ~ 15 in | 1 ft | Single | Horizontal | 23 g | 10,467.8 g |
| **Test 7** | Company B | 3.125 in | 21 in | Gun on Pallet | Single | Vertical | 21.5 g | 9,464 g |
| **Test 8** | Company B | 3.125 in | 21 in | Gun on Pallet | Multiple (6) | Horizontal | 21.5 g | 56,936 g |

## 2.5 PERSONNEL

Prior to the beginning of the test series, it was determined that a crew of approximately 20 people would be necessary to complete setup and post-test processing for both phases of testing. The core of the crew was made up of personnel from APT, ATF, IME, and R.A. McClure Inc. (RAM), with other members of industry being present for some specific tests. APT was responsible for writing the test plan, test report, and analysis of the test results. ATF was responsible for the instrumentation plan and setup of the cameras and pressure gauges. Additionally, both APT and ATF provided most of the manpower for this test series and were responsible for setting up the grid. IME was present to support all the tests and help to coordinate between the various entities that participated in the test series. RAM was responsible for establishing the GPS points for the grid, providing guidance during grid setup, and recording GPS coordinates of the recovered debris. Company A personnel were not included in the crew size but were responsible for the setting up and initiation of the JPGs.

# 3.0 Test Execution

The following sections describe the execution and results of each test in the JPG test series.

## 3.1 PHASE 1

As mentioned in Section 1.0, Phase 1 of the JPG test series consisted of one calibration shot and one test. The calibration shot and test both made use of a Company A gun with a bulkhead installed. As stated in Section 2.4.1, the results from this phase of the test series provided a better idea of what other tests could be performed in Phase 2. Therefore, the worst case was tested first to see if Company A would be comfortable with the additional, desired tests.

When planning for Phase 1 of the test series, it was determined that the search grid would consist of an inner radius extending out to 100 ft and encompass the full 360° around ground zero. The area inside the inner radius would be searched by the entire crew and treated as one big sector. In addition to being searched by the whole crew, it was planned that the area inside 100 ft would be searched a second time using a large bar magnet to recover any small fragments near ground zero that might have been initially missed. It was planned that past 100 ft, the search grid would consist of two 45° fans extending north and south. APT recommended that the fan in the north should be extended out to 1,300 ft to accommodate the bulkhead installed on the JPG. In the south, the fan would extend out to 1,000 ft. Each of these fans was broken down into nine 5° sectors. The search grid had markers placed at the 100 ft range every 5° from 337.5° to 22.5° and from 157.5° to 202.5°. Markers were also placed at the 1,000 ft range every 5° from 157.5° to 202.5° and at the 1,300 ft range every 5° from 337.5° to 22.5°. Members of ATF and APT were responsible for placing the markers according to the GPS points established by RAM. Figure 3 depicts the search grid from Phase 1.

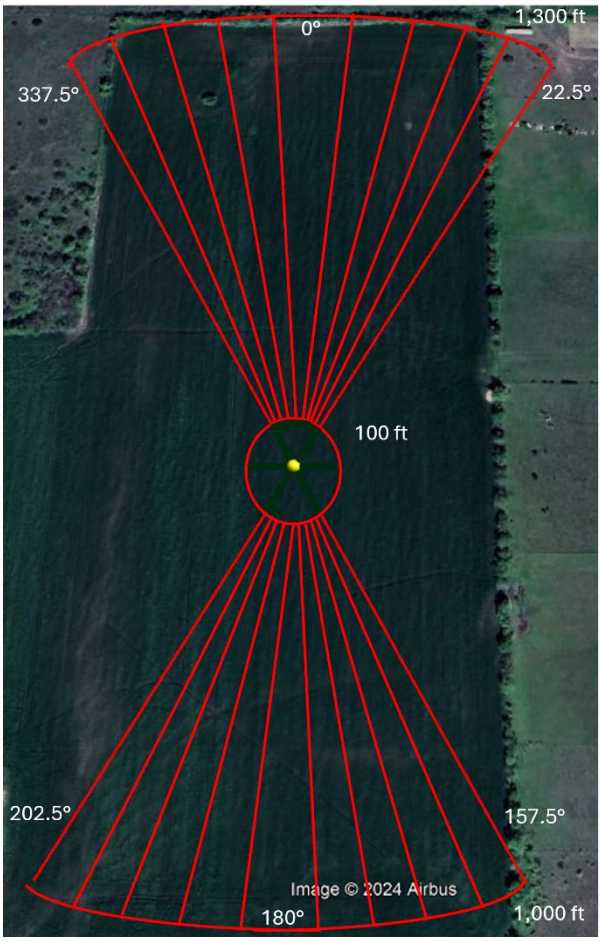


**Figure 3: Phase 1 Search Grid**

In addition to setting up the search grid, some further preparation was required before the initiation of the test. Primarily, since the field is used as farmland for part of the year, a large amount of vegetation had to be cleared so that it did not impede fragment recovery. Company A coordinated the clearing of the field with the farmer that was utilizing the field at the time of the test. Following the clearing of vegetation, a site walkthrough was performed to ensure that there was minimal metal material that might be mistaken for JPG fragments after the shot. Additionally, pressure gauges and cameras had to be set up, which was handled by ATF and is described further in Section 3.1.2.1.

### 3.1.1 Calibration

As stated in Section 3.1, only one calibration shot was performed in Phase 1. This calibration shot took place on July 15, 2024, and was performed by Company A. This shot utilized a Company A gun with a 3 1/8 in outer diameter, 23 in length, containing 6 shots per ft. Each charge had a NEW of 21.5 g. The gun was placed horizontally on a stand in a trench with sand barrels at each end to catch the bulkhead and other fragments. Upon completion of this calibration shot, it was found that the bulkhead of the gun was launched several feet into the sand

barrel. The results from this calibration shot corroborated the recommendation of extending the north side of the grid to 1,300 ft for Test 1. Unfortunately, the mass of recovered fragments from this test was not recorded and therefore an exact percentage of how much mass was recovered cannot be provided. Furthermore, there are no images showcasing the recovered fragments of the carrier tube and perforators. Figure 4 shows one of the recovered fragments of the perforators next to an intact one to provide an idea of the size of the fragments that were produced in this calibration shot.

**Figure 4: Phase 1 Calibration Shot Perforator**

### 3.1.2 Test 1

Test 1 took place on July 16, 2024, at 9:28 AM CDT. This test used the same Company A gun as described in Section 3.1.1, and had the gun positioned horizontally at a height of 1 ft above the ground, held in place by a test stand. The gun was oriented North-South with the sub facing south and the bulkhead facing north. The initiators used for this test were RP-81 and were controlled with a Teledyne RISI Inc (RISI) FS-43 Exploding Bridgewire (EBW) firing system. Company A handled the setup of the JPG and initiation of the test. Figure 5 is an example of the test setup for Test 1 and the other tests that had the JPG at 1 ft above ground.

Figure 5: Test 1 Setup (1 ft Elevation)

### 3.1.2.1 Instrumentation Results

In Test 1, pressure gauges were placed along two directions. The first line of gauges was placed in the north at distances of 10 and 20 ft from ground zero. The second line of gauges was placed in the west at distances of 5 and 10 ft. The determination of the pressure gauge locations and their setup was handled by ATF. The recordings from these gauges are listed in Table 4.

Table 4: Test 1 Pressure Gauge Readings

| Distance (ft) | Northern Gauges (psi) | Western Gauges (psi) |
|---|---|---|
| **5** | n/a | 3.34 |
| **10** | 3.7 | 1.92 |
| **20** | 1.32 | n/a |

In addition to handling the setup of the pressure gauges, ATF also developed a camera plan for all the tests in this test series and handled the setup of the cameras. The plan had one high-speed camera positioned in the west at 400-600 ft. In addition to the high-speed camera, there were also several GoPro cameras providing close-in footage and one GoPro near the high-speed camera providing footage of a wider area. Figure 6 depicts this camera layout, with north on the left-

hand side of the image. In addition to the camera plan provided by ATF, video footage was also recorded by drones operated by members of RAM.

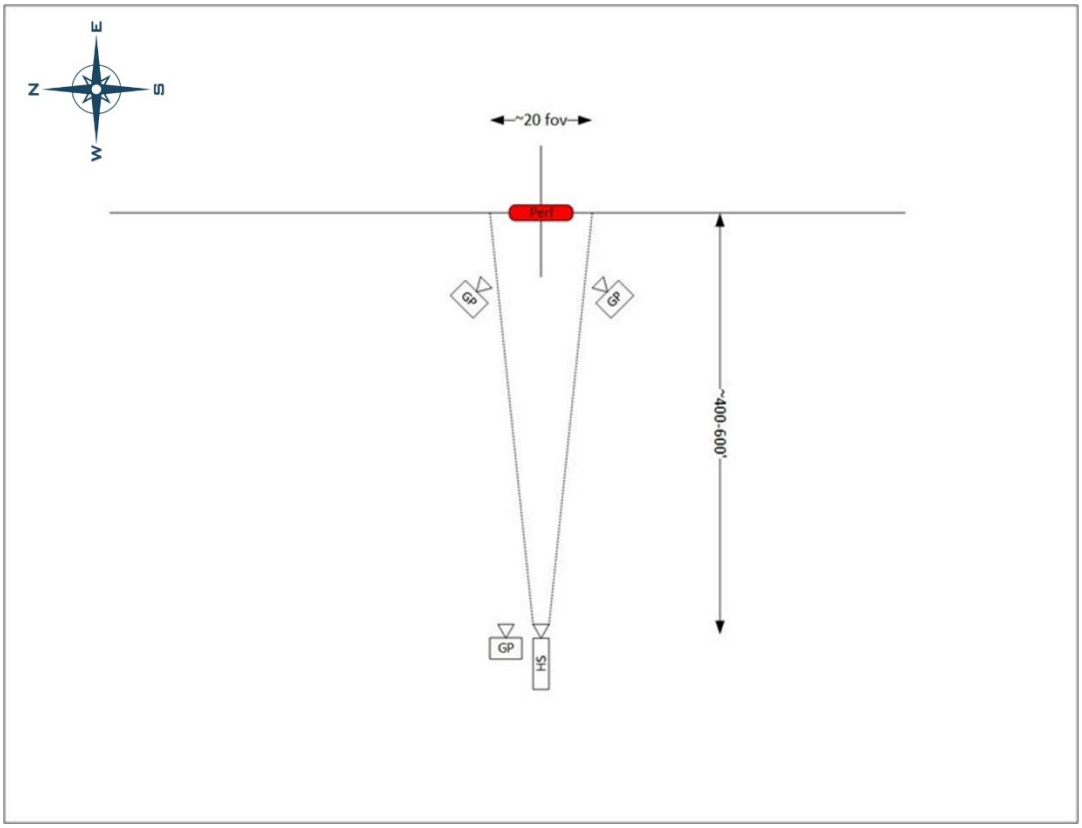


**Figure 6: Camera Plan**

In Test 1, preliminary analysis of the video footage from the high-speed camera was performed by ATF at the range to determine the velocity for the bulkhead, since it was a fragment of interest. This preliminary analysis estimated that the bulkhead was travelling with a velocity of 526 ft/s.

#### *3.1.2.2 Fragmentation*

The mass of the gun was not recorded prior to the initiation of Test 1, therefore four Company A JPGs that were as close as possible to the gun used in the test were weighed, and the average was taken. This average was used as the initial mass for the gun and was calculated to be 10,116.97 g. It should be noted that the initial and recovered mass for this test and all following tests only considered the metal mass; the mass of the plastic end caps was not included in either value. Following the completion of fragment collection, which was done in accordance with Rev 2 of DDESB TP-21 [5], all the recovered pieces were weighed to determine what percentage of the initial mass was found. The collected mass was determined to be 8,864.56 g, which means that 87.62% of the initial mass was recovered. The bulkhead accounted for roughly 7% of the total mass and was never recovered. Upon reviewing the video footage, it was determined that the

bulkhead was launched on or near the 0° line at roughly 526 ft/s. The bulkhead was not observed impacting the ground in the video and no significant impact marks were found along its flight path during fragment collection. Given the high velocity and the lack of noticeable impact marks, it was speculated to have been spinning as it bounced, leading to the bulkhead rebounding out of the test grid beyond the 1,300 ft range without leaving any clear evidence of an impact within the debris recovery area. This speculation could not be confirmed due to the suspected resting place of the bulkhead being an area with dense vegetation that prevented recovery efforts. An image showing the recovered fragments of the carrier tube and perforators is provided in Figure 7. In this figure, fragments recovered within 100 ft are on the left, fragments that were recovered from within the gun body are in the bottom right, and the recovered plastic is in the top right. Unfortunately, the fragments recovered outside of 100 ft were not captured in any images. It should be noted for this test and all following tests that while some plastic fragments were collected, the goal of the fragment collection effort was to recover metal fragments, not plastic. Therefore, the plastic fragments that were recovered were not factored into the number of fragments recovered.


**Figure 7: Test 1 Recovered Fragments**

In Test 1, a total of 25 fragments above 5 g were recovered during fragment collection and were catalogued. Of these 25 pieces, only four of them were recovered outside of 100 ft. The farthest of these pieces was found at 283.54 ft, along the 356.07° azimuth. The gun body was one of the 21 pieces recovered within 100 ft and was found 16.71 ft away from ground zero along the 150.59° azimuth. While the gun body was recovered inside of 100 ft, it was left out of Figure 7 because the image was intended to only capture the small fragments. Figure 8 provides a scatter plot depicting the fragment distribution for Test 1. The complete fragment catalogue for this test is provided in Appendix B: Fragment Catalogues

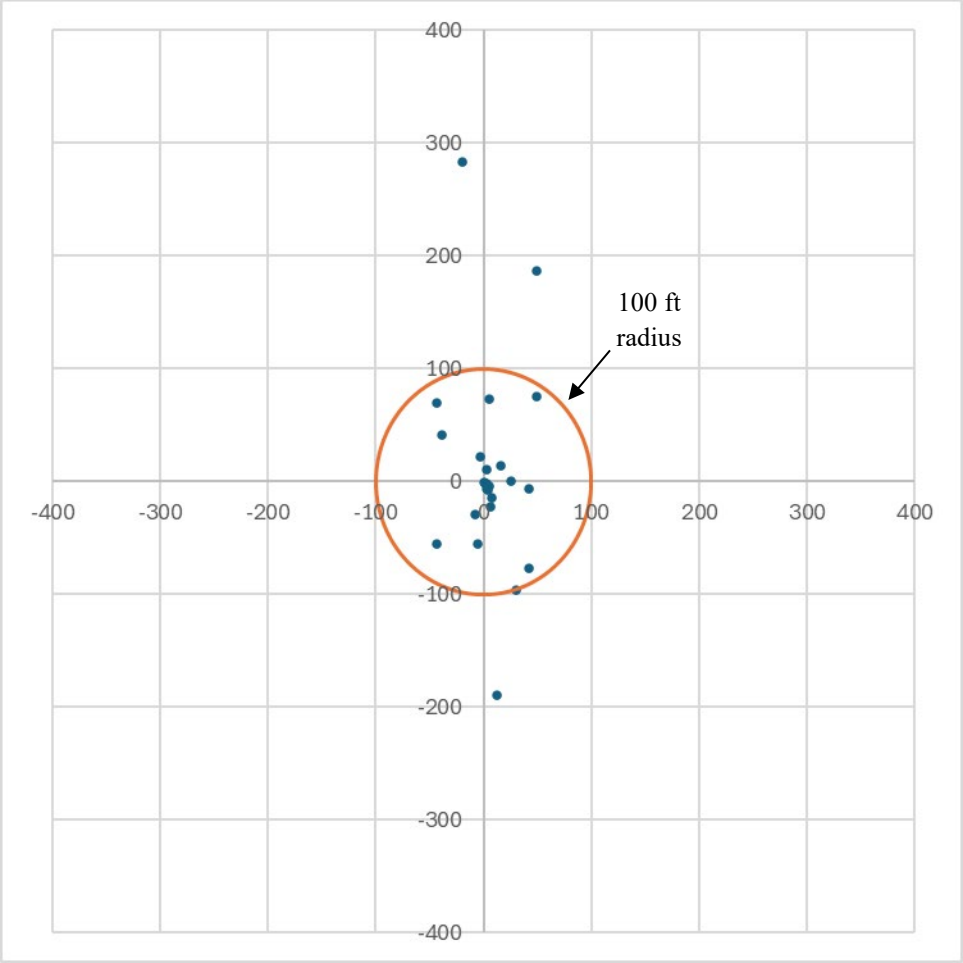


**Figure 8: Test 1 Fragment Scatter Plot (ft)**

## 3.2 PHASE 2

Phase 2 encompassed a total of five calibration shots and seven different tests. For all the tests done in this phase, fragment recovery efforts were done in accordance with TP-21. The guns tested in this phase came from several different manufacturers, as shown in Section 2.4.2 and Table 3. It should be noted that for all the tests done in this phase, the guns were oriented North-South, with the subs facing south. The exceptions to this were Test 2, in which the JPG was unintentionally aligned with the grid marker rather than true North-South, and Test 7, in which the JPG was vertically oriented. Additionally, when possible, the guns were oriented such that the majority of the charges were facing downwards. Company A handled the setup and initiation of each JPG in this phase, using the same initiation method described in Section 3.1.2. Furthermore, the determination of the pressure gauge locations and their setup was once again handled by ATF for all tests in Phase 2. Lastly, the same camera plan as described in Section 3.1.2.1 and shown in Figure 6 was used for all the tests in Phase 2.

Following the completion of Test 1, it was expected that the search grid for each test in Phase 2 could be limited to 400 ft. Additionally, for Phase 2 it was decided that debris would be collected in a full 360° area, both within and past 100 ft, rather than collecting it in two fans past 100 ft. In this phase, the grid used 10° sectors rather than 5°. Like in Phase 1, the area within 100 ft was searched by the whole crew, who then split into a north team and a south team for searching the grid past 100 ft. The area inside the 100 ft radius for all the Phase 2 tests was also searched a second time using a large bar magnet, as was done in Phase 1. As in Phase 1, the grid for Phase 2 had markers placed by ATF and APT according to GPS points established by RAM. These markers were placed every 10° starting from 5° and going clockwise to 355° at both 100 ft and 400 ft. This was done so that the normals of the JPGs would align with the center of a sector, e.g., the northern face of the gun was aligned with 0°. Figure 9 depicts the search grid for Phase 2.

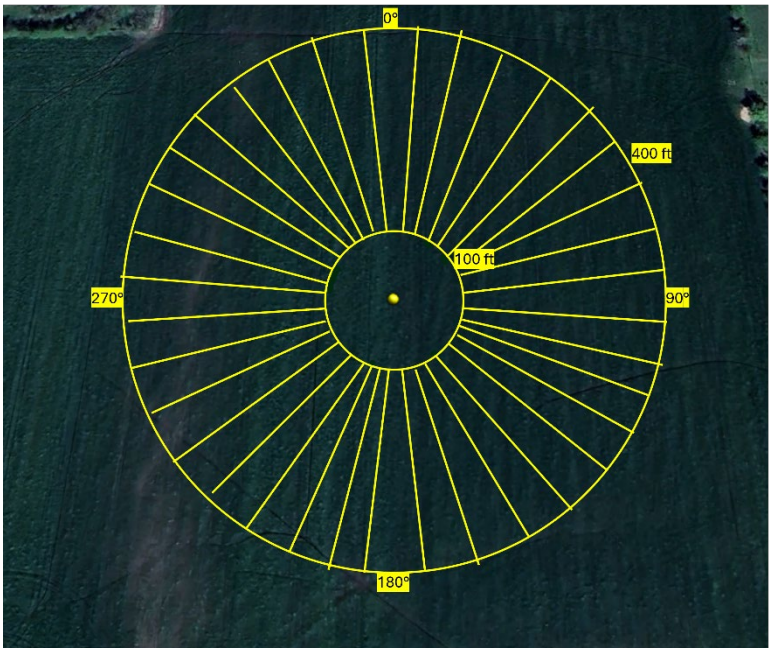


**Figure 9: Phase 2 Search Grid**

Many of the same site preparations described in Phase 1 had to be completed for Phase 2 as well. However, in addition to those preparations, the area directly surrounding ground zero had to be flattened for Tests 7 and 8. Since these would be the last two tested performed, it was expected that the ground would be somewhat uneven due to the previous tests. This could impact Tests 7 and 8 since they would be placed on pallets at ground level, rather than be held above ground by a stand like the previous tests, and uneven ground could cause the guns to tip or roll over.

### 3.2.1 Calibration

As in Phase 1, all the calibration shots for Phase 2 were done with the guns placed horizontally on a stand in a trench with sand barrels at each end to catch the fragments. It should be noted that

all of the calibration shots in Phase 2 took place on August 12, 2024. The first calibration shot used a Company C JPG with a 3 1/8 in outer diameter, a 24.5 in length, and 6 shots per foot. For this shot, each charge had a NEW of 21.5 g. Prior to the shot, this JPG had a recorded mass of 13,419 g. Of this initial mass, 13,222 g were recovered, meaning 98.5% of the gun's mass was recovered. The fragments of the carrier tube and perforators recovered from this shot are shown in Figure 10. In this figure, all the recovered metal fragments, regardless of mass, are shown on the left, while the recovered plastic is shown on the right.


**Figure 10: Phase 2 Calibration Shot 1 Recovered Fragments**

The second calibration shot was done with a Company B gun that had a 3 1/8 in outer diameter, a 21 in length, and 6 shots per foot. Each charge for this gun also had an NEW of 21.5 g. Prior to the shot, this JPG had a recorded mass of 9,428 g. Of this initial mass, 9,053 g were recovered, meaning 96% of the gun's mass was recovered. The fragments of the carrier tube and perforators recovered from this shot are shown in Figure 11. In this figure, all the recovered metal fragments, regardless of mass, are shown on the left, while the recovered plastic is shown on the right.


Figure 11: Phase 2 Calibration Shot 2 Recovered Fragments

The third calibration shot was done with another Company C JPG with the same specs as in the first calibration shot, however the NEW per charge was increased to 23 g. Prior to the shot, this JPG had a recorded mass of 13,387 g. Of this initial mass, 12,794 g were recovered, meaning 95.6% of the gun's mass was recovered. The fragments of the carrier tube and perforators recovered from this shot are shown in Figure 12. In this figure, all the recovered metal fragments, regardless of mass, are shown on the left, while the recovered plastic is shown on the right.


Figure 12: Phase 2 Calibration Shot 3 Recovered Fragments

The final calibration shot was done with a second Company B gun. Once again, this gun had the same specs as the second calibration shot, but the NEW per charge was increased to 23 g. Prior to the shot, this JPG had a recorded mass of 9,427 g. Of this initial mass, 8,485 g were recovered, meaning 90% of the gun's mass was recovered. The fragments of the carrier tube and perforators recovered from this shot are shown in Figure 13. In this figure, all the recovered metal

fragments, regardless of mass, are shown on the left, while the recovered plastic is shown on the right.

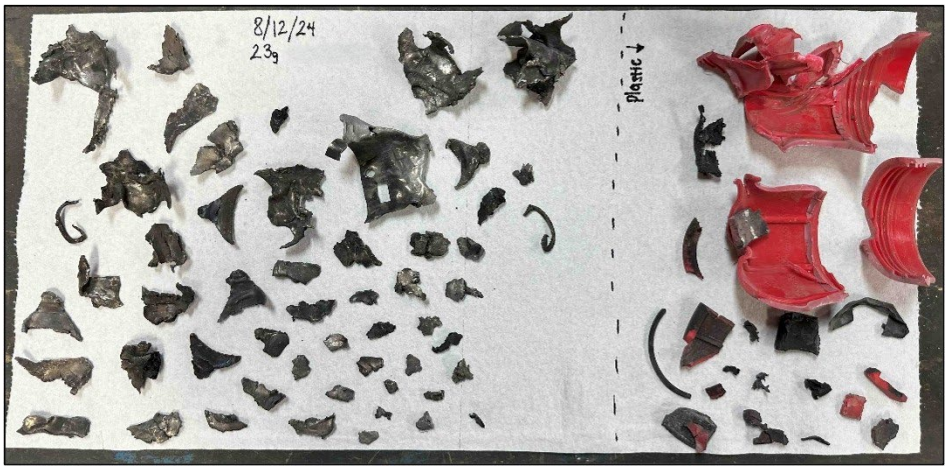


**Figure 13: Phase 2 Calibration Shot 4 Recovered Fragments**

It should be noted that a calibration shot was performed with a Company D perforating gun as well. However, this calibration shot was not performed at the Company A test site and was not witnessed by APT personnel like the other calibration shots were. Company D shared the results of this calibration shot with Company A, which is why they allowed for a test to be performed using a Company D perforating gun in Phase 2 of the test series.

### 3.2.2 Test 2

Test 2 took place on August 13, 2024, at 10:14 AM CDT. This test used a single Company B gun with a 3 1/8 in outer diameter and a 21 in length. This gun contained 6 shots per foot with each charge having an NEW of 21.5 g. This gun was oriented horizontally and positioned 1 ft above ground on a test stand. Given that this test also had the JPG positioned at 1 ft above ground, Figure 5 can be referenced for a visual of the test setup. In this test the JPG was unintentionally offset 5° clockwise of the intended axis, as the gun was aligned with the grid markers rather than true North-South during set up.

#### *3.2.2.1 Instrumentation Results*

For Test 2, pressure gauges were placed along two directions. The first line of gauges was placed to the north at distances of 5 and 10 ft from ground zero. The second line of gauges was placed to the west at distances of 5, 10, and 20 ft. The recordings from these gauges are listed in Table 5.

**Table 5: Test 2 Pressure Gauge Readings**

| Distance (ft) | Northern Gauges (psi) | Western Gauges (psi) |
|---|---|---|
| **5** | 12.91 | 3.77 |
| **10** | 7.29 | 3.88 |
| **20** | n/a | 1.38 |

There were no anticipated fragments of special interest in this test, such as the bulkhead from Test 1. Thus, there was no preliminary video analysis done at the test site to find fragment velocity. Section 4.1.2 contains the analysis of the video footage that was performed later.

#### *3.2.2.2 Fragmentation*

Prior to the initiation of Test 2, the mass was recorded as 9,448 g. Upon completion of the recovery effort, it was determined that 8,654 g were collected, equating to 91.6% of the starting mass. The fragments of the carrier tube and perforators recovered from this test are shown in Figure 14. In this figure, all the recovered metal fragments, regardless of mass, are shown on the left, while the recovered plastic is shown on the right. Unlike Test 1, in this test and all other tests done in Phase 2, the recovered fragments were not separated by distance in the pictures.


**Figure 14: Test 2 Recovered Fragments**

In Test 2, a total of 34 fragments above 5 g were recovered during fragment collection and cataloguing. Of these 34 pieces, 21 of them were recovered outside of 100 ft. The farthest of these pieces was found at 300.97 ft, along the 10.61° azimuth. The gun body was one of the 21 pieces recovered outside of 100 ft and was found 109.80 ft away from ground zero along the 180.22° azimuth. Figure 15 provides a scatter plot depicting the fragment distribution for Test 2. As mentioned previously herein, the gun in this test was offset roughly 5° clockwise; the red line in Figure 15 represents the axis the gun was aligned with. The complete fragment catalogue for this test is provided in Appendix B: Fragment Catalogues

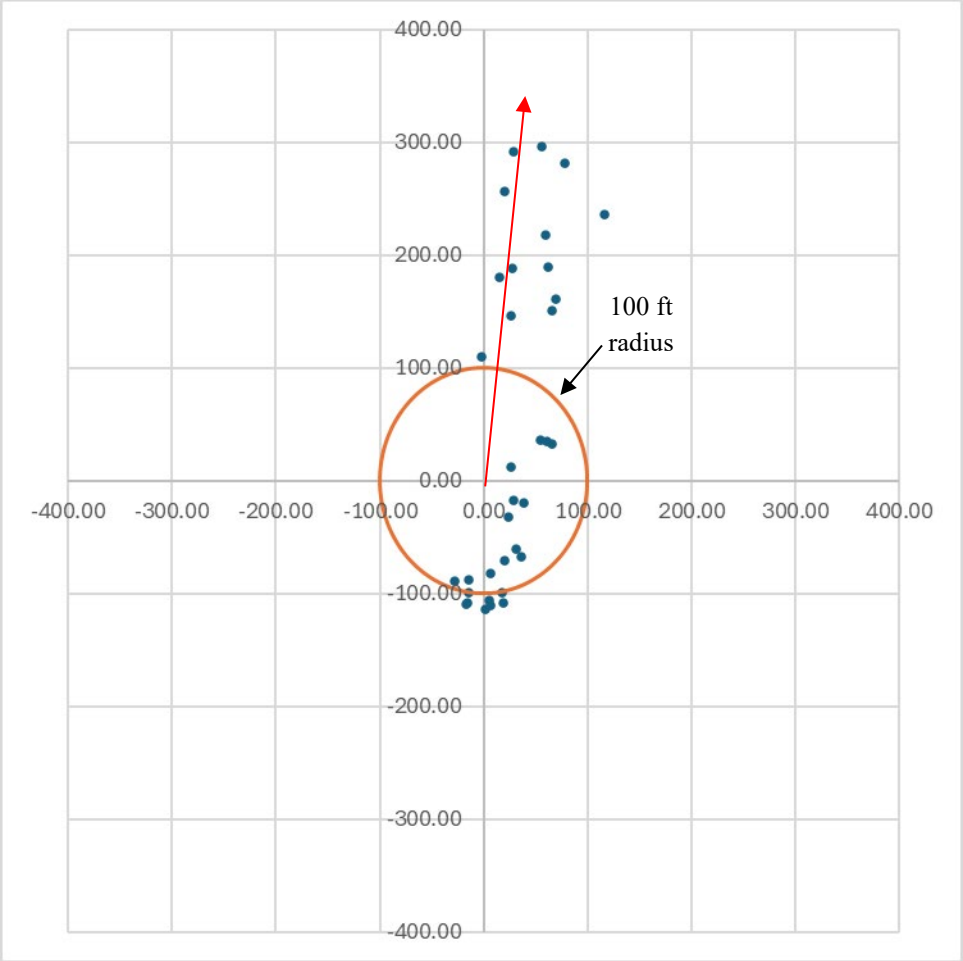


**Figure 15: Test 2 Fragment Scatter Plot**

### 3.2.3 Test 3

Test 3 took place on August 14, 2024, at 10:47 AM CDT. This test used a single Company A gun with a 3 1/8 in outer diameter and a 23 in length. This gun contained 6 shots per foot with each charge having an NEW of 21.5 g. This gun was oriented horizontally and positioned 1 ft above ground in a test stand. Given that this test also had the JPG positioned at 1 ft above ground, Figure 5 can be referenced for a visual of the test setup. It should be noted that this Company A gun had the bulkhead removed out of concern that a repeat of Test 1 would occur, i.e., the bulkhead would exit the debris collection area.

#### *3.2.3.1 Instrumentation Results*

For Test 3, pressure gauges were placed along two directions. The first line of gauges was placed to the north at distances of 5 and 10 ft from ground zero. The second line of gauges was placed to the west at distances of 5, 10, and 20 ft. The recordings from these gauges are listed in Table 6.

**Table 6: Test 3 Pressure Gauge Readings**

| Distance (ft) | Northern Gauges (psi) | Western Gauges (psi) |
|---|---|---|
| **5** | 6.49 | 6.24 |
| **10** | 4.68 | 3.66 |
| **20** | n/a | 2.32 |

Test 3 also did not have any anticipated fragments of special interest, such as the bulkhead from Test 1. Therefore, there was no preliminary video analysis done at the test site to find fragment velocity. Section 4.1.3 contains the analysis of the video footage that was performed later.

### *3.2.3.2 Fragmentation*

Prior to the initiation of Test 3, the mass was recorded as 9,639 g. Upon completion of the recovery effort, it was determined that 9,193 g were collected, equating to 95.4% of the starting mass. The carrier tube and perforator fragments recovered from this test are shown in Figure 16. Once again, in this figure all the recovered plastic is on the right-hand side, and all the recovered metal regardless of mass and recovery location is on the left-hand side.


**Figure 16: Test 3 Recovered Fragments**

In Test 3, a total of 51 fragments above 5 g were recovered during fragment collection and cataloguing. Of these 51 pieces, 19 of them were recovered outside of 100 ft. The farthest of these pieces was found at 336.90 ft, along the 172.33° azimuth. The gun body was one of the 32 pieces recovered within 100 ft and was found 2.28 ft away from ground zero along the 1.33° azimuth. Figure 17 provides a scatter plot depicting the fragment distribution for Test 3 and the complete fragment catalogue for this test is provided in Appendix B: Fragment Catalogues

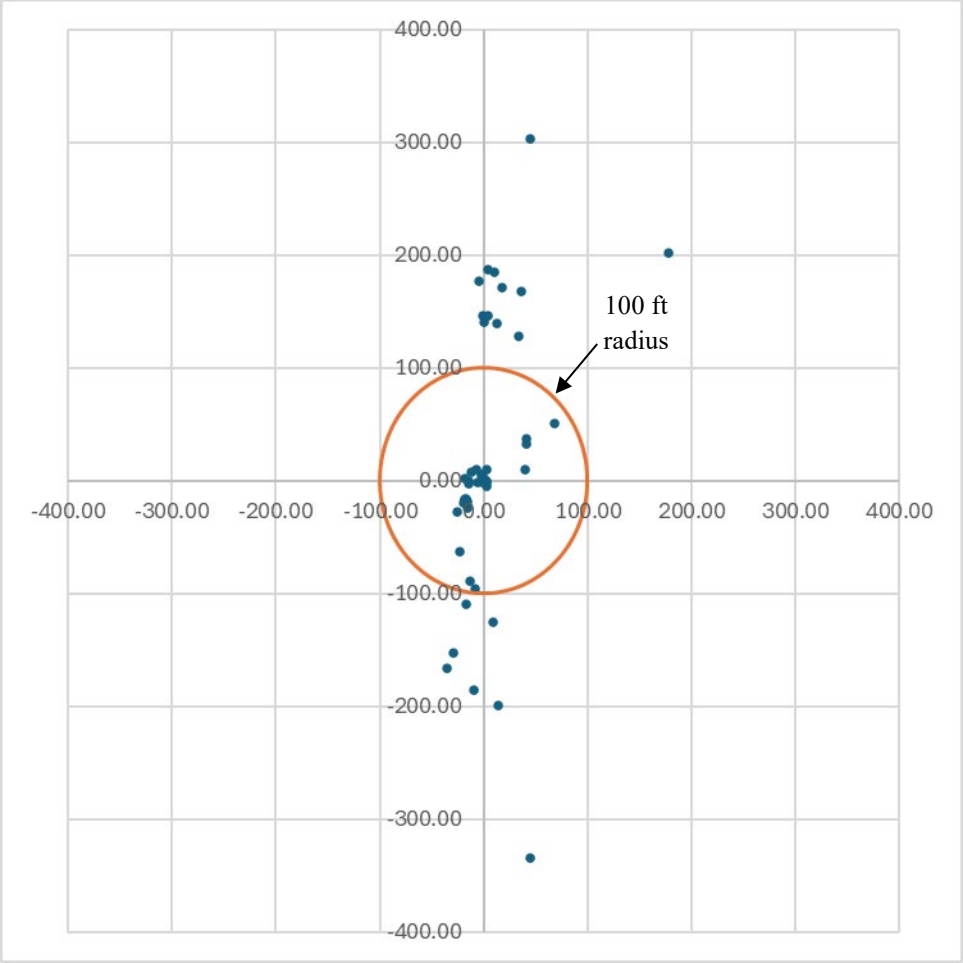


**Figure 17: Test 3 Fragment Scatter Plot**

### 3.2.4 Test 4

Test 4 took place on August 15, 2024, at 10:16 AM CDT. This test used a single Company C gun with a 3 1/8 in outer diameter and a 24.5 in length. This gun contained 6 shots per foot with each charge having an NEW of 21.5 g. This gun was oriented horizontally and positioned 1 ft above ground on a stand. Given that this test also had the JPG positioned at 1 ft above ground, Figure 5 can be referenced for a visual of the test setup.

#### *3.2.4.1 Instrumentation Results*

For Test 4, pressure gauges were placed along two directions. The first line of gauges was placed to the north at distances of 5 and 10 ft from ground zero. The second line of gauges was placed to the west at distances of 5, 10, and 20 ft. The recordings from these gauges are listed in Table 7.

**Table 7: Test 4 Pressure Gauge Readings**

| Distance (ft) | Northern Gauges (psi) | Western Gauges (psi) |
|---|---|---|
| **5** | 8.34 | 3.19 |
| **10** | 6.02 | 2.76 |
| **20** | n/a | 1.6 |

There were no anticipated fragments of special interest in Test 4, so there was no preliminary video analysis done at the test site to find fragment velocity. Section 4.1.4 contains the analysis of the video footage that was performed later.

### *3.2.4.2 Fragmentation*

Prior to the initiation of Test 4, the mass was recorded as 13,416 g. Upon completion of the recovery effort, it was determined that 12,835.4 g were collected, equating to 95.7% of the starting mass. The carrier tube and perforator fragments recovered from this test are shown in Figure 18. It can be seen on the far left of this image that the carrier tube largely remained intact. The pattern of having metal fragments on the left and plastic on the right of the photo continues for this test. Once again, this image contains all the recovered fragments regardless of the distance they were recovered at or their mass.


**Figure 18: Test 4 Recovered Fragments**

In Test 4, a total of 44 fragments above 5 g were recovered during fragment collection and cataloguing. Of these 44 pieces, 16 of them were recovered outside of 100 ft. The farthest of these pieces was found at 334.69 ft, along the 27.13° azimuth. The gun body was one of the 28 pieces recovered within 100 ft and was found 78.89 ft away from ground zero along the 190° azimuth. Figure 19 provides a scatter plot depicting the fragment distribution for Test 4 and the complete fragment catalogue for this test is provided in Appendix B: Fragment Catalogues

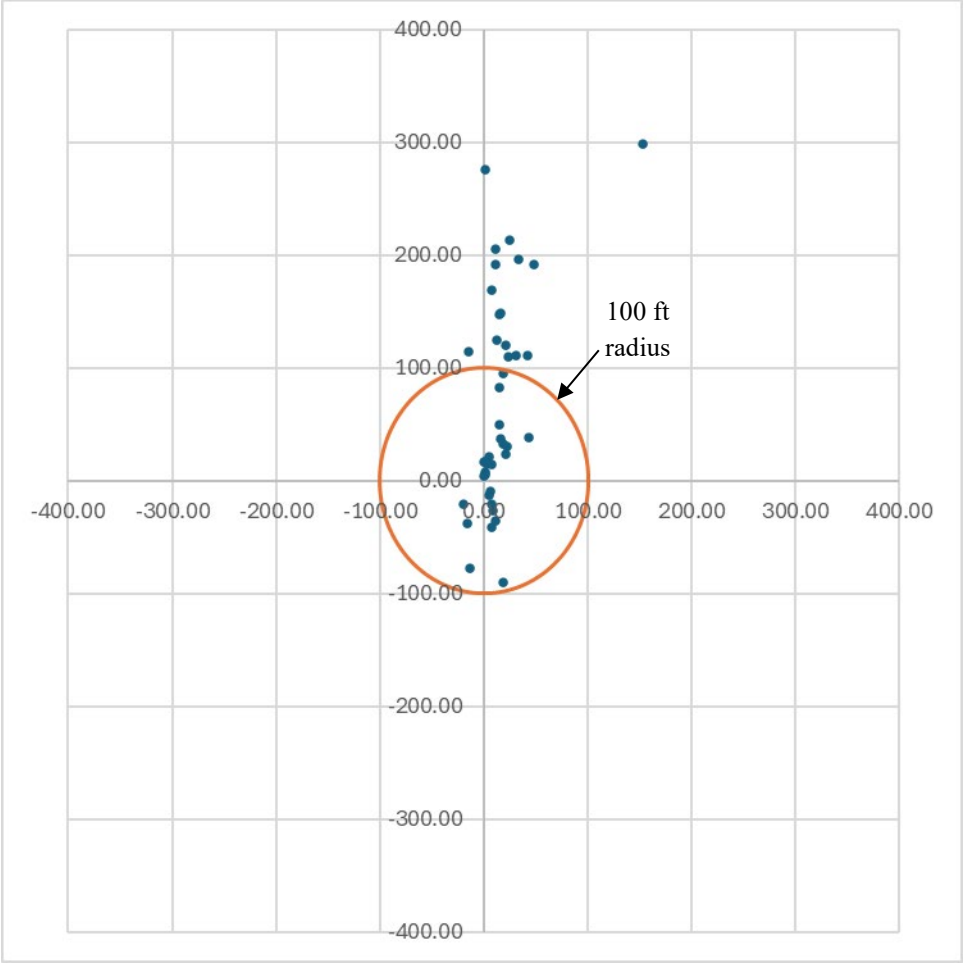


**Figure 19: Test 4 Fragment Scatter Plot**

### 3.2.5 Test 5

Test 5 took place on August 16, 2024, at 10:14 AM CDT. This test used a single Company B gun with a 3 1/8 in outer diameter and a 21 in length. This gun contained 6 shots per foot with each charge having an NEW of 21.5 g. This gun was oriented horizontally and positioned 3 ft above ground on a stand. Figure 20 depicts the test setup for Test 5.

Figure 20: Test 5 Set Up (3 ft Elevation)

### 3.2.5.1 Instrumentation Results

For Test 5, pressure gauges were placed along two directions. The first line of gauges was placed to the north at distances of 5 and 10 ft from ground zero. The second line of gauges was placed to the west at distances of 5, 10, and 20 ft. The recordings from these gauges are listed in Table 8.

Table 8: Test 5 Pressure Gauge Readings

| Distance (ft) | Northern Gauges (psi) | Western Gauges (psi) |
|---|---|---|
| **5** | 6.56 | 4.31 |
| **10** | 4.31 | 2.76 |
| **20** | n/a | 2.07 |

Test 5 was another test in which there were no anticipated fragments of special interest. Consequently, there was no preliminary video analysis done at the test site to find fragment velocity. Section 4.1.5 contains the analysis of the video footage that was performed later.

### 3.2.5.2 Fragmentation

Prior to the initiation of Test 5, the mass was recorded as 9,502 g. Upon completion of the recovery effort, it was determined that 9,083 g were collected, equating to 95.6% of the starting mass. The carrier tube and perforator fragments recovered from this test are shown in Figure 21. In this test the plastic fragments were left out of the image. Instead, it can be seen that Figure 21 displays all the recovered metal fragments with the largest of them on the top left and the smallest on the bottom right. The fragments displayed in this image were recovered both within and beyond the 100 ft range.


**Figure 21: Test 5 Recovered Fragments**

In Test 5, a total of 57 fragments above 5 g were recovered during fragment collection and cataloguing. Of these 57 pieces, 16 of them were recovered outside of 100 ft. The farthest of these pieces was found at 287.71 ft, along the 14.45° azimuth. The gun body was one of the 16 pieces recovered outside of 100 ft and was found 159.56 ft away from ground zero along the 184.71° azimuth. Figure 22 provides a scatter plot depicting the fragment distribution for Test 5 and the complete fragment catalogue for this test is provided in Appendix B: Fragment Catalogues

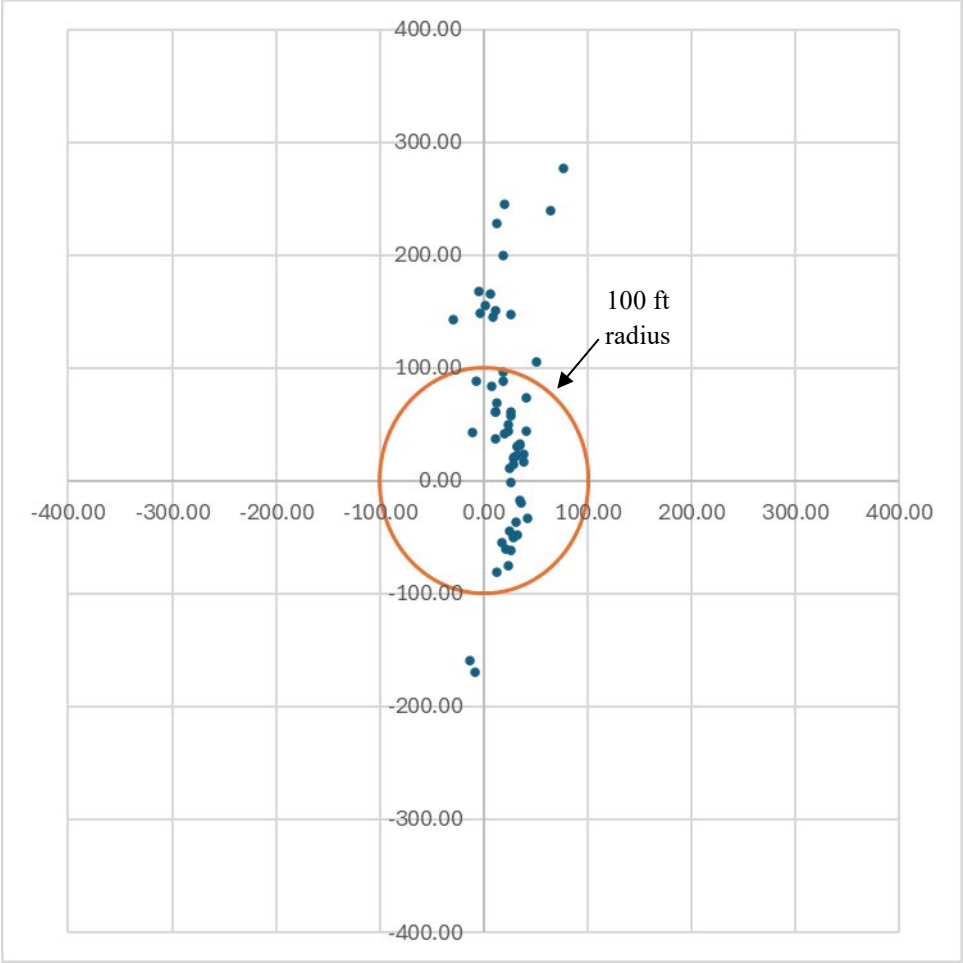


**Figure 22: Test 5 Fragment Scatter Plot**

### 3.2.6 Test 6

Test 6 took place on August 19, 2024, at 9:58 AM CDT. This test used a single Company D gun with a 3 1/8 in outer diameter and a length of ~15 in. This gun contained 6 shots per foot with each charge having an NEW of 23 g. This gun was oriented horizontally and positioned 1 ft above ground on a stand. Given that this test also had the JPG positioned at 1 ft above ground, Figure 5 can be referenced for a visual of the test setup.

#### *3.2.6.1 Instrumentation Results*

For Test 6, pressure gauges were placed along two directions. The first line of gauges was placed to the north at distances of 5 and 10 ft from ground zero. The second line of gauges was placed to the west at distances of 5, 10, and 20 ft. The recordings from these gauges are listed in Table 9.

Table 9: Test 6 Pressure Gauge Readings

| Distance (ft) | Northern Gauges (psi) | Western Gauges (psi) |
|---|---|---|
| **5** | 9.46 | 8.56 |
| **10** | 3.73 | 9.9 |
| **20** | n/a | 1.85 |

Notably, the trend that was observed in all the previous tests was not present in this test. Specifically, the highest pressure in this test was recorded by the Western Gauges and not the Northern Gauges as in the previous tests. This is theorized as being due to the gun body in this test breaking apart and failing to constrain the blast wave.

While the gun body breaking apart was an unexpected result, it was decided not to perform any preliminary video analysis while at the testing site, given the fragments of the gun body were easily found and there were no other anticipated fragments of special interest. The video analysis for this test can be found in Section 4.1.6.

### 3.2.6.2 Fragmentation

Prior to the initiation of Test 6, the mass was recorded as 10,467.8 g. Upon completion of the recovery effort, it was determined that 10,134 g were collected, equating to 96.8% of the starting mass. The perforator fragments recovered from this test are shown in Figure 23. As shown on the right side of Figure 23, this test produced many plastic fragments. This is because the internal carrier tube of this gun was made of plastic and not metal like the other guns used in this test series. On the left side of the figure, the metal fragments are once again arranged with the largest in the top left and the smallest in the bottom center of the figure. Furthermore, as with all other tests in this phase, the fragments displayed in this image were recovered at any distance.


Figure 23: Test 6 Recovered Fragments

In Test 6, a total of 62 fragments above 5 g were recovered during fragment collection and catalogued. Of these 62 pieces, 28 of them were recovered outside of 100 ft. The farthest of these pieces was found at 367.89 ft, along the 351.70° azimuth. During fragment collection and

cataloguing, it was found that the gun body in this test had broken apart into three pieces. The exact range and bearing of these pieces are listed in Table 10.

**Table 10: Test 6 Gun Body Fragment Locations**

| | Fragment 1 | Fragment 2 | Fragment 3 |
|---|---|---|---|
| **Range (ft)** | 31.60 | 74.87 | 100.48 |
| **Bearing (°)** | 301.89 | 145.63 | 156.63 |

Figure 24 provides a scatter plot depicting the fragment distribution for Test 6 and the complete fragment catalogue for this test is provided in Appendix B: Fragment Catalogues

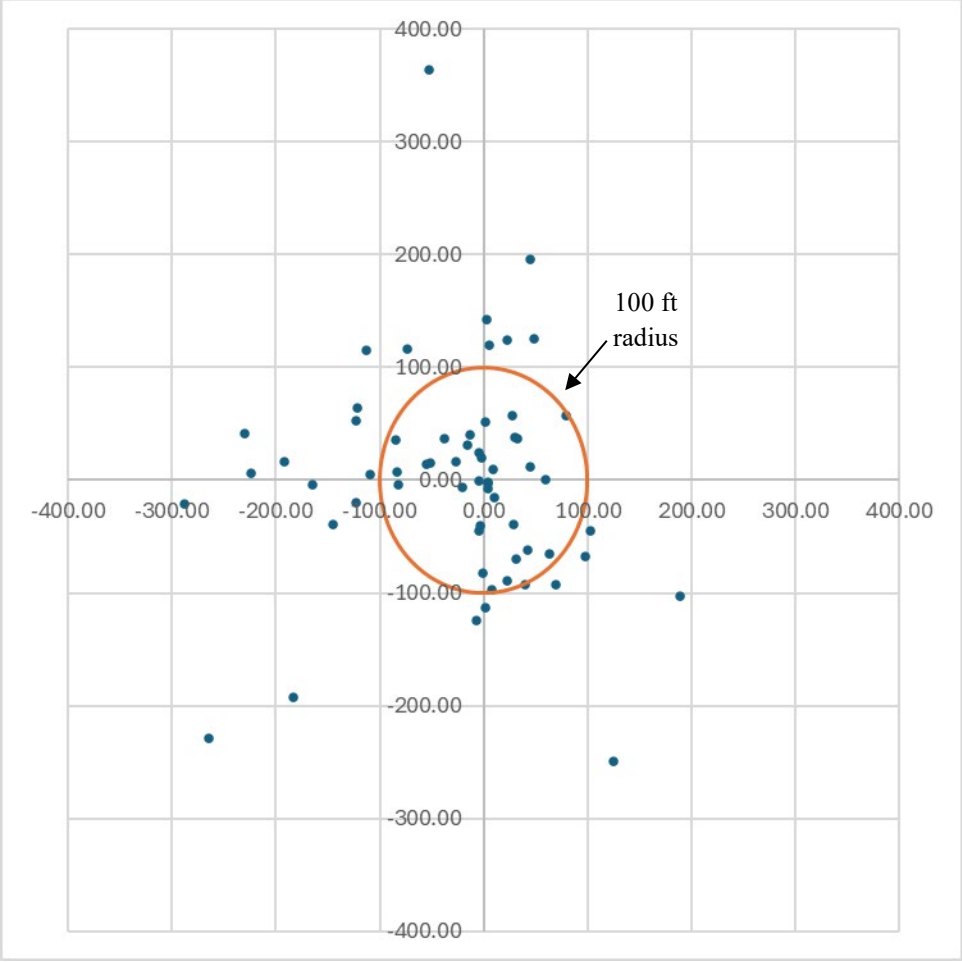


**Figure 24: Test 6 Fragment Scatter Plot**

The scatter plot for Test 6 shows that this test did not follow the expected trend that was observed in the previous tests. Whereas the previous test all had the majority of the fragments focused along the North-South axis, this test had many fragments distributed to the west. This may have been the result of the gun breaking apart and therefore not directing the fragments along the North-South axis, but it is noteworthy that the farthest fragment was still to the north.

### 3.2.7 Test 7

Test 7 took place on August 20, 2024, at 10:00 AM CDT. This test used a single Company B gun with a 3 1/8 in outer diameter and a 21 in length. This gun contained 6 shots per foot with each charge having an NEW of 21.5 g. This gun was oriented vertically and positioned upright on a pallet. For this test, the sub was facing downwards into the pallet. Furthermore, the gun was oriented such that the charges were not aimed directly at the cameras to help maintain visual clarity. Figure 25 depicts the test setup for Test 7.

**Figure 25: Test 7 Setup (Vertical Orientation)**

#### 3.2.7.1 Instrumentation Results

For Test 7, pressure gauges were placed along two directions. The first line of gauges was placed to the north at distances of 5 and 10 ft from ground zero. The second line of gauges was placed to the west at distances of 5, 10, and 20 ft. The recordings from these gauges are listed in Table 11.

**Table 11: Test 7 Pressure Gauge Readings**

| Distance (ft) | Northern Gauges (psi) | Western Gauges (psi) |
|---|---|---|
| **5** | 3.52 | 4.64 |
| **10** | 2.94 | 3.12 |
| **20** | n/a | 1.49 |

Similar to Test 6, this was another test in which the highest pressure was recorded by the Western Gauges. However, in this test it would be expected that this is a result of the gun's orientation and not the result of the gun breaking apart. As stated in Section 3.2.7, this test had the gun oriented vertically rather than horizontally, and therefore the blast was not concentrated along the North-South axis as it was in the other tests.

While Test 7 was uniquely the sole test with a vertical configuration, no fragments of special interest were anticipated. The analysis of the video footage from this test is described in Section 4.1.7.

#### 3.2.7.2 Fragmentation

Prior to the initiation of Test 7, the mass was recorded as 9,494 g. Upon completion of the recovery effort, it was determined that 9,145 g were collected, equating to 96.3% of the starting mass. The carrier tube and perforator fragments recovered from this test are shown in Figure 26. In this figure the metal fragments are once again laid out with the largest in the top left and the smallest in the bottom center of the figure. This figure also includes the various sub 5 g fragments that were recovered from ground zero by magnet in the center of the image. Once again, these fragments were recovered at all distances from ground zero to 400 ft. The recovered pieces of plastic are on the right side of the image.


Figure 26: Test 7 Recovered Fragments

In Test 7, a total of 35 fragments above 5 g were recovered during fragment collection and cataloguing. Of these 35 pieces, 14 of them were recovered outside of 100 ft. The farthest of these pieces was found at 297.96 ft, along the 311.96° azimuth. The gun body was one of the 21 pieces recovered within 100 ft and was found 1.69 ft away from ground zero along the 277.26° azimuth. Figure 27 provides a scatter plot depicting the fragment distribution for Test 7 and the complete fragment catalogue for this test is provided in Appendix B: Fragment Catalogues.

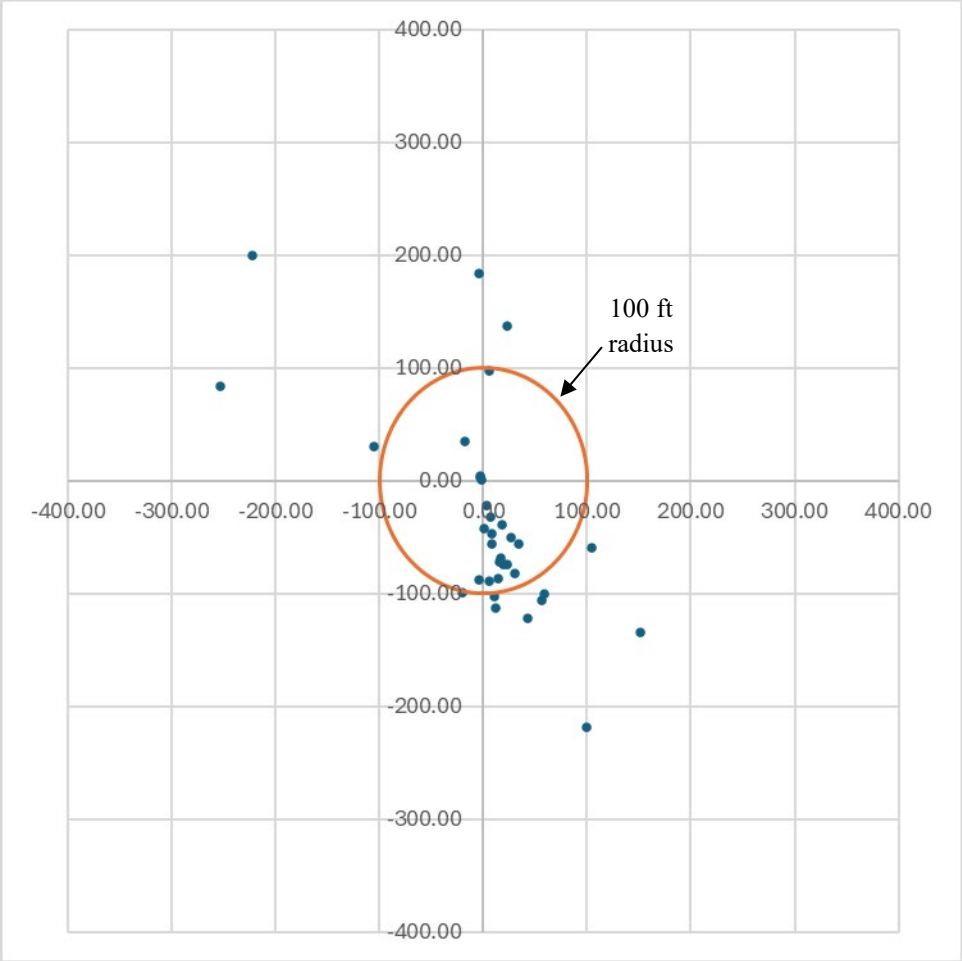


Figure 27: Test 7 Fragment Scatter Plot

Test 7 did not have the same expectations for fragment distribution as the other tests did. All the other tests aligned the JPG along the North-South axis and thus it was expected that the majority of the fragments would be distributed about that axis. However, as stated in Section 3.2.7, this test oriented the gun vertically, so a different fragment distribution was to be expected. That said, this test did perform slightly different than expected; given that a large amount of the fragments would be projected vertically into the air, a more uniform fragment distribution was expected. In actuality, most of the fragments were focused in the Southeast quadrant instead. It is believed that this is because the gun "slipped" slightly as it fired. This resulted in the gun pushing through the pallet slightly to the Northwest of its original location and thus perhaps causing the fragment bias to the Southeast.

### 3.2.8 Test 8

Test 8 took place on August 21, 2024, at 10:45 AM CDT. This test made use of six Company B guns, each with a 3 1/8 in outer diameter and a 21 in length. These guns contained six shots per foot with each charge having a NEW of 21.5 g. These guns were oriented horizontally and, as

was stated in Section 3.2, positioned such that the subs were all facing south; they were not positioned in an alternating “nose-tail” configuration. Furthermore, it is important to note that the guns in this test were all forced to initiate, as this was not a test to see if sympathetic detonation would occur. The JPGs in this test were arranged in a 3-2-1 stack on top of a pallet. Going from west to east, Guns 1 through 3 made up the base of the stack, Guns 4 and 5 were in the middle, and Gun 6 was on the top. Figure 28 depict the test set up for Test 8.

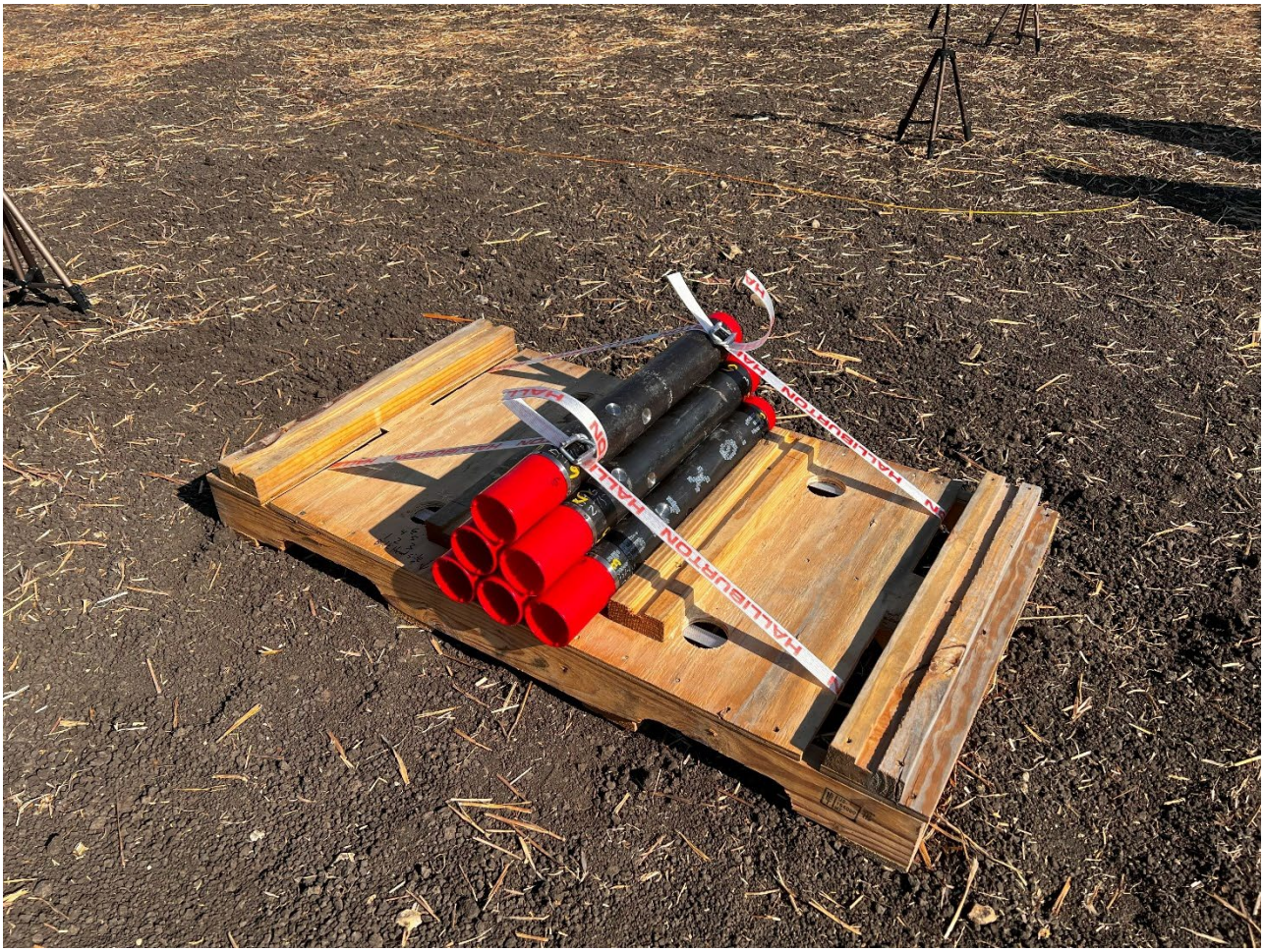


**Figure 28: Test 8 Set Up (Multi Gun Test)**

#### *3.2.8.1 Instrumentation Results*

For Test 8, pressure gauges were placed along two directions. The first line of gauges was placed to the north at distances of 5 and 10 ft from ground zero. The second line of gauges was placed to the west at distances of 5, 10, and 20 ft. The recordings from these gauges are listed in Table 12.

Table 12: Test 8 Pressure Gauge Readings

| Distance (ft) | Northern Gauges (psi) | Western Gauges (psi) |
|---|---|---|
| **5** | 23.57 | 18.67 |
| **10** | 10.73 | 4.75 |
| **20** | n/a | 1.96 |

There were no anticipated fragments of special interest in Test 8, despite it being the largest test in Phase 2. Therefore, there was no preliminary video analysis done at the test site to find fragment velocity. Section 4.1.8 contains the analysis of the video footage that was performed later.

#### *3.2.8.2 Fragmentation*

Prior to the initiation of Test 8, the total mass of all guns was recorded as 56,936 g. Upon completion of the recovery effort, it was determined that 53,521 g were collected, equating to 94% of the starting mass. The carrier tube and perforator fragments recovered from this test are shown in Figure 29. In this figure the recovered carrier tube fragments are in the far left of the image, the recovered perforator fragments are then arranged in order of largest to smallest moving from the upper left to the lower right of the image. The recovered pieces of plastic are in the upper right corner of the image with the sub 5 g fragments that were recovered at ground zero via magnet placed directly beneath them in the figure. The fragments displayed in this image were recovered at any distance.

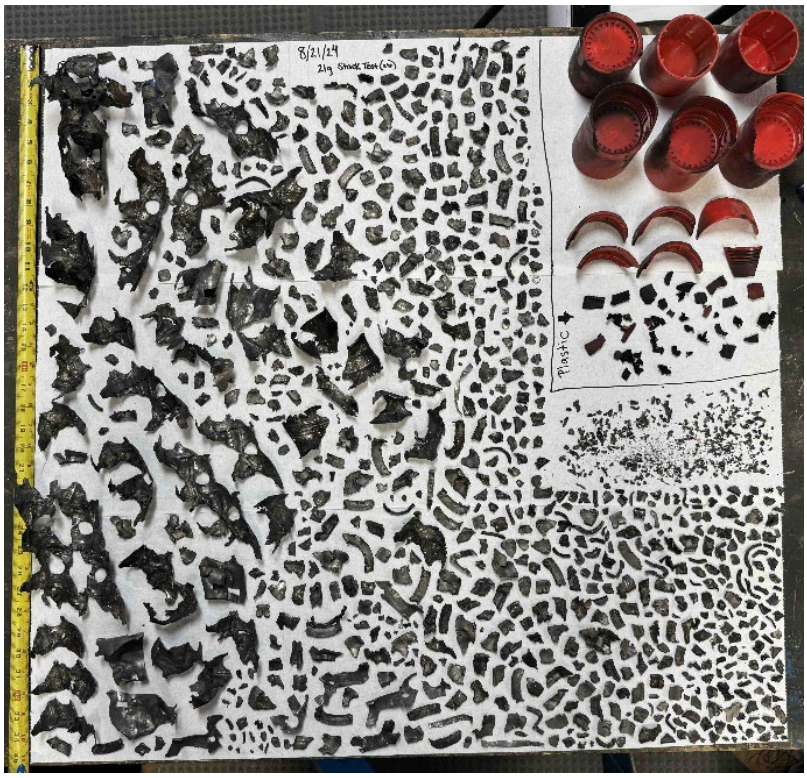


Figure 29: Test 8 Recovered Fragments

In Test 8, a total of 266 fragments above 5 g were recovered during fragment collection and cataloguing. Of these 266 pieces, 150 of them were recovered outside of 100 ft. The farthest of these pieces was found at 393.94 ft, along the 351.71° azimuth. Of the six JPGs used in this test, the bodies of Guns 1, 4, 5, and 6 were recovered outside of 100 ft, while the bodies of Guns 2 and 3 were recovered within 100 ft. The exact range and bearing of each gun's body are listed in Table 13.

Table 13: Test 8 Gun Body Locations

| | Shell 1 | Shell 2 | Shell 3 | Shell 4 | Shell 5 | Shell 6 |
|---|---|---|---|---|---|---|
| **Range (ft)** | 119.07 | 98.02 | 93.89 | 327.76 | 244.49 | 273.77 |
| **Bearing (°)** | 209.81 | 184.62 | 136.20 | 214.48 | 138.20 | 181.45 |

Figure 30 provides a scatter plot depicting the fragment distribution for Test 8 and the complete fragment catalogue for this test is provided in Appendix B: Fragment Catalogues

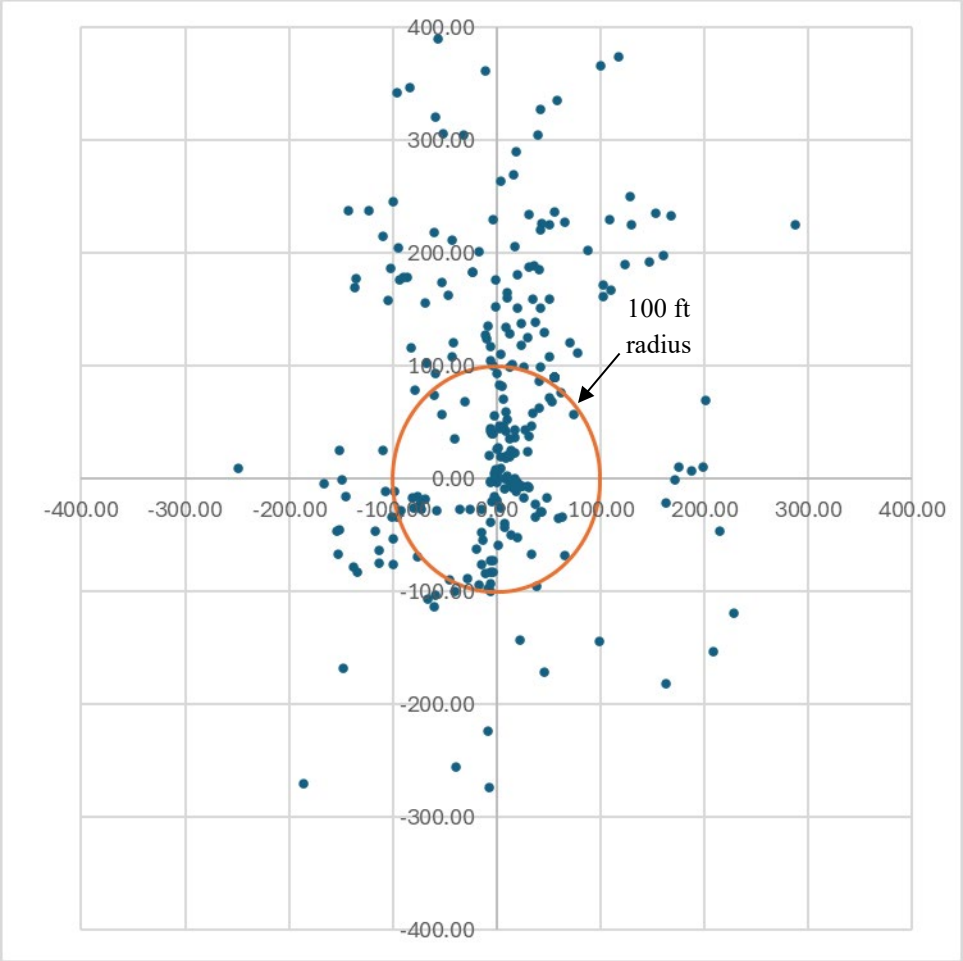


**Figure 30: Test 8 Fragment Scatter Plot**

## 3.3 CREW SIZE ASSESSMENT

As stated in Section 2.5, for this test series a crew of roughly 20 was present for each test. The members of this crew were primarily made up of APT, ATF, IME, and RAM personnel with volunteers from Companies B, C, and D there for some of the tests. The crew was able to recover more than 90% of the mass for each test, other than Test 1 due to the bulkhead never being recovered. Across all tests, the crew had an average recovery rate of roughly 0.48 pieces per manhour. It would be misleading to present the recovery rate of the crew without also providing some context concerning the conditions present at the testing site. While the crew was out at the Company A site, the average temperature every day was around 108°F and so, out of concern for the crew, the time spent out in the field – as well as the pace of the crew while working – had to be limited. Despite wanting to limit the crew's time exposed to the heat, testing could not be initiated too early in the day because the lack of proper lighting would have an impact on the video footage and make it make it harder to find fragments.

# 4.0 Post-Test

The following sections describe the analysis work that was performed after obtaining the results of the JPG test series outlined in Section 3.0.

## 4.1 INSTRUMENTATION RESULT ANALYSIS

The test configurations were recreated in IMESAFR v2.2 utilizing the existing JPG model so that a comparison could be made between the current model and the pressure gauge readings from the tests. It is important to remember that, as stated in Section 1.2, the pressure measurements are largely being used to confirm that the test went as expected. No groundbreaking discoveries were expected to result from this part of the analysis.

In addition to the comparison between the pressure gauge readings and the calculated values, this section also contains the analysis of the video footage from the test series. Upon receiving the video footage, it was uploaded into video analysis software that would allow for the video to be viewed on a frame-by-frame basis. Fragments would then be marked and tracked by the software so that velocity could be calculated. The specific software that was used to analyze the video footage from this test series was a free, open-source, video analysis tool called Tracker 6 [6].

### 4.1.1 Test 1

Figure 31 depicts the comparison between the pressure gauge readings from Test 1 and the predicted pressure values from IMESAFR using the Kingery-Bulmash hemispherical TNT equations. It is important to note that, as stated in Section 1.2, IMESAFR does not currently have directionality implemented for pressure and impulse calculations for JPGs. Therefore, it was not surprising to see that IMESAFR predicted a much higher pressure than what the Western Gauges measured. If pressure data were available for a Northern Gauge at 5 ft, it would have been expected to be significantly closer to what IMESAFR predicted than what the Western Gauge recorded. The most important thing to take away from this comparison is that as the figure approaches the 20 ft mark, the predicted pressure and the actual pressure begin to converge upon one another, showing that the test happened at a scale that was expected.

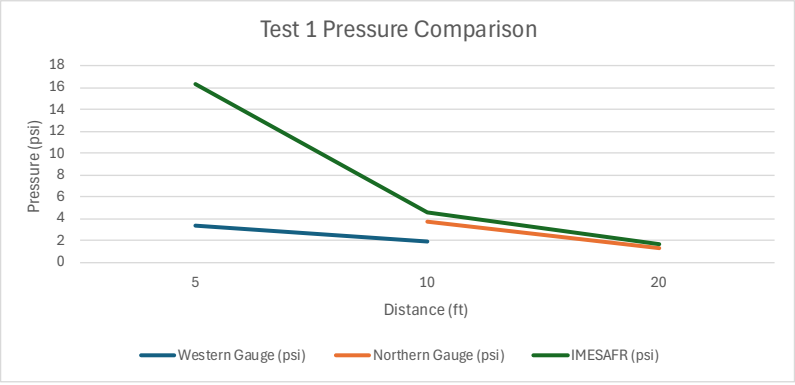


**Figure 31: Test 1 Pressure Comparison**

As stated in Section 3.2.2.1, some preliminary analysis of the video footage from Test 1 was performed by ATF at the test site. This preliminary analysis was only done for the bulkhead since it was a fragment of special interest, and it was determined to be traveling at a speed of 526 ft/s. In addition to the preliminary analysis that was done at the range, the video footage for this test was further analyzed by APT. For Test 1, a total of 18 fragments (not counting the bulkhead) were tracked across all video sources. Of these 18 fragments, the fastest of them was found to be traveling at a speed of 208.26 ft/s, while the slowest one was the gun body which was observed traveling almost perfectly vertical from ground zero with a speed of roughly 22.81 ft/s. The overall average velocity for this test was calculated to be approximately 130.57 ft/s, which, it should be noted, does not include the velocity of the bulkhead. Table 14 contains further details concerning how many fragments were tracked for each video source.

**Table 14: Test 1 Fragment Velocity**

| Footage | Number of Fragments Tracked | Minimum Velocity (ft/s) | Maximum Velocity (ft/s) | Average Velocity (ft/s) |
|---|---|---|---|---|
| **High Speed** | 5 | 22.81 | 208.26 | 151.48 |
| **GoPros** | 11 | 23.1 | 188.12 | 162.78 |
| **Drone** | 2 | 34.19 | 120.69 | 77.44 |

Concerning the observed behavior of the fragments that were tracked, most of the fragments appeared to be tumbling, however the gun body showed some interesting behavior. Specifically, the gun body was observed spinning rapidly or “helicoptering” as it traveled upwards, sending smaller fragments in every direction. Figure 32 depicts a sample of the GoPro footage in the tracking software.

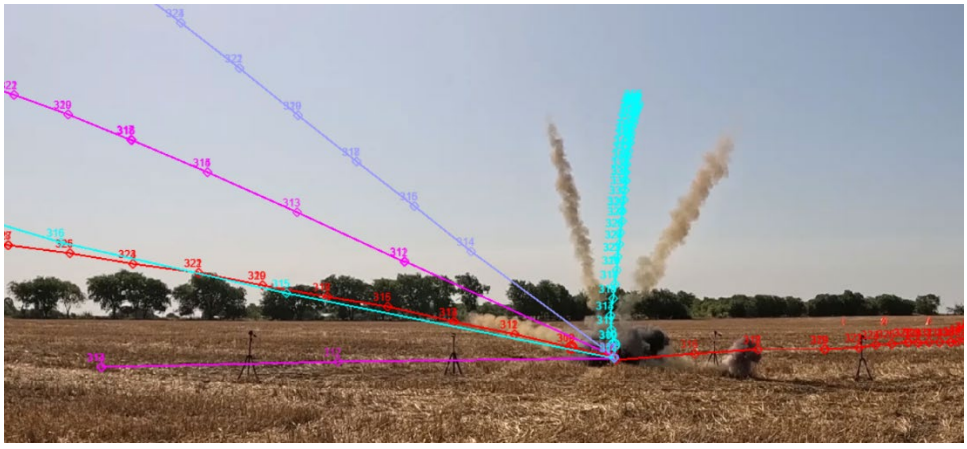

**Figure 32: Test 1 Video Tracking**

### 4.1.2 Test 2

Figure 33 depicts the predicted pressure values from IMESAFR that are nearly the same as those seen in Figure 31. This is because both of these tests, and a number of the other tests, all had the

same NEW. Figure 33 does show that the calculated pressure and the actual pressure at 5 ft are significantly closer to one another as was expected and stated in Section 4.1.1. As predicted, both the actual and the IMEASFR predicted pressure values begin to converge upon one another as the figure approaches the 20 ft mark, showing the test performed as expected.

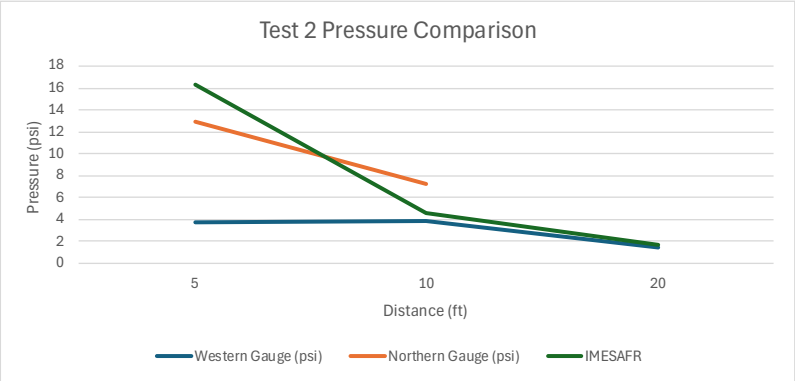


**Figure 33: Test 2 Pressure Comparison**

For Test 2, a total of 12 fragments were tracked across all video sources. Of these 12 fragments, the fastest of them was found to be traveling at a speed of 248.88 ft/s, while the slowest was traveling at a speed of 107.34 ft/s. The overall average velocity was calculated to be approximately 167.92 ft/s. Table 15 contains further details concerning how many fragments were tracked for each video source.

**Table 15: Test 2 Fragment Velocity**

| Footage | Number of Fragments Tracked | Minimum Velocity (ft/s) | Maximum Velocity (ft/s) | Average Velocity (ft/s) |
|---|---|---|---|---|
| **High Speed** | 4 | 181.59 | 226.29 | 187.81 |
| **GoPros** | 6 | 170.5 | 248.88 | 186.07 |
| **Drone** | 2 | 107.34 | 152.42 | 129.88 |

Many of the fragments that were tracked in this test appeared to be tumbling. However, the gun body was observed traveling south with very little tumbling until it impacted the ground around 52 ft away from ground zero and tumbled until it came to a rest around 109 ft away from ground zero. Figure 34 depicts a sample of the GoPro footage in the tracking software.

Figure 34: Test 2 Video Tracking

### 4.1.3 Test 3

Figure 35 shows some unexpected results, specifically the very low pressure reading from the Northern Gauge at 5 ft. While this was strange, it is important to remember that the main concern was at farther distances, and it is clear to see that the predicted pressure is quickly converging upon the actual outside of 5 ft.

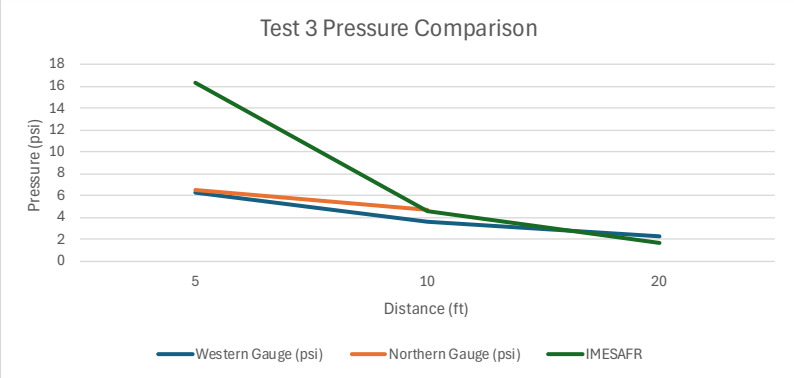


Figure 35: Test 3 Pressure Comparison

For Test 3, a total of 14 fragments were tracked across all video sources. Of these 14 fragments, the fastest of them was found to be traveling at a speed of 283.8 ft/s, while the slowest fragment was traveling at a speed of 41.25 ft/s. The overall average velocity for this test was calculated to be approximately 127.74 ft/s. Table 16 contains further details concerning how many fragments were tracked for each video source.

Table 16: Test 3 Fragment Velocity

| Footage | Number of Fragments Tracked | Minimum Velocity (ft/s) | Maximum Velocity (ft/s) | Average Velocity (ft/s) |
|---|---|---|---|---|
| **High Speed** | 3 | 51.56 | 115.38 | 93.06 |
| **GoPros** | 8 | 41.25 | 283.8 | 166.4 |
| **Drone** | 3 | 77.53 | 155.86 | 123.77 |

Once again, most of the fragments that were observed in this test appeared to be tumbling. The gun body in this test could not be tracked. The gun body stayed very close to ground zero (it was recovered about 2 ft away) and was largely obscured by the gas byproducts and dust from the event. However, the drone footage provides a brief glimpse of how the gun body was behaving. It can be seen spinning in a similar manner to the gun body from Test 1; however, it does not achieve anywhere near the same height. Figure 36 depicts a sample of the GoPro footage in the tracking software.

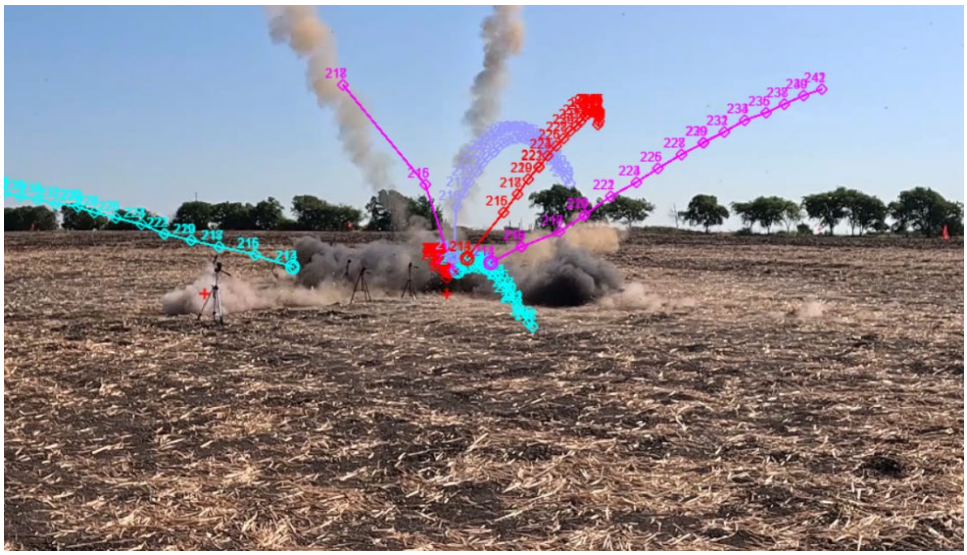

Figure 36: Test 3 Video Tracking

### 4.1.4 Test 4

Figure 37 shows some results that are more in line with expectations than those seen in Figure 35. While the predicted pressure is still higher than the actual, it was expected due to the impact of directionality and close-in effects. Once again, what was most important was that the predicted pressure and the actual pressure appeared to begin converging upon one another around the 20 ft mark.

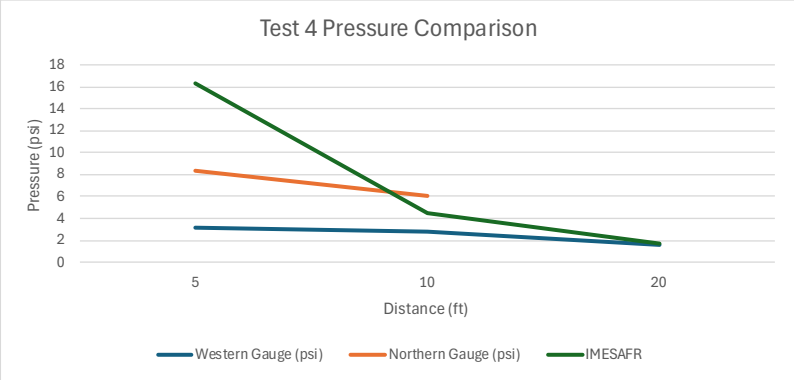


**Figure 37: Test 4 Pressure Comparison**

Similar to Test 3, in Test 4, a total of 14 fragments were tracked across all video sources. Of these 14 fragments, the fastest of them was found to be traveling with a speed of 307.69 ft/s while the slowest fragment was found to be the gun body which was observed traveling with a speed of 52.53 ft/s. The overall average velocity for this test was calculated to be approximately 179.72 ft/s. Table 17 contains further details concerning how many fragments were tracked for each video source.

**Table 17: Test 4 Fragment Velocity**

| Footage | Number of Fragments Tracked | Minimum Velocity (ft/s) | Maximum Velocity (ft/s) | Average Velocity (ft/s) |
|---|---|---|---|---|
| **High Speed** | 4 | 52.53 | 292.16 | 169.4 |
| **GoPros** | 8 | 66.2 | 307.69 | 197.87 |
| **Drone** | 2 | 82.5 | 261.3 | 171.9 |

As with the previous tests, most fragments appeared to be tumbling through the air. The gun body was found traveling south slowly spinning vertically in a “tomahawk” fashion. The gun body then impacted the ground and bounced several times, tumbling more erratically each time. Figure 38 depicts a sample of the GoPro footage for this test in the tracking software.

Figure 38: Test 4 Video Tracking

### 4.1.5 Test 5

Figure 39 is similar to Figure 37; the recorded pressure from the close-in Northern Gauge was low compared to the predicted pressure but was not anything concerning. Once again, the expected behavior can be seen at the 20 ft range; the predicted and the actual lines appear to start converging.

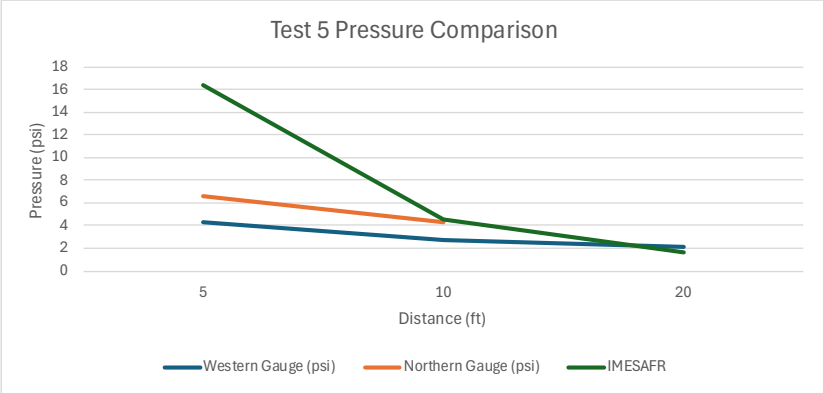


Figure 39: Test 5 Pressure Comparison

In Test 5, a total of 12 fragments were tracked across all video sources. Of the 12 fragments that were tracked the fastest was found to be traveling with a speed of 288.57 ft/s while the slowest fragment was traveling with a speed of 93.23 ft/s. The overall average velocity for this test was calculated to be approximately 187.94 ft/s. Table 18 contains further details concerning how many fragments were tracked for each video source. It should be noted that, despite several attempts, the tracking software was unable to load the drone footage from this test, which resulted in the footage being unable to be properly analyzed.

Table 18: Test 5 Fragment Velocity

| Footage | Number of Fragments Tracked | Minimum Velocity (ft/s) | Maximum Velocity (ft/s) | Average Velocity (ft/s) |
|---|---|---|---|---|
| **High Speed** | 5 | 159.6 | 276.32 | 201.06 |
| **GoPros** | 7 | 93.23 | 288.57 | 174.82 |
| **Drone** | n/a | n/a | n/a | n/a |

Once again, the majority of fragments in this test appeared to be tumbling. The gun body was observed tumbling as it traveled south, even before it first impacted the ground. Figure 40 depicts a sample of the GoPro footage in the tracking software.

Figure 40: Test 5 Video Tracking

### 4.1.6 Test 6

Figure 41 shows some interesting results for Test 6. Specifically, it can be seen that the actual pressure reading for the Western Gauge at 10 ft was higher than both the predicted pressure and the pressure measured by the Northern Gauge. It is important to remember that Test 6 not only had a higher NEW per charge than the others but was also the test in which the gun body broke apart into three pieces. Therefore, the gun may have failed to provide any directionality to the pressure wave. Additionally, as was stated in Section 3.2.6.2, this test had most of its fragments recovered in the west, so it is very likely that a fragment from the gun perforator impacted the pressure gauge resulting in the spike shown. Looking at the 20 ft mark it is clear that despite this unexpected behavior, the predicted and the actual lines still appear to start converging.

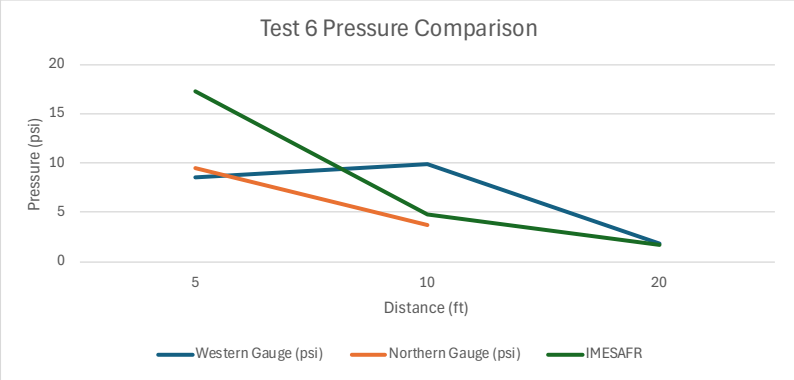


**Figure 41: Test 6 Pressure Comparison**

Due to unforeseen circumstances, high-speed and GoPro video footage are unavailable for Test 6. However, the drone footage was still available and could be used for some analysis instead. In the drone footage, a total of 5 fragments were tracked, the fastest of which was found to have a speed of 203.03 ft/s, while the slowest had a speed of 56.4 ft/s. Given that only the drone footage was available for analysis for this test it is likely that the calculated average velocity of 119.45 ft/s is underestimating the actual velocity. This is because the available drone footage for this test does not provide the ideal point of view or level of fidelity. Therefore, it is likely that some fast-moving fragments were not able to be identified and tracked in the video. Table 19 contains all the details of the fragment velocity that was already stated but is provided again for consistency.

**Table 19: Test 6 Fragment Velocity**

| Footage | Number of Fragments Tracked | Minimum Velocity (ft/s) | Maximum Velocity (ft/s) | Average Velocity (ft/s) |
|---|---|---|---|---|
| **High Speed** | n/a | n/a | n/a | n/a |
| **GoPros** | n/a | n/a | n/a | n/a |
| **Drone** | 5 | 56.4 | 203.03 | 119.45 |

As was stated previously, the drone footage for this test does not provide a high level of fidelity so it is difficult to say for certain how the majority of fragments were behaving. However, given the observed trend in the previous tests and the behavior of the fragments that were able to be properly observed, it is likely that the majority of fragments were tumbling. The gun body in this test broke apart into three pieces, which were observed to be tumbling as well. Figure 42 depicts the drone footage in the tracking software.

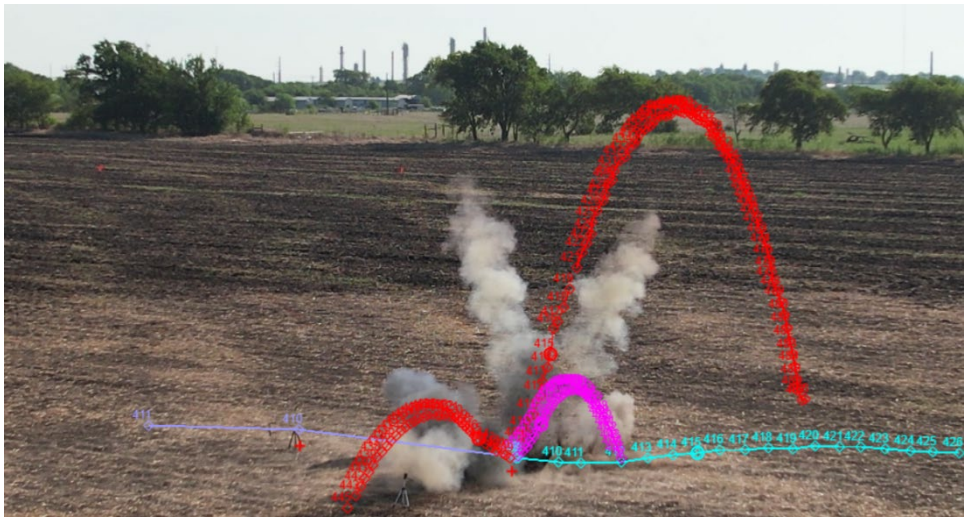

Figure 42: Test 6 Video Tracking

### 4.1.7 Test 7

Figure 43 and Test 7 overall are quite interesting. In this test the pressure readings from the Northern Gauges were always less than the readings from the Western Gauges. While this would have normally been concerning, it is important to remember that this test was done with the JPG in a vertical configuration. Therefore, the gun directed the blast wave into the ground and into the air rather than towards the Northern Gauges. Despite this, the pressure comparison shows that as the blast wave approaches the 20 ft gauge the predicted and the actual lines appear to start converging.

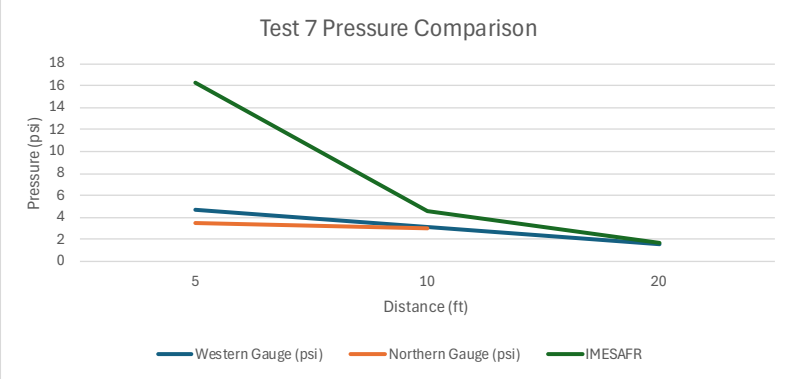


Figure 43: Test 7 Pressure Comparison

Thankfully, despite the unforeseen circumstances mentioned in Section 4.1.6, some high-speed video footage was available for Test 7; however, the GoPro video footage for this test remained unavailable. In Test 7, only six fragments were tracked across the available video sources. The first reason why so few fragments were tracked was that the drone footage for this test had the same fidelity problem as stated previously in Test 6. Furthermore, since this test had the JPG vertically oriented, most of the fragments went upwards and could not be effectively tracked in

the high-speed footage due to the glare from the sunlight. The fastest fragment that was tracked was observed to have a speed of 180.44 ft/s, while the slowest had a speed of 65.72 ft/s. The overall average velocity for this test was calculated to be approximately 121.25 ft/s. Table 20 contains further details concerning how many fragments were tracked for each video source.

**Table 20: Test 7 Fragment Velocity**

| Footage | Number of Fragments Tracked | Minimum Velocity (ft/s) | Maximum Velocity (ft/s) | Average Velocity (ft/s) |
|---|---|---|---|---|
| **High Speed** | 3 | 65.72 | 180.44 | 130.99 |
| **GoPros** | n/a | n/a | n/a | n/a |
| **Drone** | 3 | 82.52 | 160.2 | 111.51 |

The fragments that were tracked for this test all appeared to be tumbling, which is in line with what had been observed in previous tests. The gun body could not be tracked for this test. This is because this test had the gun in a vertical orientation, which resulted in the gun body being forced downwards into the pallet during detonation and embedding itself there. Therefore, velocity could not be determined for the gun body. Figure 44 depicts the footage from the drone in the tracking software and shows just how high some of the fragments were observed going in this test.

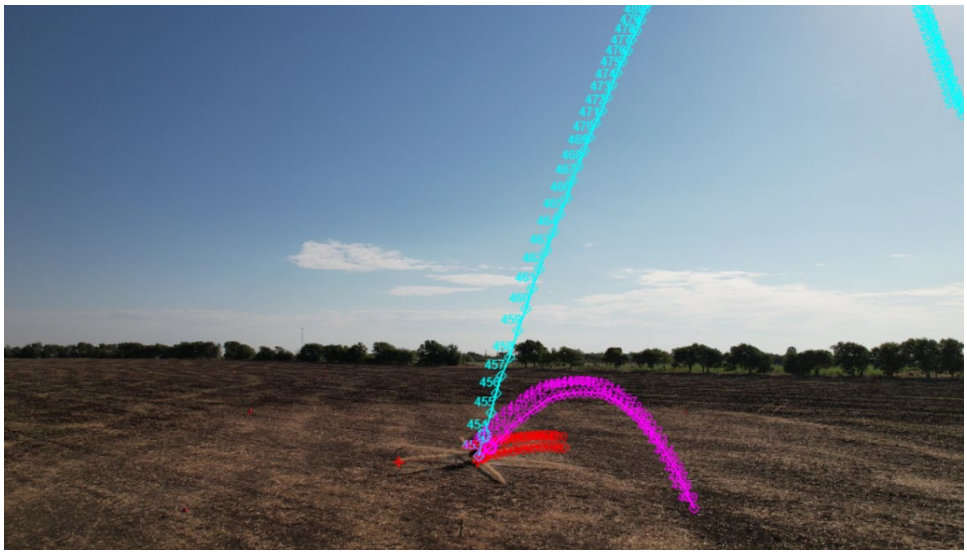

**Figure 44: Test 7 Video Tracking**

### 4.1.8 Test 8

Figure 45 shows some results that are fairly standard given what has been observed in the previous tests. Given that this test was done with multiple JPGs there were some concerns that unexpected behavior would be an issue. The only major difference between this figure and the others is the scale that this figure is working with; since this test did have six times the NEW of

most of the tests, the pressure values were much higher across the board. However, it can still be seen that as the 20 ft mark is approached the predicted and the actual lines appear to start converging.

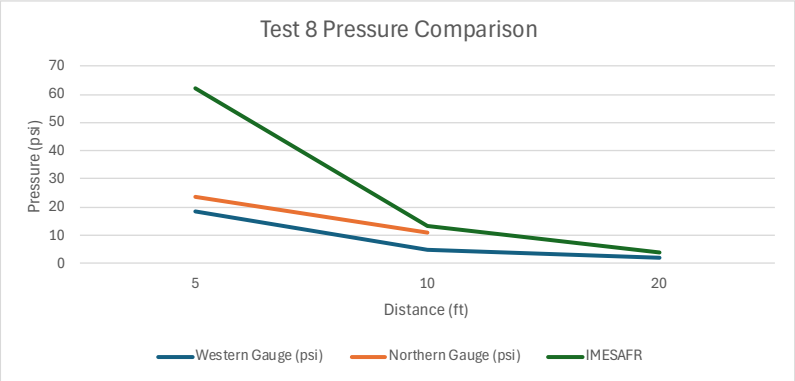


**Figure 45: Test 8 Pressure Comparison**

Like Test 7, Test 8 thankfully had some high-speed footage available for analysis despite unforeseen circumstances, and the GoPro video footage for this test also remained unavailable. In Test 8, a total of 20 fragments were tracked across the available video sources. The fastest of these 20 fragments was found to have a velocity of 318.62 ft/s, while the slowest fragment was found to be one of the gun bodies of the JPGs used in this test and had a velocity of 97.19 ft/s. The overall average velocity for this test was calculated to be approximately 170.82 ft/s. Table 21 contains further details concerning how many fragments were tracked for each video source.

**Table 21: Test 8 Fragment Velocity**

| Footage | Number of Fragments Tracked | Minimum Velocity (ft/s) | Maximum Velocity (ft/s) | Average Velocity (ft/s) |
|---|---|---|---|---|
| **High Speed** | 9 | 112.87 | 318.62 | 168.56 |
| **GoPros** | n/a | n/a | n/a | n/a |
| **Drone** | 11 | 97.19 | 268.49 | 173.07 |

Test 8 continues the trend observed in the previous tests and all the fragments that were tracked in this test appeared to be tumbling. The gun bodies of the JPGs used in this test were observed behaving in one of two ways. Firstly, the gun bodies near the top of the stack were observed to have been launched at high angles, while spinning horizontally or “helicoptering” at differing speeds. Secondly, the gun bodies near the bottom of the stack were launched almost perfectly parallel to the ground with very shallow vertical launch angles; and were observed tumbling and impacting the ground several times. Figure 46 depicts the high-speed camera footage in the tracking software.

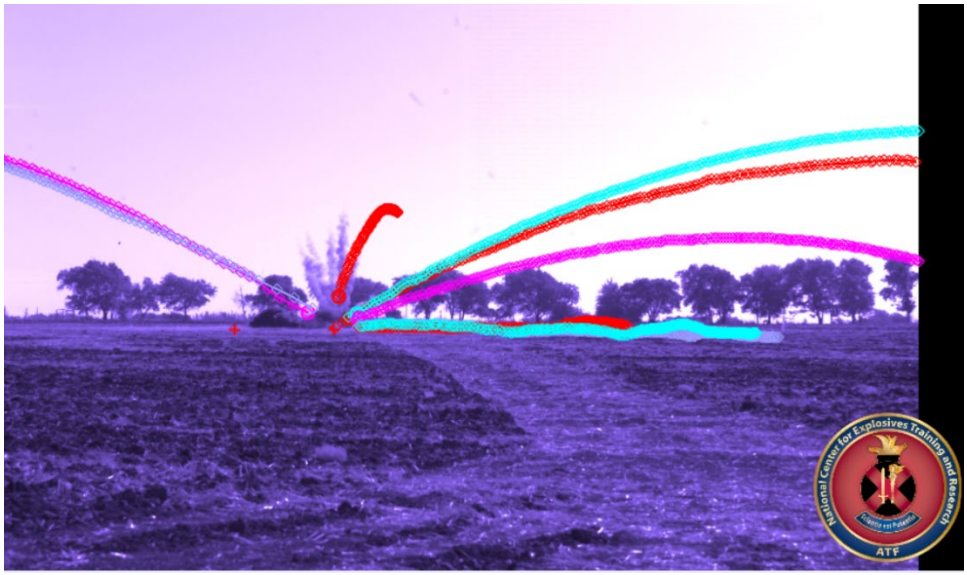

Figure 46: Test 8 Video Tracking

## 4.2 DEBRIS REDUCTION AND ANALYSIS

The ultimate goal of the debris reduction and analysis is the creation of a new debris probability density function backed up by empirical test data that could be implemented into the IMESAFR model for JPGs. The debris probability function has two components: the downrange function, which is dependent upon distance, and the cross-range function, which is dependent on the angle. Therefore, the fragment catalogues for this test series were analyzed to create the figures in this section that depict the fragment density by distance and azimuth.

Another goal of the debris reduction and analysis was the determination of the mass bin distribution for each test. The mass bin system is a method of categorizing pieces of debris or fragmentation of similar size and mass into one of eleven bins, ten of which are used for debris modeling (the eleventh is only used to assess conservation of mass). This makes predicting the potential behavior and calculating the impact kinetic energy of these pieces simpler since it can be done for each mass bin rather than for every possible size and mass. Rev 2 of DDESB TP-21 [5] provides a more in-depth description of the mass bin system and provides the bounds of the mass bins. The relevant mass bin information for this test series that was taken from TP-21 is summarized in Table 22.

Table 22: TP-21 Mass Bin Limits for Steel

| | Bin 1 | Bin 2 | Bin 3 | Bin 4 | Bin 5 | Bin 6 | Bin 7 | Bin 8 | Bin 9 | Bin 10 | Bin G |
|---|---|---|---|---|---|---|---|---|---|---|---|
| **Upper Mass (g)** | n/a | 11,800 | 4,540 | 2,040 | 820 | 360 | 140 | 64 | 27 | 11 | <6 |
| **Lower Mass (g)** | >11,800 | 4,540 | 2,040 | 820 | 360 | 140 | 64 | 27 | 11 | 6 | n/a |

### 4.2.1 Test 1

Figure 47 depicts the fragment distribution by distance for Test 1 and followed a fairly predictable trend with most of the fragments being found close to ground zero while the amplitude gradually decreases as distance increases.

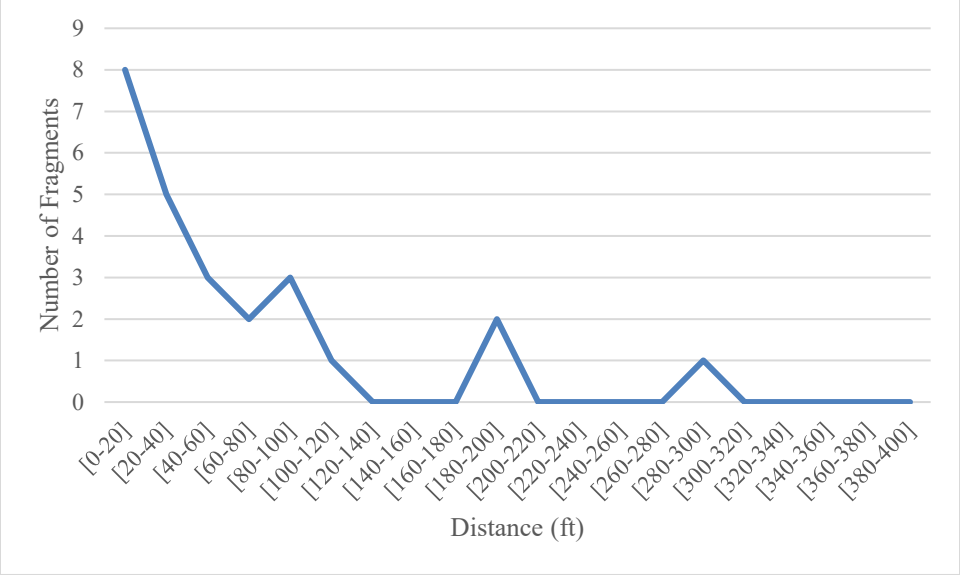


Figure 47: Test 1 Fragments by Distance

Figure 48 and Figure 49 depict the fragment distribution by azimuth for Test 1. These figures are broken down into 5° bands similar to the search grid that was used for this test. In Figure 48, only the fragments that were above 5 g and that made it outside of the 100 ft range are depicted. For this test, only a total of four fragments that made it past 100 ft were recovered and two of them were recovered near the North-South axis. Figure 49, however, depicts all the fragments that were above 5 g regardless of their distance and shows a much more varied distribution for the fragments when considering the fragments within 100 ft, with most being found off the North-South axis. In total, only 20% of the fragments recovered in this test were found with ±10° of the North-South axis, which was lower than expected. The shaded areas in these figures represent the azimuths where most fragments were expected to land: 0°±10° and 180°±10°.

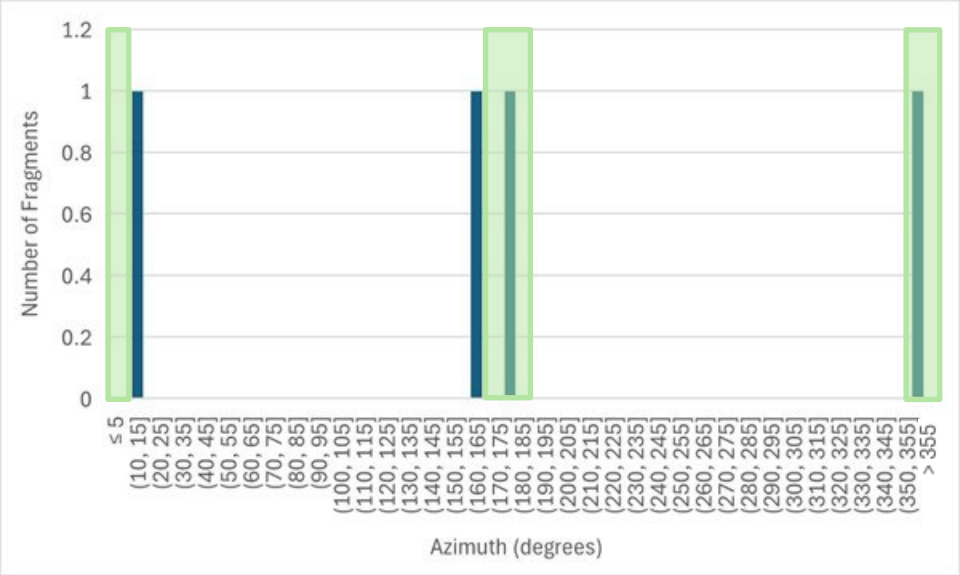


**Figure 48: Test 1 Fragments by Azimuth Outside 100 ft**

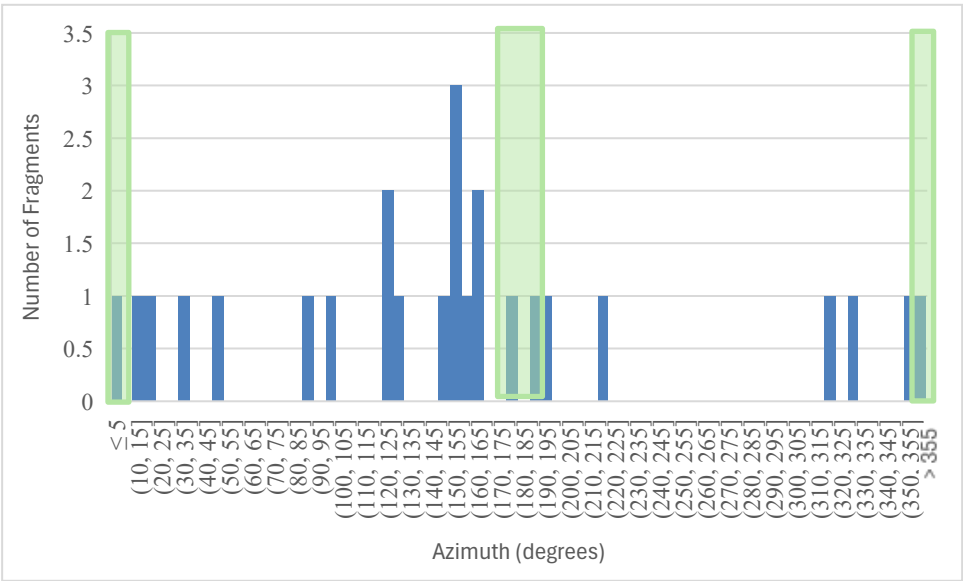


**Figure 49: Test 1 Fragments by Azimuth**

As displayed in Figure 50, in Test 1 the vast majority of the fragments were found to be in Mass Bin 10, followed by Bins 9 and G. During fragment collection, two fairly large pieces were recovered and are shown in Figure 7; these pieces are the Bin 6 entries. The sole fragment shown in Bin 2 was the gun body. It should be noted that if the bulkhead for this test had been recovered it would have been in Mass Bin 5.

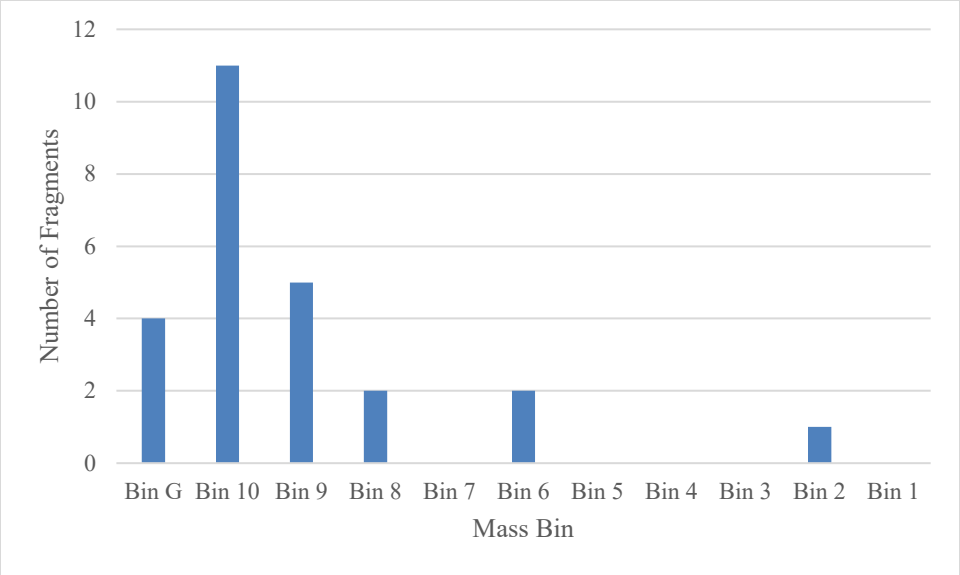


**Figure 50: Test 1 Fragments per Mass Bin**

### 4.2.2 Test 2

Figure 51 shows that unlike Test 1, which had a fairly predictable fragment distribution by distance, in Test 2 there were actually very few fragments close to ground zero. As stated in Section 3.2.2.2, most of the fragments for this test, 21 to be exact, were recovered beyond 100 ft. Figure 51 provides a more detailed look at the results and shows how a large number of the fragments were only slightly outside the 100 ft radius and made it to the 100-120 ft range.

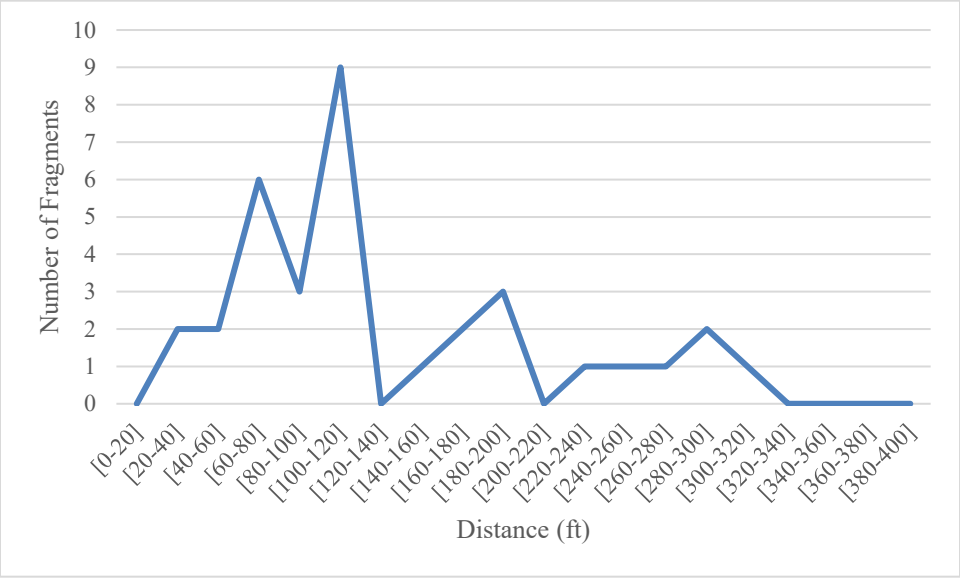


**Figure 51: Test 2 Fragments by Distance**

Figure 52 and Figure 53 are depicting the fragment distribution by radial azimuth for Test 2. In Figure 52, the expected trend is depicted, with all the fragments being located on or near the

North-South axis. Figure 53 does show a slightly more varied fragment distribution, but many of the fragments in this test were still focused along the North-South axis, even when including fragments within 100 ft. To be exact, in this test 44.12% of all fragments above 5 g were found within ±10° of the North-South axis, which was much more in line with expectations. It should be noted that the fragments by azimuth were adjusted to account for the 5° offset that was present in this test. The shaded areas in these figures represent the azimuths where most fragments were expected to land: 0°±10° and 180°±10°.

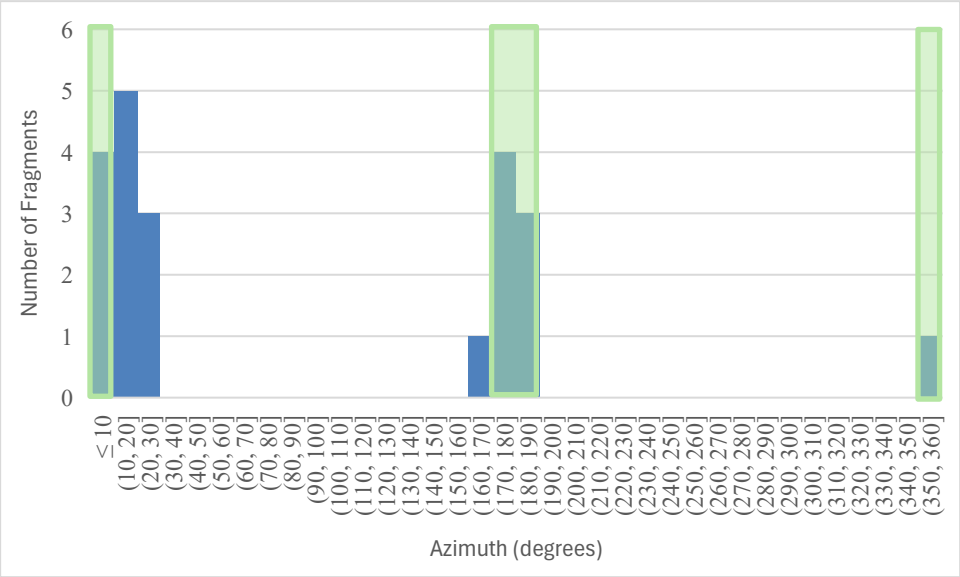


**Figure 52: Test 2 Fragments by Azimuth Outside 100 ft**

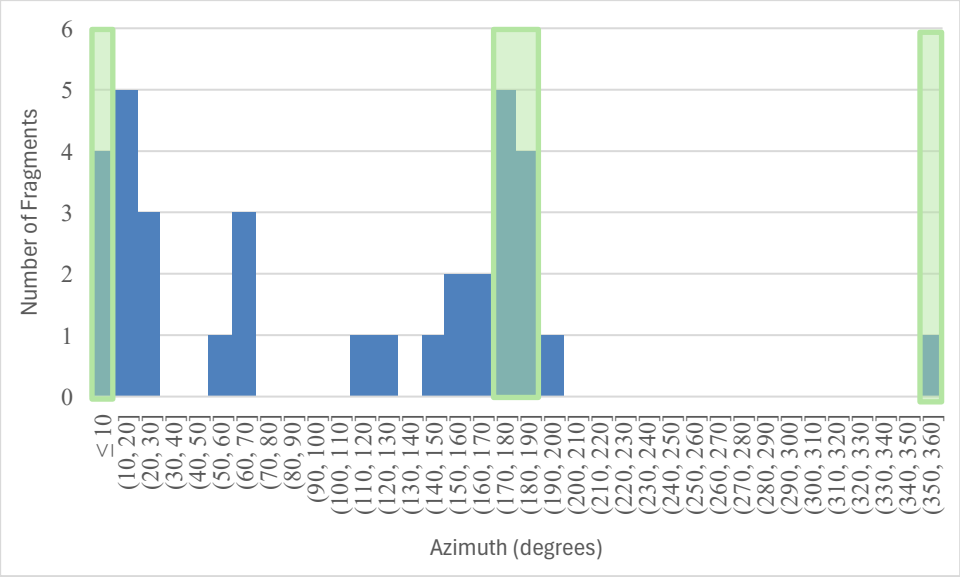


**Figure 53: Test 2 Fragments by Azimuth**

Figure 54 is the mass bin breakdown for Test 2. In this test, Bin 10 still contained the most fragments overall, but it was a much closer distribution between Bin G and Bin 10. Unlike Test 1, there were no fragments recovered that were larger than Bin 8. Similar to Test 1 however, the gun body for this test also made up the sole entry for Mass Bin 2.

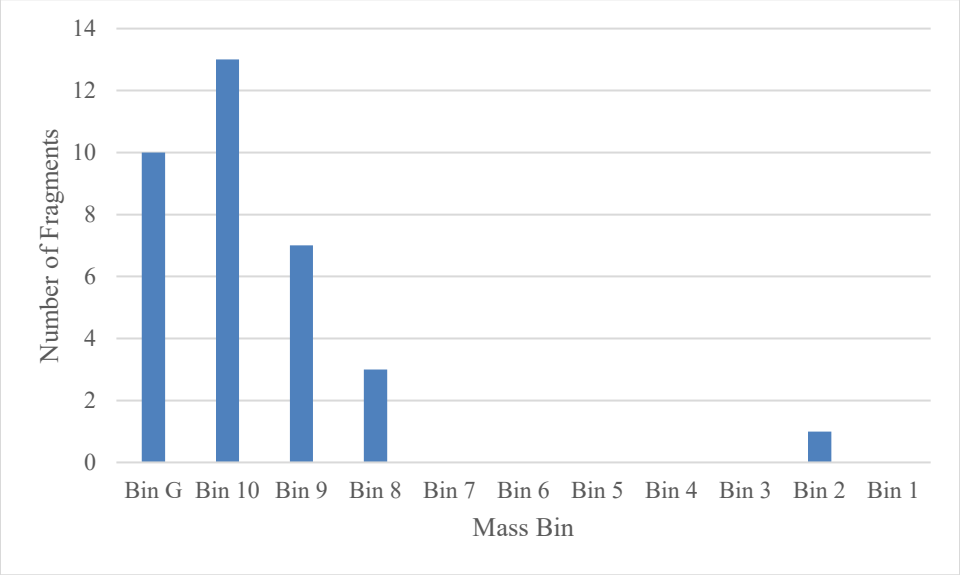


**Figure 54: Test 2 Fragments per Mass Bin**

### 4.2.3 Test 3

Figure 55 shows the results of Test 3, which demonstrate a return to the expected trend for the fragment distribution by distance. It was already stated in Section 3.2.3.2 that 32 of the 51 fragments that were recovered were found within 100 ft, but looking at Figure 55 shows that most the fragments were found even closer to ground zero and were recovered within 40 ft.

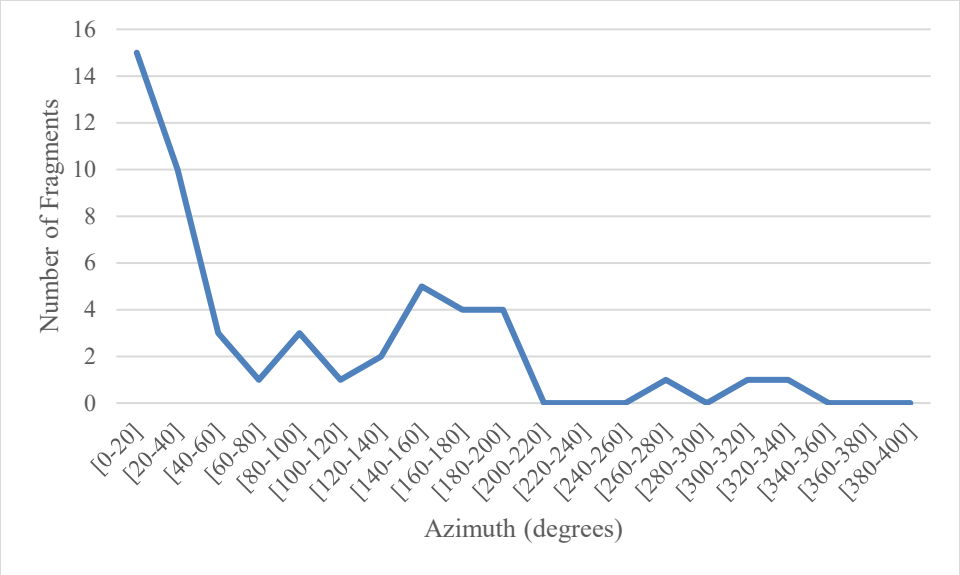


**Figure 55: Test 3 Fragments by Distance**

Figure 56 and Figure 57 depict the fragment distribution by radial azimuth for Test 3. Figure 56 shows that the fragments past 100 ft were primarily found where they were expected to be, with a large amount being recovered within the 0° - 10° band. In Figure 57, the fragment distribution became significantly more varied when considering fragments inside 100 ft, with the 220° - 230° band now containing the majority. In Test 3 a total of 33.34% of all fragments were recovered within ±10° of the North-South axis. The shaded areas in these figures represent the azimuths where most fragments were expected to land: 0°±10° and 180°±10°.

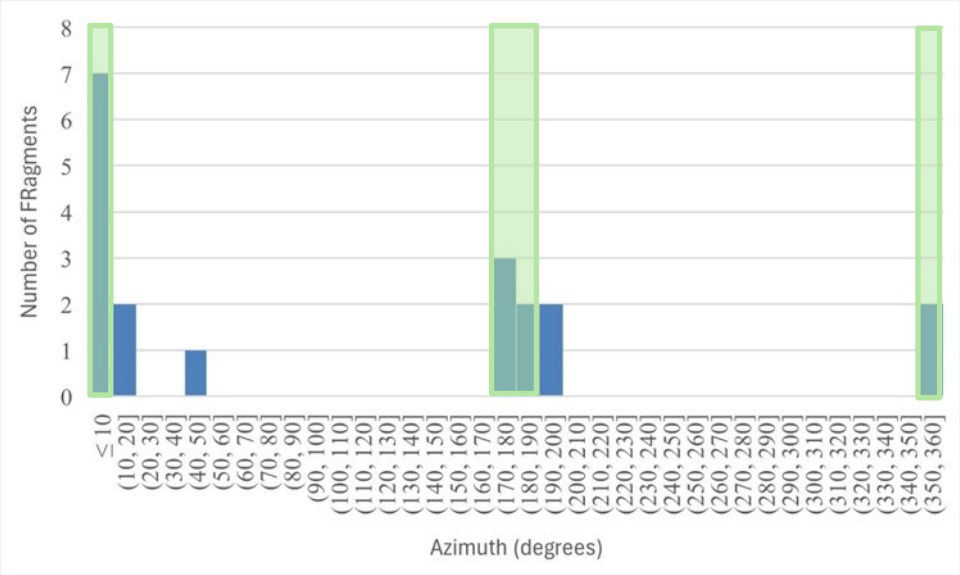


**Figure 56: Test 3 Fragments by Azimuth Outside 100 ft**

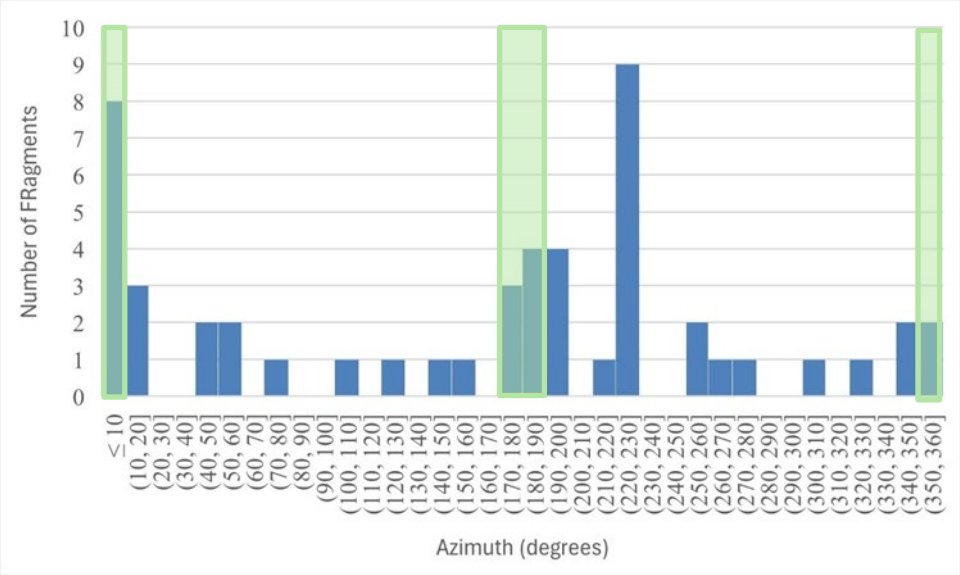


**Figure 57: Test 3 Fragments by Azimuth**

Figure 58 shows the mass bin breakdown for Test 3 and shows that Bin 10 had the most fragments, as in the previous tests. Bins G and 9 contained similar numbers of fragments in this test. This is the first test in which there was an entry in Mass Bin 7. Once again it can be seen that some larger fragments were recovered, making up the Bin 6 entries, while the gun body itself is still the sole entry for Mass Bin 2.

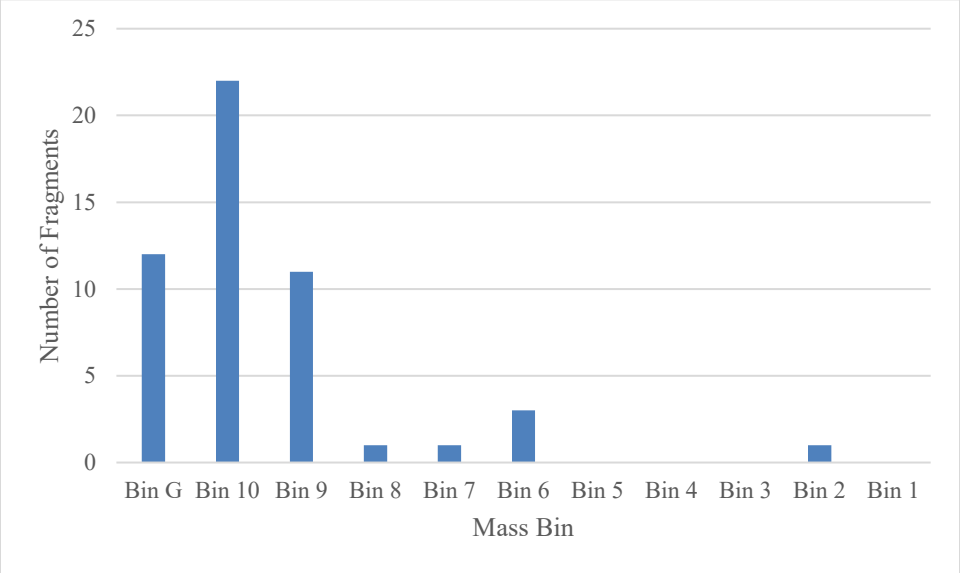


**Figure 58: Test 3 Fragments per Mass Bin**

### 4.2.4 Test 4

Figure 59 depicts the results of Test 4 and was quite similar to Figure 55 (Test 3) in its general shape and trends. In both figures, the number of fragments was generally decreasing from 0 – 80 ft, followed by some spikes around the same distances. Furthermore, it was stated in Section 3.2.4.2 that 28 of the 44 pieces that were recovered were found within 100 ft, which was close to the numbers from Test 3 as well.

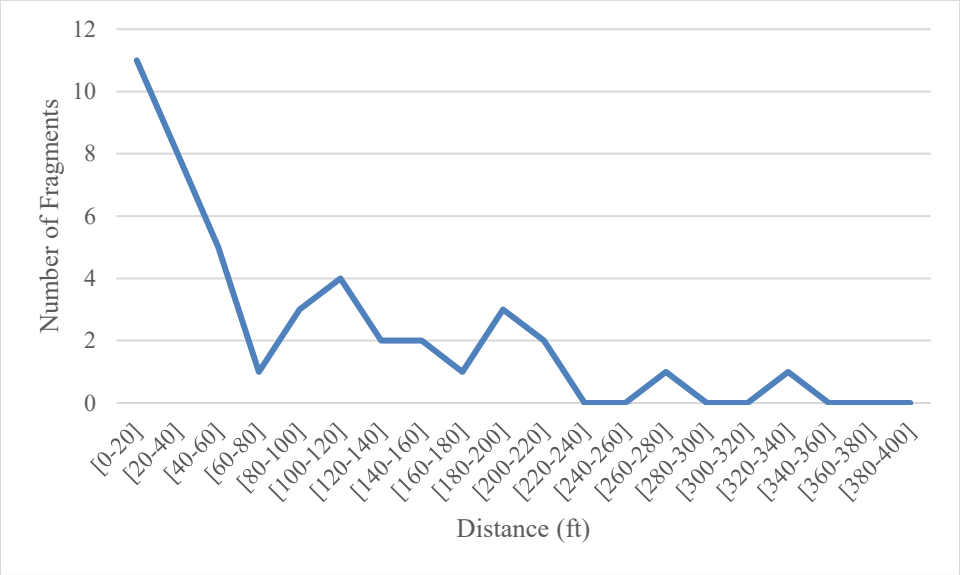


**Figure 59: Test 4 Fragments by Distance**

Figure 60 and Figure 61 depict the fragment distribution by radial azimuth for Test 4. Figure 60 shows some interesting results, namely that outside 100 ft, fragments were only found near the North axis with none recovered near the South axis. Moving on, Figure 61 shows that some fragments within 100 ft were recovered near or on the South axis, but the majority were still focused on the north, with some entries on the diagonals. In total, 38.63% of all fragments were recovered within ±10° of the North-South axis. Breaking that number down shows that 36.36% was recovered within ±10° of the North axis, while only 2.27% was recovered within ±10° of the South axis. The shaded areas in these figures represent the azimuths where most fragments were expected to land: 0°±10° and 180°±10°.

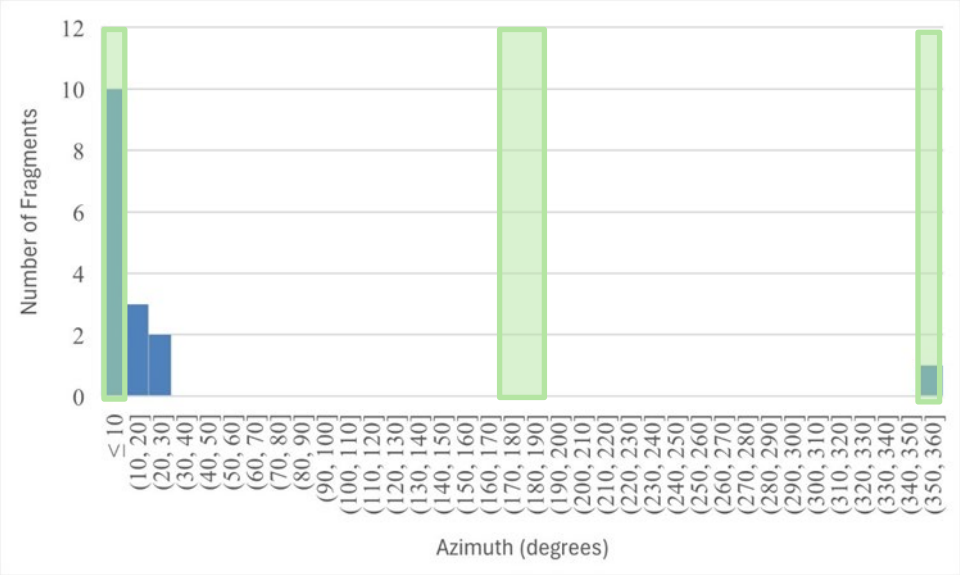


Figure 60: Test 4 Fragments by Azimuth Outside 100 ft

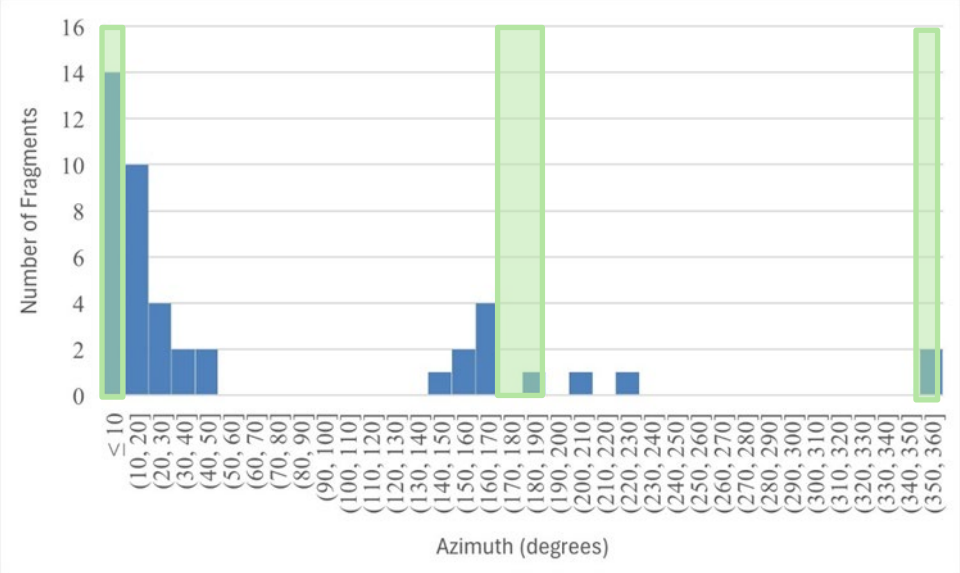


Figure 61: Test 4 Fragments by Azimuth

Figure 62 shows the mass bin breakdown for Test 4 and, as has come to be expected, mass bin 10 still contained the majority of fragments. For this test, Bins G and 9 contained the exact same number of entries while, for the first time, Bin 8 did not contain any entries. For this test the gun's body was not included in Bin 2, as it was large enough to qualify for Mass Bin 1.

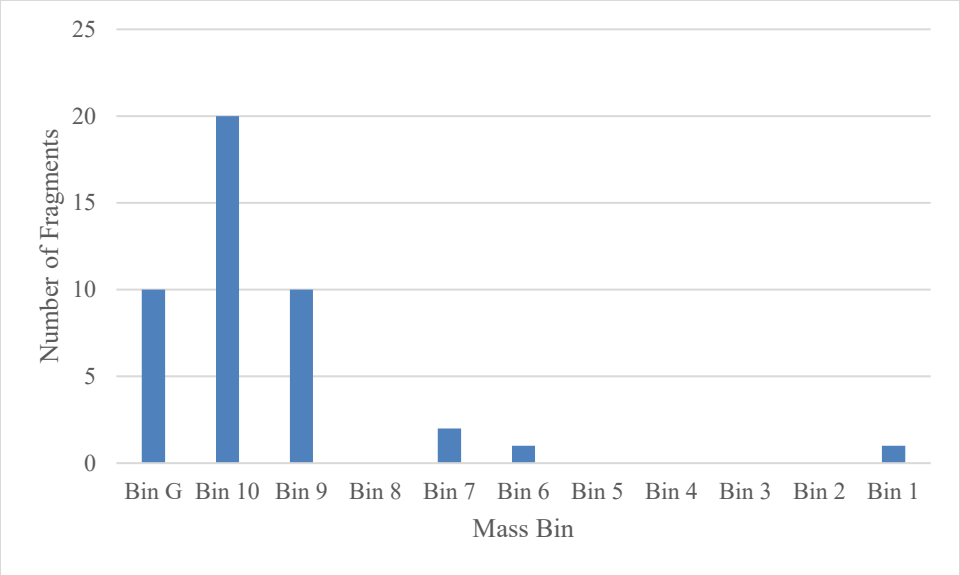


**Figure 62: Test 4 Fragments per Mass Bin**

### 4.2.5 Test 5

Similar to Figure 51 for Test 2, Figure 63 shows a fragment distribution by distance for Test 5 that had its peak downrange from ground zero. However, unlike Test 2, which had most of its fragments outside of 100 ft, Section 3.2.5.2 indicates that only 16 out of 57 fragments for Test 5 were found outside of 100 ft. The 41 pieces found within 100 ft were primarily focused around 40 – 60 ft.

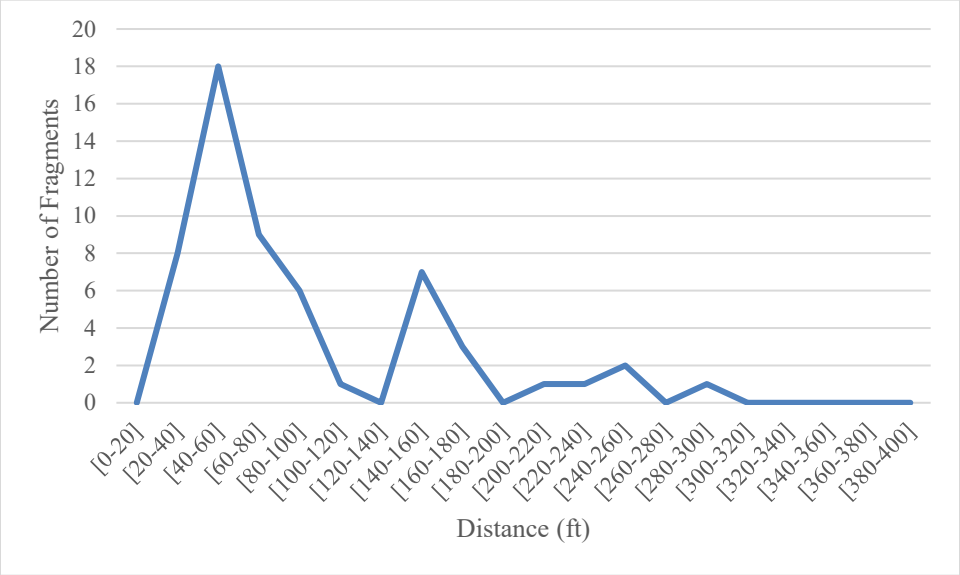


**Figure 63: Test 5 Fragments by Distance**

Figure 64 and Figure 65 depict the fragment distribution by radial azimuth for Test 5. Figure 64 is somewhat similar to Figure 59 (Test 4) in that the majority of the fragments past 100 ft were focused in the 0° - 10° band and nearly no fragments were found on or near the South axis. Figure 65 shows a slightly more varied fragment distribution, but it very clearly was still focused near the North axis with very few entries near the South axis, even when considering fragments within 100 ft. In total, 26.31% of all fragments were recovered within ±10° of the North-South axis. However, much like Test 4, when that number is broken down it shows that the percentage of fragments within ±10° of the North axis was significantly larger than the percentage within ±10° of the South axis. Specifically, 21.05% of fragments were recovered within ±10° of the North axis, while only 5.26% of fragments were recovered within ±10° of the South axis. The shaded areas in these figures represent the azimuths where most fragments were expected to land: 0°±10° and 180°±10°.

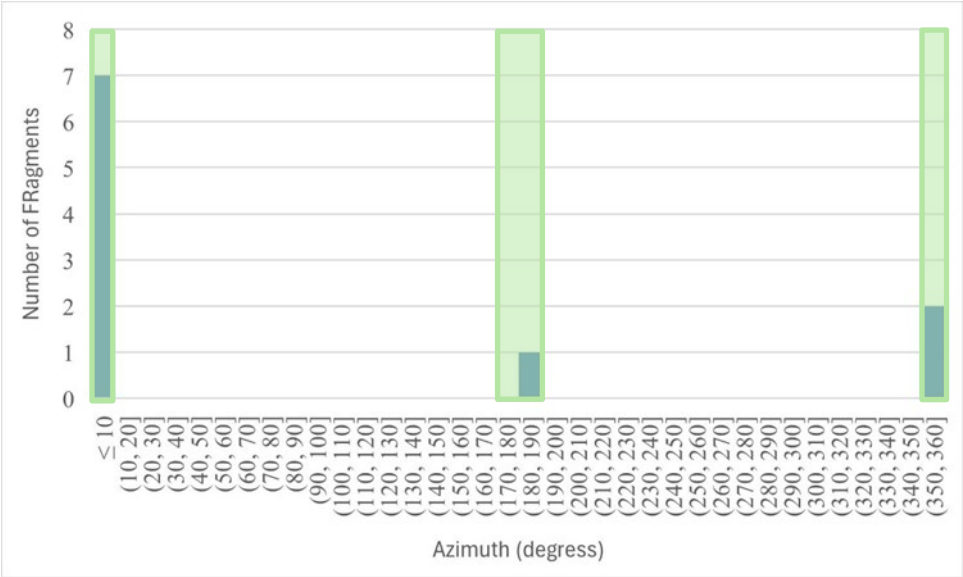


**Figure 64: Test 5 Fragments by Azimuth Outside 100 ft**

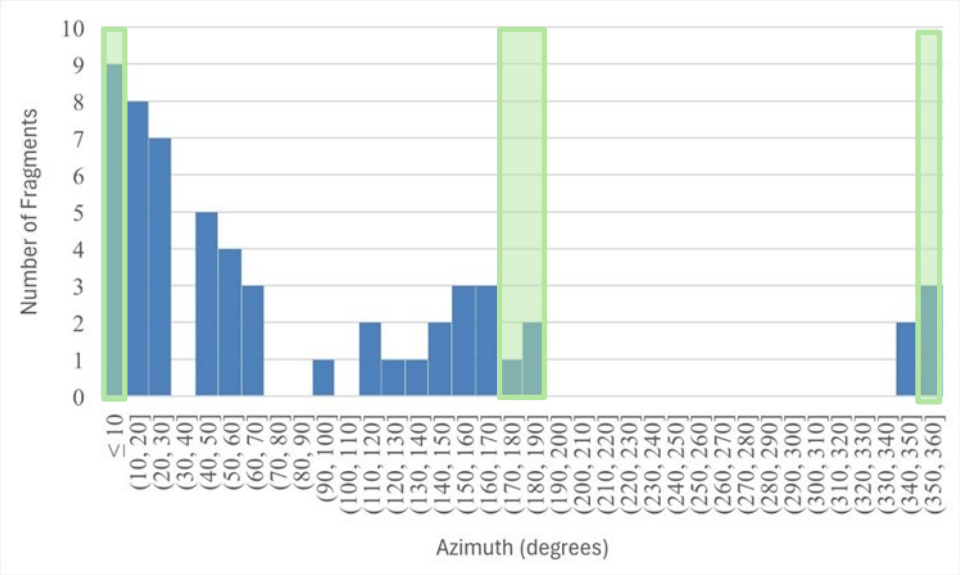


**Figure 65: Test 5 Fragments by Azimuth**

Figure 66 shows the mass bin breakdown for Test 5 and as expected Mass Bin 10 still contained the most fragments. Test 5 had more fragments in Mass Bin 10 than any of the previous tests. Mass Bin G contained the second-most number of fragments, followed by Bin 9, which was not out of the ordinary for this test series. As with all previous tests other than Test 4, the gun's body for this test was the sole entry for Mass Bin 2.

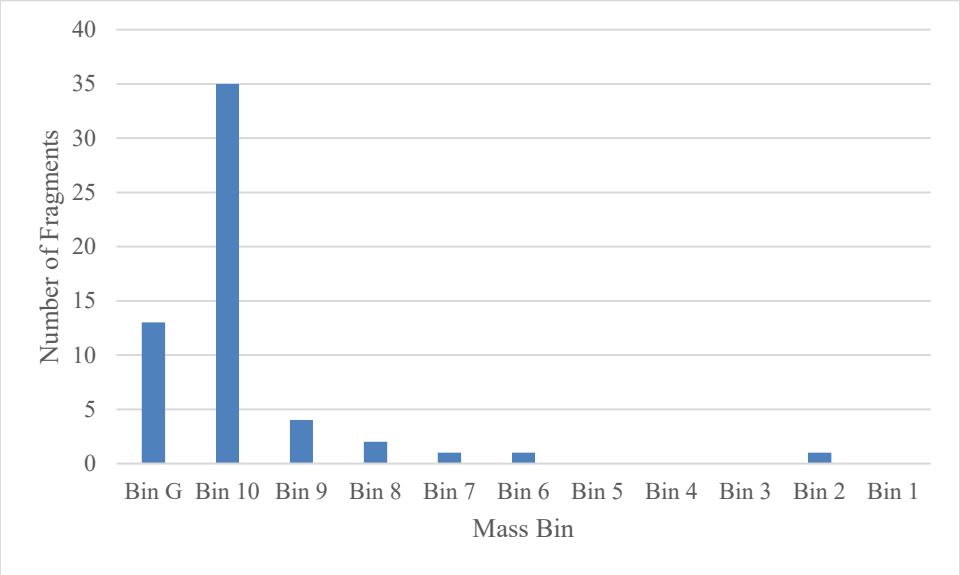


**Figure 66: Test 5 Fragments per Mass Bin**

### 4.2.6 Test 6

Figure 67 shows the results for Test 6 and is interesting in the sense that it appeared to be a combination of the trends observed in all the previous tests. Like Figure 51 (Test 2) and Figure

63 (Test 5), the peak fragment distribution was away from ground zero. Furthermore, the fragment distribution by distance for Test 6 starts at a nonzero value, which was similar to Figure 47 (Test 1), Figure 55 (Test 3), and Figure 59 (Test 4). It was stated in Section 3.2.6.2, of the 62 fragments that were recovered, 28 of them were outside 100 ft, while 34 were inside 100 ft. Of the fragments found inside 100 ft, most were in the 40 - 60 ft range, while outside 100 ft, most were in the 120 - 140 ft region.

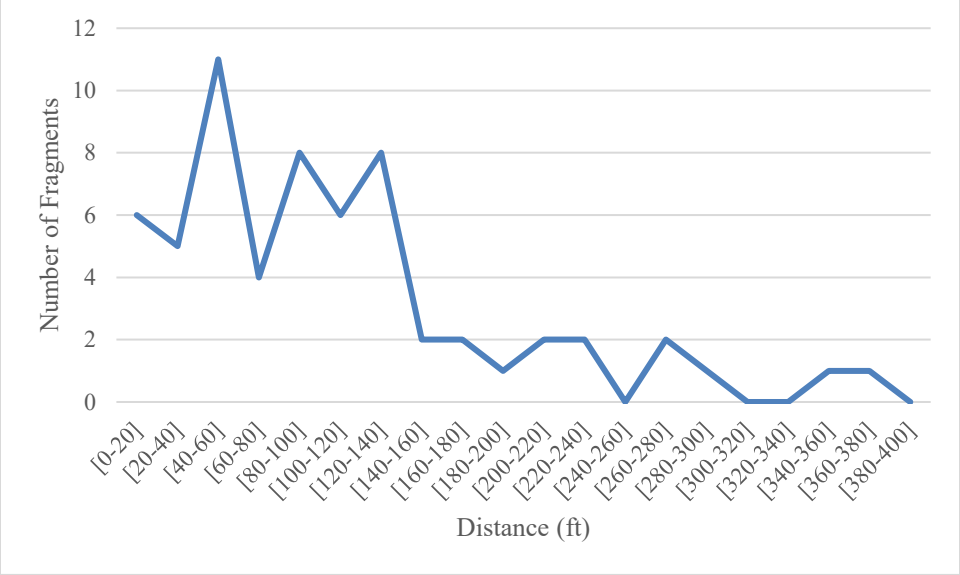


**Figure 67: Test 6 Fragments by Distance**

Figure 68 and Figure 69 depict the fragment distribution by azimuth for Test 6. As pointed out in Section 3.2.6.2, the gun body in this test broke apart into three pieces and did not seem to constrain or direct the blast and fragments to the same degree as the other tests. Therefore, it was not expected that the fragments would be focused on the North-South axis; instead, a more varied distribution overall was expected. In Figure 68 it can already be seen that most of the fragments past 100 ft were focused on or near the West-East axis at 270°. There were still some fragments near the North axis but very little near the South axis. Moving on to Figure 69, when taking into account the fragments within 100 ft the majority of the fragments were still focused out to the west, but the amount of fragmentation in the south had increased slightly. Unsurprisingly, the percentage of fragments recovered within ±10° of the North-South axis was only 17.74%. The shaded areas in these figures represent the azimuths where most fragments were expected to land: 0°±10° and 180°±10°.

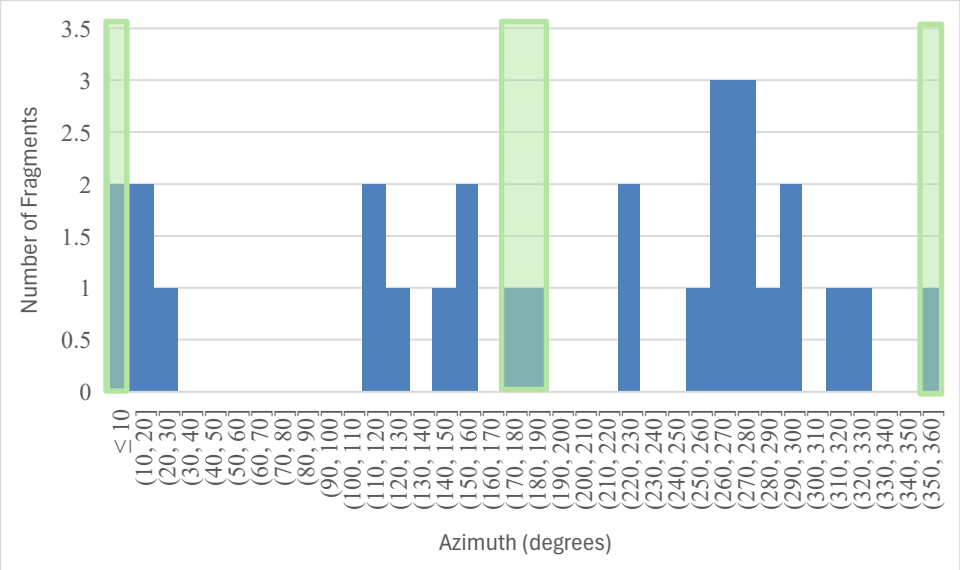


**Figure 68: Test 6 Fragments by Azimuth Outside 100 ft**

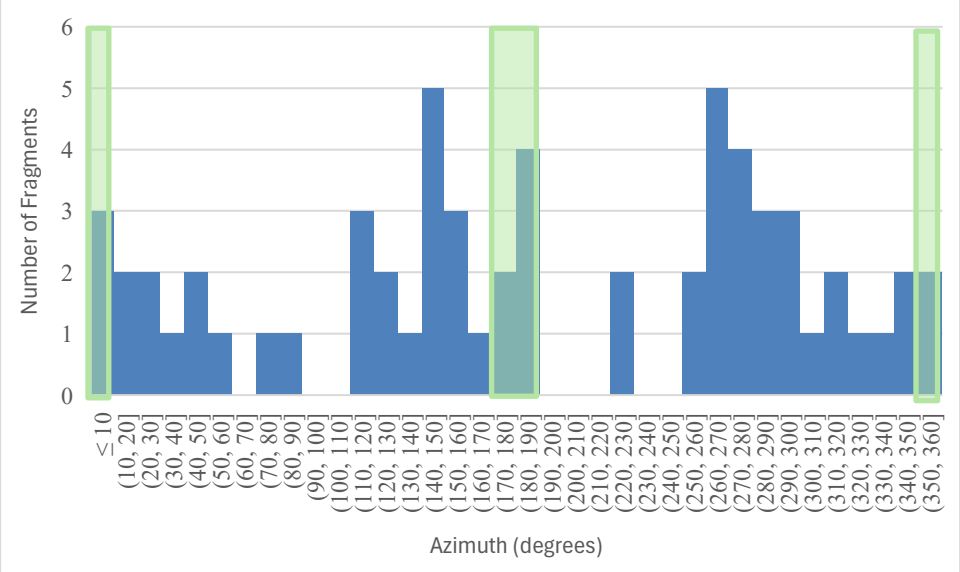


**Figure 69: Test 6 Fragments by Azimuth**

Figure 70 shows the mass bin breakdown for Test 6 and was quite different from any of the other mass bin distributions in the previous tests. First, in this test Mass Bin 9 contained the most fragments, followed by Mass Bin 10 and Mass Bin G with the second and third most fragments, respectively. The other main difference is that since the gun's body broke apart into three pieces, there was no entry for Mass Bin 2. Instead, two of the pieces of the gun body were in Mass Bin 3 while the third piece was in Mass Bin 4.

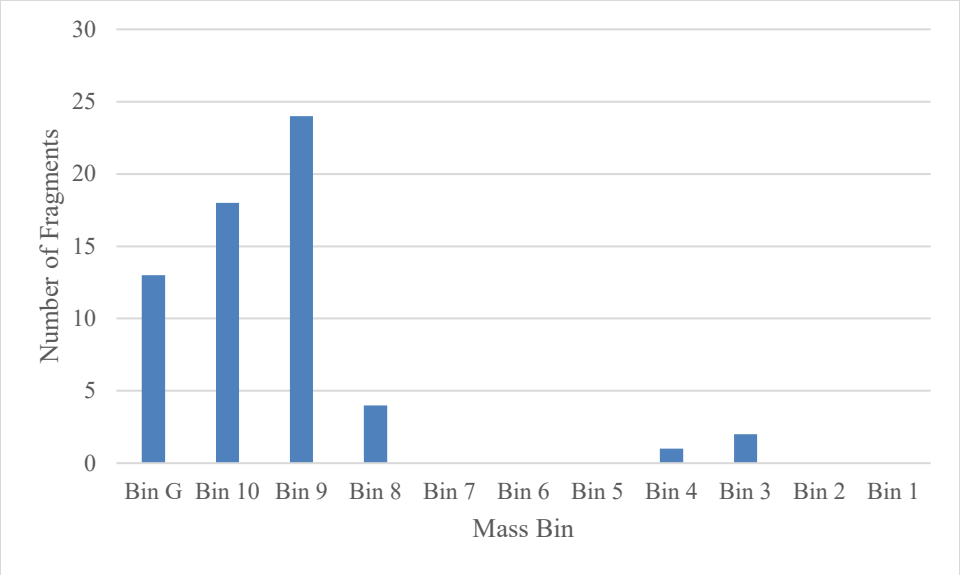


**Figure 70: Test 6 Fragments per Mass Bin**

### 4.2.7 Test 7

Figure 71 shows the fragment distribution by distance for Test 7 and followed the same trend as Figure 67 (Test 6). It started at a nonzero value yet did not reach its peak until it was some distance away from ground zero. This figure was unique amongst these tests since its peak was a plateau. In Section 3.2.7.2, it was stated that of the 35 fragments recovered, 21 of them were recovered within 100 ft and 14 were recovered outside 100 ft. Figure 71 shows the majority of recovered pieces were in the 40 – 120 ft range.

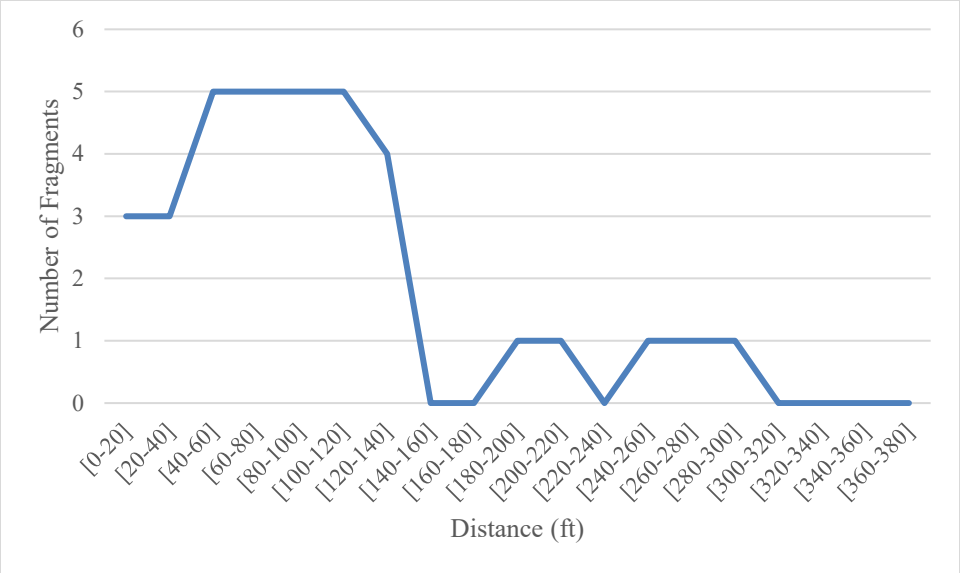


**Figure 71: Test 7 Fragments by Distance**

Figure 72 and Figure 73 depict the fragment distribution by azimuth for Test 7. Considering that Test 7 was the test in which the JPG was oriented vertically, it was not expected that the fragments would be focused on the North-South axis. Instead, a more uniform distribution was expected regardless of distance. However, looking at Figure 72 and Figure 73 shows that the distribution was not uniform. Figure 72 shows that, of the fragments that made it past 100 ft, most of them were focused in the Southeast quarter from 90° - 180°. Adding in the fragments within 100 ft only increased the difference in fragments in the Southeast quarter and the others, as shown in Figure 73. Of the 31.43% of fragments that were recovered within ±10° of the North-South axis, 22.86% of them were found within ±10° of the South axis. The shaded areas in these figures represent the azimuths where most fragments were expected to land: 0°±10° and 180°±10°.

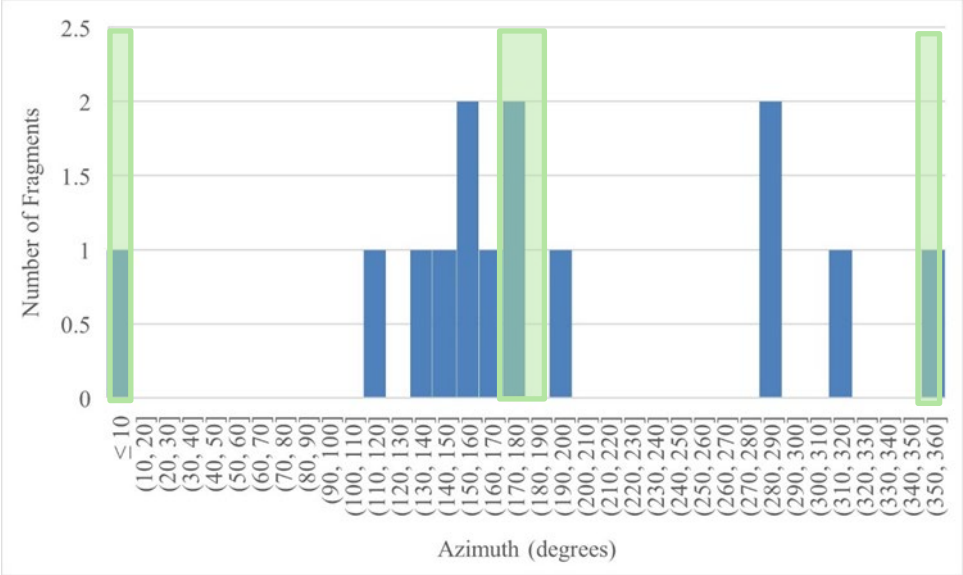


**Figure 72: Test 7 Fragments by Azimuth Outside 100 ft**

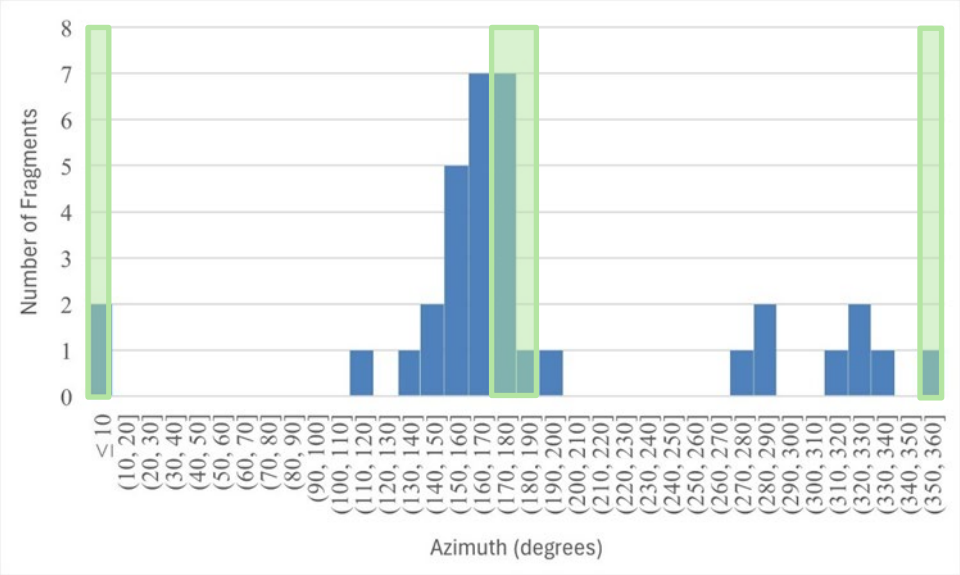


**Figure 73: Test 7 Fragments by Azimuth**

Figure 74 shows the mass bin breakdown for Test 7 and depicts a return to the expected trend with most of the fragments being contained within Mass Bin 10. Following Mass Bin 10 was Bin G with the second most fragments, and then Bin 9 with the third most fragments, similar to Test 5. As seen in the majority of the previous tests, the gun body remained the sole entry for Mass Bin 2.

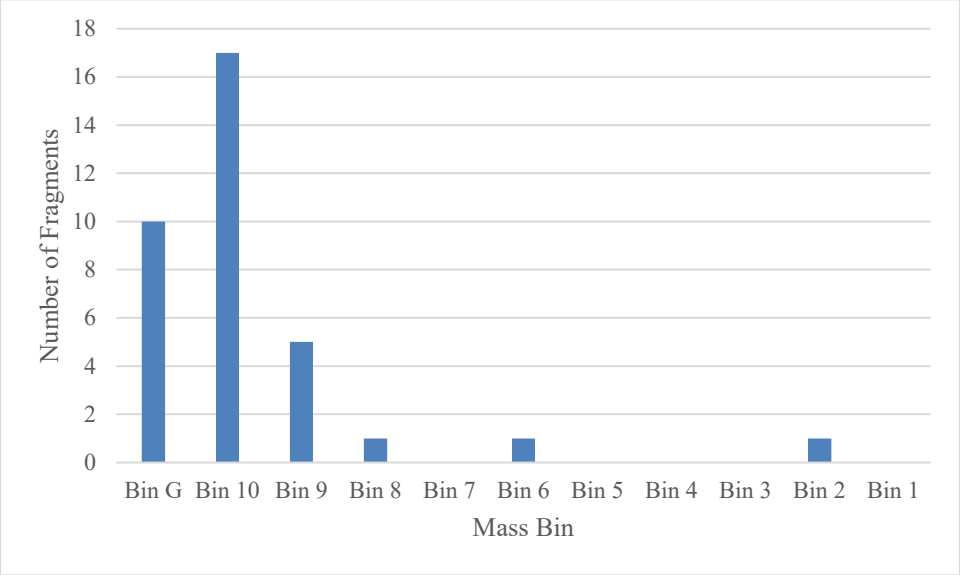


**Figure 74: Test 7 Fragments per Mass Bin**

### 4.2.8 Test 8

Similar to Tests 6 and 7 in terms of fragment distribution by distance, Test 8 also had a peak value higher than the starting value, as shown in Figure 75. However, unlike any other test, Test 8 was the only one to have a data entry for all the ranges. Similar to Test 2, this test had the majority of its fragments land outside 100 ft. In Section 3.2.8.2, it was stated that of the 266 fragments that were recovered in this test, 150 of them were recovered outside 100 ft, while the remaining 116 fragments were recovered inside 100 ft. Another similarity between these two tests was the range at which the peak distribution was found; in both Figure 51 and Figure 75 the peak was at the range of 100 – 120 ft.

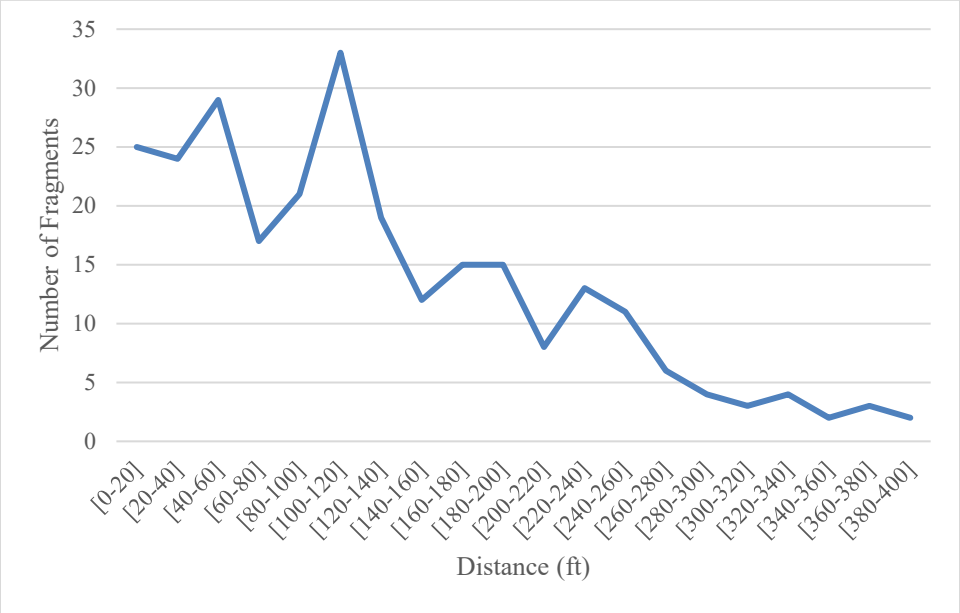


**Figure 75: Test 8 Fragments by Distance**

Figure 76 and Figure 77 depict the fragment distribution by azimuth for Test 8. While this test was unique in being the only test that was performed using multiple JPGs, it was still expected that most of the debris would be focused along the North-South axis. Looking at Figure 76 shows that most of the fragments outside of 100 ft were primarily focused on the North axis and not the South axis, similar to Tests 4 and 5. In Figure 77 adding in the fragments within 100 ft resulted in an increase across all the Southern azimuths but still did not push them to the same level seen near the North axis. Specifically, 20.3% of all fragments were recovered within ±10° of the North axis but only 7.52% of all fragments were recovered within ±10° of the South axis. The shaded areas in these figures represent the azimuths where most fragments were expected to land: 0°±10° and 180°±10°.

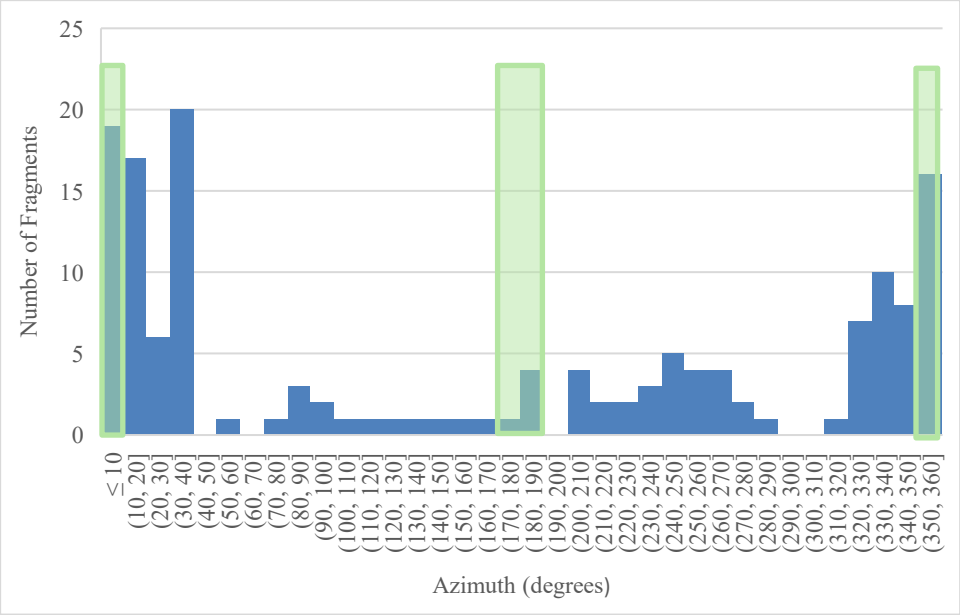


**Figure 76: Test 8 Fragments by Azimuth Outside 100 ft**

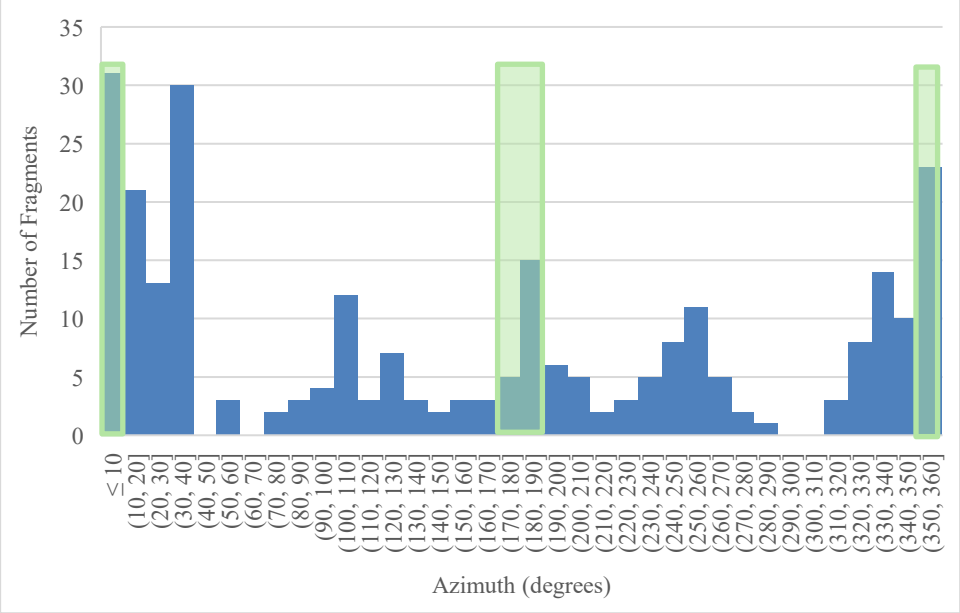


**Figure 77: Test 8 Fragments by Azimuth**

Figure 78 shows the mass bin breakdown for Test 8 and to no surprise Mass Bin 10 still contained the most fragments. In general, the mass bin breakdown is similar to that of Test 5. It is important to note that all the JPGs' bodies in this test remained intact and therefore they were all in Mass Bin 2.

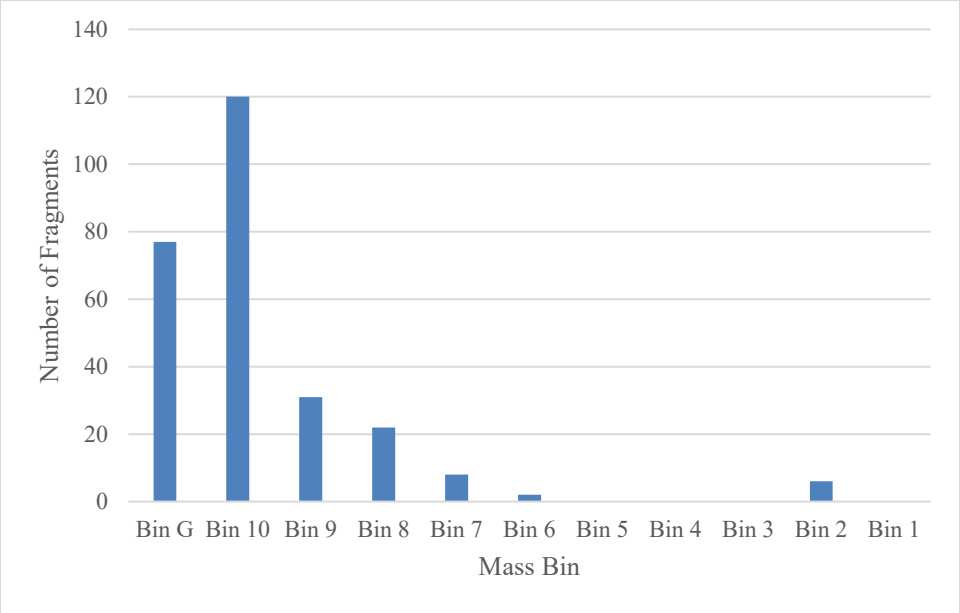


**Figure 78: Test 8 Fragments per Mass Bin**

## 4.3 MODEL COMPARISON

As was stated in Section 1.2, it was unknown how accurate the existing JPG model in IMESAFR would be in comparison to the results of this test series. To assess this, some simple comparisons were made by reproducing the test setup in IMESAFR 2.2 and comparing the results to the gathered test data. While these comparisons were made for every test, only Test 8 will be covered in this paper.

The first comparison is the differences in the actual mass distribution and the projected mass distribution. This comparison was made by determining the total number of fragments recovered per mass bin versus the total number of fragments per mass bin IMESAFR had predicted. As it turned out, IMESAFR predicted significantly fewer fragments than what was recovered. Specifically, IMESAFR predicted a total of 21.27 fragments that qualified for Mass Bin 10 or greater, whereas the test resulted in 189 of the 266 fragments that were recovered qualifying for Mass Bin 10 or greater. Table 23 shows the exact breakdown of the mass distribution comparison. The remaining 77 fragments from Test 8 were above 5 g and therefore cataloged, but only qualified for Mass Bin G. To make a fair comparison to IMESAFR, which only uses Mass Bin 10 or greater for risk calculations, the Mass Bin G fragments were left out of Table 23.

**Table 23: Mass Distribution Comparison**

| Total Number of Fragments | | | | | | | | | | |
|---|---|---|---|---|---|---|---|---|---|---|
| | Bin 1 | Bin 2 | Bin 3 | Bin 4 | Bin 5 | Bin 6 | Bin 7 | Bin 8 | Bin 9 | Bin 10 |
| **Test** | 0 | 6 | 0 | 0 | 0 | 2 | 8 | 22 | 31 | 120 |
| **Model** | 0 | 0 | 0 | 0 | 0 | 0 | 0.58 | 2.77 | 6.41 | 11.5 |

As described in Section 1.2, IMESAFR scales the amount of fragmentation according to the ratio of the charge weights between the surrogate item the model was based on and the item being modeled in the program. Since the JPGs that were tested in this test series were smaller than the surrogate item it was unknown how accurately IMESAFR would predict the number of fragments. Table 23 makes it quite clear that IMESAFR is underpredicting the number of fragments that should be generated in this case. This is likely due to the large difference in size and NEW between the surrogate item and the items tested, as well as the basic idea that the surrogate item was not actually a JPG. The difference in NEW between the JPGs and the surrogate item was large enough that even though Test 8 utilized six JPGs, the total NEW of the test was still less than that of the singular surrogate item. So, when this smaller NEW was input into IMESAFR, the program scaled the number of items down and therefore calculated fewer fragments than what the model shows (based on the surrogate item's NEW), though more than it predicted for the single-item tests.

In addition to the mass distribution, a comparison of the debris density was also made. Figure 79 and Figure 80 depict the comparison of the total debris density contour for Test 8 in IMESAFR and the actual debris scatter plot that was created using the debris catalog. The most noticeable part of these figures was the lack of directionality in the contour. As mentioned previously it is clear that by assuming a uniform 360° distribution, IMESAFR is overpredicting the number of fragments in some areas while underpredicting the number of fragments in others. To further help make the comparison for debris density, some reference points were made using the test data. Table 24 was created to accompany Figure 79 and Figure 80. The table contains the calculated debris density for the test in five different bands: 0-20 ft, 20-100 ft, 100-200 ft, 200-300 ft, 300-400 ft, and compares them to the debris density IMESAFR predicted at the midpoint of each band. The debris density values from the test data were calculated by taking all the debris above 5 g within the respective annular ring (in all directions) and dividing by the area of said annular ring. This density was then further adjusted to account for the difference in the number of fragments. In Test 8 it was found that the test produced 8.89 times the number fragments than IMESAFR predicted, so the test density values were divided by 8.89 to account for this. Table 24 makes it clear to see that in most cases IMESAFR is underpredicting the debris density even after the test's density values have been scaled down to account for the difference in total number of pieces. Interestingly, IMESAFR was predicting that the density will increase in the 300-400 ft band; this may be due to the initial velocity in IMESAFR being too high, resulting in the tool predicting fragments traveling farther than was observed in the test. Furthermore, while it cannot be seen in the images, IMESAFR is predicting debris densities as far out as 1,800 ft,

though the density predictions at that distance are extremely low. While no fragments were recovered past 400 ft in Test 8, that does not necessarily mean that IMESAFR was wrong in predicting that there is a (low) probability that fragments could travel that far. After all, in Test 1 (which was a single item test) it was confirmed that the bulkhead made it past 1,300 ft and was never recovered, so it is possible for a fragment to travel that far even if the likelihood of it happening is extremely low, as IMESAFR predicted.

**Table 24: Debris Density Comparison**

| | 0 – 20 ft | 20 – 100 ft | 100 – 200 ft | 200 – 300 ft | 300 – 400 ft |
|---|---|---|---|---|---|
| **Test** | 3.04E-03 | 2.20E-04 | 8.00E-05 | 2.51E-05 | 5.12E-06 |
| **Model** | 7.89E-03 | 2.03E-06 | 4.17E-06 | 7.52E-06 | 1.07E-05 |

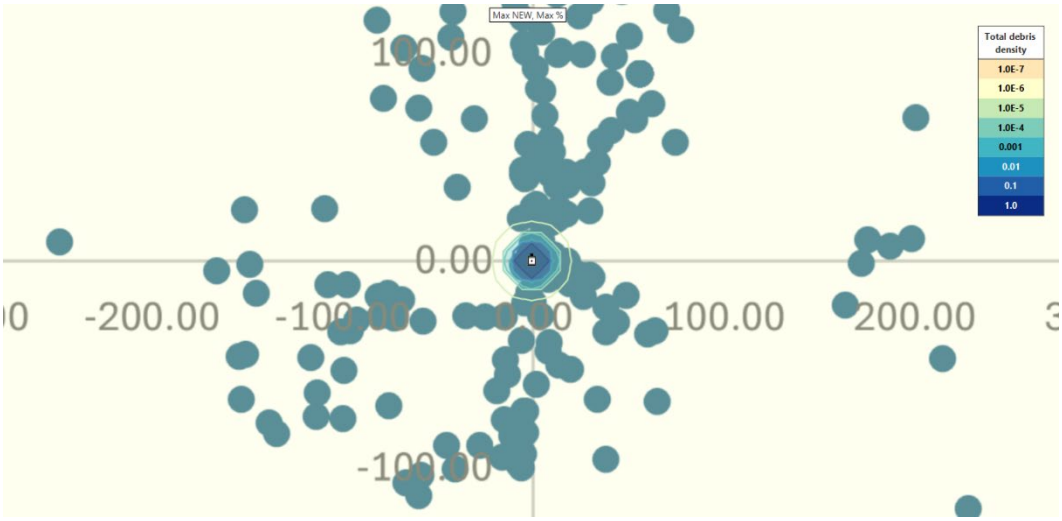


**Figure 79: Test 8 Debris Density Contour Close-In**

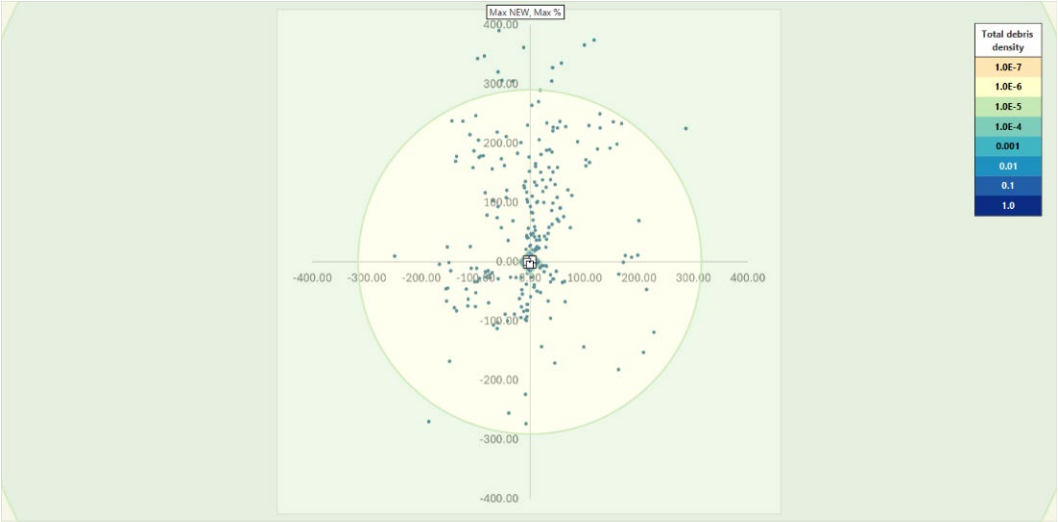


**Figure 80: Test 8 Debris Density Comparison Zoomed Out**

To summarize the results of the comparison between the model and the results from this test series; the model in IMESAFR is predicating debris traveling farther than what was observed in the tests, most likely due to the initial velocities associated with the model being too high, and it is underpredicting the amount of fragments being generated due to the difference in size and NEW of the surrogate item and modern JPGs.

## 5.0 Future Plans

As stated in Sections 1.3 and 2.2, the original plan for this test series had more tests envisioned but had to be limited to eight tests due to time, funding, and range constraints. Therefore, it was determined that more testing will need to be done in the future. Specifically, testing needs to be done to observe the effects of different gun sizes, phasing angles, number of shots-per-foot, and total number of charges, as all these parameters may influence the behavior of the JPG during detonation. In addition to the remaining parameters that need to be tested, it is desirable to perform further testing to fully capture the behavior of the bulkhead, since that was not accomplished in Test 1.

## 6.0 Summary and Conclusions

To summarize, the primary goal of this test series was to collect empirical data that could be used to improve IMESAFR, especially the range, bearing, and mass of the JPG fragments. The test results will be used to improve the existing IMESAFR JPG model and therefore improve the program's ability to perform QRA for scenarios involving JPGs. Originally, it was believed that the results from this test series would be used to reduce conservatism in the model. However, upon comparing the test results to the model, it was determined that the model was conservative in some areas but non-conservative in other aspects. Overall, this test series has provided a significant amount of data that can be used to begin the process of looking into possible

improvements to the model. However, there are numerous additional parameters that still need to be tested.

## 7.0 References

1. Bureau of Alcohol, Tobacco, Firearms and Explosives (ATF), "Table of Distances," 26 October 2021.
2. J. Tatom, B. Evans, J. Hoffman, C. Fritz, M. Duncan, M. Robinson, “IMESAFR Overview” in *National Defense Industrial Association (NDIA), International Explosives Safety Symposium & Exposition, San Diego, CA, August 2018.*
3. Institute of Makers of Explosives (IME), “Guide to Obtaining DOT Approval of Jet Perforating Guns using AESC/IME Perforating Gun Specifications Version 02,” 1 September 2017.
4. Department of Defensive Ammunition and Explosives Hazard Classification Procedures (TB 700-2). Various editions
5. Swisdak, Michael M., Tatom, John W., and Conway, Robert T., “Procedures for the Collection, Analysis, and Interpretation of Explosion-Produced Debris—Revision 2,” DDESB Technical Paper 21, 30 November 2017.
6. Open Source Physics. (2025). Tracker Video Analysis and Modeling Tool (Version 6.3.1). Retrieved from https://opensourcephysics.github.io/tracker-website/

# APPENDIX A: ATF REGULATIONS

The tests are being conducted to represent a model of a potential accidental detonation of the JPGs in both the stored (horizontal) singularly and in a deployed (vertical) positions. The storage of these configured guns has been authorized per ATF Rule 2010-7 (Reference 1) which relates to Title 18 U.S.C. 842 (j): Storage of explosives and also under both 27 CFR 555.22: Alternate methods or procedures and 27 CFR 555.205: Movement of explosives materials which generally authorizes the loaded JPGs to be stored in an indoor location if the following conditions are met at all times:

1. No more than 50 pounds of explosives may be stored inside any facility used for indoor explosives storage. This means that the combined net explosives weight (NEW) contained in the magazines and outside of magazines in any one building must not exceed 50 pounds.
2. All loaded JPGs must either lie flat on the floor or be placed in stable racks to prevent accidental movement or discharge.

If the JPGs are stored in an outdoor location the following additional conditions must be met at all times:

1. No more than 200 loaded JPGs or 2,500 pounds of net explosive weight (NEW) may be kept outside a magazine. Each outdoor area or vehicle containing loaded JPGs must comply with the table of distances requirements set forth in 27 CFR 555.218.
2. The loaded JPGs may be stored in a covered or uncovered area as long as the guns are placed flat on a concrete or paved floor, offshore well tool pallets, or placed on permanently mounted racks to prevent accidental movement or discharge. Loaded JPGs that have exposed explosives that are not contained within a secure tube (e.g., tube-less strips or wire guns) may not be stored in an outdoor location.

The aforementioned information relating to both the indoor and outdoor storage requirements of the JPGs is only a portion of the requirements detailed in ATF Rule 2010-7. The remaining requirements are related to security (e.g., locks, fencing) and are not pertinent to the current testing parameters.

**Reference**

1. ATF Rule 2010-7, U.S. Department of Justice, Bureau of Alcohol, Tobacco, Firearms and Explosives, Office of the Director Washington, DC 20226, 18 U.S.C. 842(j): Storage of Explosives, 27 CFR 555.22: Alternative Methods or Procedures, 27 CFR 555.205 Movement of Explosive Materials

# APPENDIX B: FRAGMENT CATALOGUES

## Test 1

| PT_ID | East | North | Elev | Description | Mass (g) | Distance (ft) | Azimuth (°) |
|---|---|---|---|---|---|---|---|
| 14 | 2256175.80 | 6862983.66 | 1034.05 | PERFORATOR-21.3 | 21.3 | 26.02 | 88.35 |
| 16 | 2256165.95 | 6862996.99 | 1034.12 | PERFORATOR-5.9 | 5.9 | 21.43 | 48.95 |
| 17 | 2256153.08 | 6862993.12 | 1033.97 | WELD-CARRIER-TUBE-PERFORATOR-48.8 | 48.8 | 10.72 | 17.83 |
| 20 | 2256146.76 | 6863004.56 | 1033.97 | WELD-CARRIER-TUBE-PERFORATOR-5.9 | 5.9 | 21.86 | 352.02 |
| 21 | 2256198.98 | 6863058.47 | 1034.96 | PERFORATOR-7.9 | 7.9 | 90.16 | 33.07 |
| 22 | 2256155.53 | 6863056.02 | 1034.69 | CARRIER-TUBE-15.2 | 15.2 | 73.33 | 4.49 |
| 23 | 2256111.64 | 6863024.12 | 1034.00 | CARRIER-TUBE-5.4 | 5.4 | 56.16 | 317.20 |
| 24 | 2256106.57 | 6863052.46 | 1034.13 | WELD-CARRIER-TUBE-PERFORATOR-14.2 | 14.2 | 81.88 | 328.14 |
| 25 | 2256150.22 | 6862982.63 | 1033.63 | PERFORATOR-3FTRAD-9.1 | 9.1 | 0.52 | 123.51 |
| 26 | 2256179.67 | 6862886.16 | 1033.14 | PERFORATOR-26.8 | 26.8 | 101.27 | 162.84 |
| 27 | 2256161.88 | 6862793.27 | 1031.96 | CARRIER-TUBE-200.3 | 200.3 | 190.03 | 176.35 |
| 30 | 2256130.37 | 6863265.79 | 1036.82 | PERFORATOR-10.4 | 10.4 | 283.54 | 356.07 |
| 31 | 2256198.51 | 6863169.45 | 1036.35 | CARRIER-TUBE-205.3 | 205.3 | 192.79 | 14.64 |
| 1000 | 2256151.27 | 6862980.63 | 1033.81 | PERFORATOR-7.4 | 7.4 | 2.72 | 147.06 |
| 1001 | 2256152.66 | 6862980.82 | 1033.84 | PERFORATOR-2.5 | 2.5 | 3.55 | 126.05 |
| 1002 | 2256152.46 | 6862981.06 | 1033.89 | PERFORATOR-8.2 | 8.2 | 3.25 | 124.84 |
| 1003 | 2256154.94 | 6862979.04 | 1034.01 | PERFORATOR-7.9 | 7.9 | 6.44 | 126.97 |
| 1004 | 2256153.62 | 6862975.64 | 1033.56 | PERFORATOR-5 | 5 | 8.22 | 152.27 |
| 1006 | 2256152.17 | 6862976.67 | 1033.90 | PERFORATOR-9.5 | 9.5 | 6.68 | 159.18 |
| 1013 | 2256156.68 | 6862960.04 | 1033.75 | CARRIER-TUBE-31.3 | 31.3 | 23.89 | 163.24 |
| 1017 | 2256191.79 | 6862906.50 | 1033.66 | PERFORATOR-10.8 | 10.8 | 87.20 | 151.21 |
| 1021 | 2256144.11 | 6862928.13 | 1033.35 | PERFORATOR-7.8 | 7.8 | 55.08 | 185.92 |
| 1022 | 2256106.08 | 6862927.93 | 1032.94 | CARRIER-TUBE-9.8 | 9.8 | 70.24 | 218.49 |
| 1023 | 2256142.00 | 6862953.24 | 1033.44 | CARRIER-TUBE-13.8 | 13.8 | 30.68 | 194.72 |
| 1028 | 2256192.50 | 6862975.96 | 1034.16 | PERFORATOR-9.3 | 9.3 | 43.27 | 99.25 |
| 1029 | 2256158.00 | 6862968.36 | 1033.84 | GUN_BODY | 8065.98 | 16.71 | 150.59 |

## Test 2

| PT_ID | East | North | Elev | Description | Mass (g) | Distance (ft) | Azimuth (°) |
|---|---|---|---|---|---|---|---|
| 1000 | 2256103.15 | 6863020.52 | 1033.53 | PERFORATOR-11.9 | 11.9 | 198.84 | 18.25 |
| 1001 | 2256100.95 | 6863049.33 | 1033.93 | PERFORATOR-12 | 12 | 225.78 | 15.43 |
| 1002 | 2256110.81 | 6862992.47 | 1033.30 | PERFORATOR-6.3 | 6.3 | 175.33 | 23.51 |
| 1003 | 2256106.07 | 6862981.89 | 1033.24 | PERFORATOR-5.9 | 5.9 | 163.74 | 23.46 |
| 2001 | 2256094.92 | 6862867.36 | 1031.85 | CARRIER-PERFORATOR-WELD-5 | 5 | 64.75 | 56.57 |
| 2002 | 2256102.09 | 6862866.86 | 1031.88 | PERFORATOR-5.4 | 5.4 | 70.60 | 60.12 |
| 2003 | 2256106.40 | 6862863.98 | 1031.91 | PERFORATOR-10.1 | 10.1 | 73.05 | 63.76 |
| 2004 | 2256067.68 | 6862843.84 | 1031.38 | CARRIER-TUBE-6 | 6 | 29.43 | 65.62 |
| 2005 | 2256069.10 | 6862814.36 | 1031.13 | PERFORATOR-7.9 | 7.9 | 33.11 | 121.55 |
| 2006 | 2256079.92 | 6862812.41 | 1031.18 | PERFORATOR-14.8 | 14.8 | 43.54 | 116.28 |
| 2007 | 2256064.31 | 6862799.20 | 1030.86 | CARRIER-TUBE-18.5 | 18.5 | 40.06 | 144.20 |
| 2008 | 2256072.14 | 6862770.77 | 1030.69 | CARRIER-TUBE-37.2 | 37.2 | 68.48 | 152.83 |
| 2009 | 2256076.48 | 6862764.04 | 1030.80 | PERFORATOR-10.5 | 10.5 | 76.44 | 152.24 |
| 2010 | 2256060.67 | 6862760.75 | 1030.57 | PERFORATOR-5.4 | 5.4 | 73.64 | 164.41 |
| 2011 | 2256026.32 | 6862743.81 | 1029.88 | PERFORATOR-7.2 | 7.2 | 89.08 | 189.41 |
| 2012 | 2256013.03 | 6862742.99 | 1029.77 | PERFORATOR-6.7 | 6.7 | 92.97 | 197.43 |
| 2013 | 2256026.20 | 6862731.87 | 1029.80 | PERFORATOR-6.7 | 6.7 | 100.89 | 188.36 |
| 2014 | 2256024.05 | 6862722.25 | 1029.69 | PERFORATOR- 10.2 | 10.2 | 110.72 | 188.74 |
| 2015 | 2256065.77 | 6862944.71 | 1032.42 | PERFORATOR- 4.6 | 4.6 | 115.74 | 12.42 |
| 2016 | 2256066.70 | 6862977.37 | 1032.87 | PERFORATOR- 15.7 | 15.7 | 147.96 | 10.05 |
| 2017 | 2256055.60 | 6863011.40 | 1033.05 | PERFORATOR- 11 | 11 | 180.31 | 4.68 |
| 2018 | 2256067.82 | 6863019.77 | 1033.36 | CARRIER-TUBE- 57.9 | 57.9 | 190.00 | 8.15 |
| 2019 | 2256060.78 | 6863087.83 | 1033.95 | PERFORATOR - 5.6 | 5.6 | 256.91 | 4.44 |
| 2020 | 2256070.01 | 6863123.08 | 1034.35 | PERFORATOR - 5.2 | 5.2 | 292.84 | 5.71 |
| 2021 | 2256077.22 | 6863140.70 | 1034.55 | PERFORATOR - 4.5 | 4.5 | 311.15 | 6.71 |
| 2022 | 2256096.27 | 6863127.52 | 1034.70 | PERFORATOR - 5 | 5 | 300.97 | 10.61 |
| 2023 | 2256118.45 | 6863112.83 | 1034.80 | PERFORATOR - 9.6 | 9.6 | 291.65 | 15.43 |
| 2024 | 2256157.05 | 6863067.61 | 1034.55 | CARRIER-TUBE - 48.6 | 48.6 | 262.98 | 26.22 |
| 2025 | 2256025.17 | 6862723.02 | 1029.79 | GUN_BODY | 8196 | 109.80 | 188.22 |
| 2026 | 2256047.84 | 6862749.07 | 1030.22 | PERFORATOR - 8.7 | 8.7 | 82.91 | 175.18 |
| 2027 | 2256059.74 | 6862723.78 | 1030.14 | PERFORATOR-5.5 | 5.5 | 109.55 | 170.09 |
| 2028 | 2256058.92 | 6862732.36 | 1030.25 | PERFORATOR-5.6 | 5.6 | 100.95 | 169.71 |
| 2029 | 2256047.20 | 6862720.63 | 1029.95 | PERFORATOR-12.2 | 12.2 | 111.24 | 176.74 |
| 2030 | 2256042.98 | 6862717.23 | 1029.81 | PERFORATOR-5.1 | 5.1 | 114.48 | 178.95 |
| 2031 | 2256045.76 | 6862725.86 | 1029.87 | PERFORATOR-6.2 | 6.2 | 105.95 | 177.36 |
| 2032 | 2256038.70 | 6862941.67 | 1032.18 | PERFORATOR-7.9 | 7.9 | 110.00 | 358.86 |

## Test 3

| PT_ID | East | North | Elev | Description | Mass (g) | Distance (ft) | Azimuth (°) |
|---|---|---|---|---|---|---|---|
| 2001 | 2256018.35 | 6862768.89 | 1030.27 | CARRIER-PERFORATOR-WELD-7.2 | 7.2 | 66.72 | 199.74 |
| 2002 | 2256027.20 | 6862742.26 | 1029.91 | PERFORATOR-5.4 | 5.4 | 90.47 | 188.70 |
| 2004 | 2256015.52 | 6862804.53 | 1030.59 | PERFORATOR-17.6 | 17.6 | 37.16 | 223.04 |
| 2005 | 2256021.39 | 6862811.78 | 1030.65 | PERFORATOR-5.1 | 5.1 | 27.86 | 224.40 |
| 2006 | 2256025.31 | 6862813.32 | 1030.79 | CARRIER-TUBE-169 | 169 | 24.08 | 220.29 |
| 2007 | 2256024.28 | 6862813.77 | 1030.72 | PERFORATOR-22.7 | 22.7 | 24.42 | 222.81 |
| 2008 | 2256023.15 | 6862814.34 | 1030.71 | PERFORATOR-6.3 | 6.3 | 24.80 | 225.63 |
| 2009 | 2256023.19 | 6862814.87 | 1030.69 | PERFORATOR-15 | 15 | 24.40 | 226.45 |
| 2010 | 2256022.70 | 6862814.59 | 1030.74 | PERFORATOR-12.2 | 12.2 | 24.95 | 226.75 |
| 2011 | 2256022.71 | 6862814.58 | 1030.73 | PERFORATOR-5.4 | 5.4 | 24.96 | 226.72 |
| 2012 | 2256023.78 | 6862815.34 | 1030.74 | PERFORATOR-8.6 | 8.6 | 23.66 | 226.29 |
| 2013 | 2256043.55 | 6862826.78 | 1031.00 | PERFORATOR-8.3 | 8.3 | 5.59 | 151.43 |
| 2014 | 2256043.86 | 6862829.74 | 1030.93 | PERFORATOR-6.2 | 6.2 | 3.56 | 123.14 |
| 2015 | 2256043.88 | 6862830.98 | 1031.03 | PERFORATOR-12.7 | 12.7 | 3.09 | 103.34 |
| 2016 | 2256041.54 | 6862830.74 | 1030.92 | PERFORATOR-7.8 | 7.8 | 1.16 | 145.20 |
| 2017 | 2256040.58 | 6862830.06 | 1030.99 | PERFORATOR-5.1 | 5.1 | 1.65 | 190.43 |
| 2018 | 2256035.34 | 6862829.71 | 1030.99 | PERFORATOR-7.8 | 7.8 | 5.88 | 250.38 |
| 2019 | 2256025.88 | 6862830.72 | 1030.88 | PERFORATOR-5.1 | 5.1 | 15.03 | 266.31 |
| 2020 | 2256026.08 | 6862828.45 | 1030.94 | PERFORATOR-7.3 | 7.3 | 15.15 | 257.66 |
| 2021 | 2256022.93 | 6862833.55 | 1030.94 | PERFORATOR-26.7 | 26.7 | 18.05 | 275.91 |
| 2022 | 2256029.54 | 6862839.28 | 1031.06 | PERFORATOR-15.9 | 15.9 | 13.65 | 303.78 |
| 2023 | 2256033.44 | 6862842.04 | 1031.13 | PERFORATOR-5.8 | 5.8 | 12.75 | 324.29 |
| 2024 | 2256039.28 | 6862836.79 | 1031.03 | PERFORATOR-6.8 | 6.8 | 5.34 | 342.56 |
| 2025 | 2256039.27 | 6862836.78 | 1031.03 | CARRIER-TUBE-88.4 | 88.4 | 5.34 | 342.52 |
| 2026 | 2256040.93 | 6862833.97 | 1030.92 | GUN_BODY | 7894 | 2.28 | 1.33 |
| 2027 | 2256044.00 | 6862841.64 | 1031.04 | PERFORATOR-12.6 | 12.6 | 10.43 | 17.44 |
| 2028 | 2256082.04 | 6862864.23 | 1031.78 | PERFORATOR-5.0 | 5 | 52.47 | 51.67 |
| 2029 | 2256081.90 | 6862868.69 | 1031.85 | PERFORATOR-6.8 | 6.8 | 55.24 | 47.95 |
| 2030 | 2256109.66 | 6862882.53 | 1032.15 | PERFORATOR-8.5 | 8.5 | 85.53 | 53.53 |
| 2031 | 2256023.52 | 6862721.80 | 1029.64 | PERFORATOR-7.8 | 7.8 | 111.25 | 188.98 |
| 2032 | 2256011.65 | 6862679.39 | 1028.97 | PERFORATOR-5.5 | 5.5 | 155.08 | 190.87 |
| 2033 | 2256005.17 | 6862665.81 | 1028.87 | PERFORATOR-6.9 | 6.9 | 169.68 | 192.15 |
| 2034 | 2256054.14 | 6862971.09 | 1032.58 | CARRIER-TUBE-32 | 32 | 140.03 | 5.44 |
| 2035 | 2256058.18 | 6863003.24 | 1032.99 | PERFORATOR-5.5 | 5.5 | 172.42 | 5.76 |
| 2036 | 2256051.72 | 6863016.07 | 1032.86 | PERFORATOR-5.7 | 5.7 | 184.70 | 3.37 |
| 2037 | 2256085.29 | 6863134.97 | 1034.56 | PERFORATOR-8.0 | 8 | 306.52 | 8.33 |
| 2038 | 2256219.23 | 6863033.60 | 1034.55 | CARRIER-TUBE-15.6 | 15.6 | 269.41 | 41.45 |
| 2039 | 2256074.55 | 6862960.12 | 1032.64 | PERFORATOR-8.6 | 8.6 | 132.77 | 14.69 |
| 2040 | 2256044.51 | 6862977.52 | 1032.50 | PERFORATOR-5.0 | 5 | 145.87 | 1.43 |
| 2041 | 2256041.75 | 6862971.90 | 1032.32 | PERFORATOR-6.0 | 6 | 140.21 | 0.36 |

| | | | | | | | |
|---|---|---|---|---|---|---|---|
| 2042 | 2256039.77 | 6862978.20 | 1032.38 | CARRIER-TUBE-199 | 199 | 146.52 | 359.57 |
| 2043 | 2256050.40 | 6862705.85 | 1029.70 | PERFORATOR-11.3 | 11.3 | 126.19 | 175.67 |
| 2044 | 2256031.54 | 6862645.96 | 1028.90 | PERFORATOR-7.7 | 7.7 | 185.96 | 182.88 |
| 2045 | 2256054.99 | 6862632.63 | 1029.22 | PERFORATOR-6.3 | 6.3 | 199.56 | 175.94 |
| 2046 | 2256085.84 | 6862497.80 | 1027.44 | CARRIER-TUBE-181.4 | 181.4 | 336.90 | 172.33 |
| 2047 | 2256032.02 | 6862736.03 | 1029.94 | PERFORATOR-6.9 | 6.9 | 96.07 | 185.29 |
| 2048 | 2256077.30 | 6862999.59 | 1033.04 | PERFORATOR-7.2 | 7.2 | 171.80 | 12.24 |
| 2049 | 2256045.21 | 6863018.72 | 1032.95 | PERFORATOR-5.2 | 5.2 | 187.08 | 1.33 |
| 2050 | 2256036.18 | 6863008.22 | 1032.70 | PERFORATOR-11.0 | 11 | 176.59 | 358.48 |
| 2051 | 2256024.95 | 6862807.84 | 1030.66 | PERFORATOR-8.0 | 8 | 28.68 | 213.74 |
| 2052 | 2256080.28 | 6862841.49 | 1031.61 | PERFORATOR-8.7 | 8.7 | 40.61 | 76.04 |

## Test 4

| PT_ID | East | North | Elev | Description | Mass (g) | Distance (ft) | Azimuth (°) |
|---|---|---|---|---|---|---|---|
| 2001 | 2256026.91 | 6862754.15 | 1030.08 | GUN_BODY | 11844 | 78.79 | 190.00 |
| 2002 | 2256024.34 | 6862793.58 | 1030.50 | PERFORATOR-8.2 | 8.2 | 41.54 | 203.45 |
| 2003 | 2256021.80 | 6862811.37 | 1030.66 | PERFORATOR-7.5 | 7.5 | 27.87 | 223.19 |
| 2004 | 2256048.25 | 6862790.00 | 1030.68 | PERFORATOR-7.2 | 7.2 | 42.33 | 169.97 |
| 2005 | 2256051.52 | 6862796.30 | 1030.69 | PERFORATOR-16.8 | 16.8 | 36.96 | 163.26 |
| 2006 | 2256049.44 | 6862805.41 | 1030.91 | PERFORATOR-7.7 | 7.7 | 27.64 | 161.95 |
| 2007 | 2256048.52 | 6862811.19 | 1030.96 | PERFORATOR-16.6 | 16.6 | 21.88 | 159.54 |
| 2008 | 2256046.27 | 6862818.27 | 1030.90 | PERFORATOR-8.8 | 8.8 | 14.46 | 158.10 |
| 2009 | 2256046.73 | 6862822.36 | 1030.95 | PERFORATOR-5.6 | 5.6 | 11.01 | 147.92 |
| 2010 | 2256040.35 | 6862836.16 | 1031.05 | PERFORATOR-14.3 | 14.3 | 4.51 | 353.23 |
| 2011 | 2256041.98 | 6862837.37 | 1031.08 | PERFORATOR-6.4 | 6.4 | 5.79 | 10.94 |
| 2012 | 2256042.71 | 6862839.61 | 1031.06 | PERFORATOR-9.1 | 9.1 | 8.13 | 13.05 |
| 2013 | 2256047.86 | 6862845.67 | 1031.23 | CARRIER-TUBE-230 | 230 | 15.63 | 26.54 |
| 2014 | 2256043.86 | 6862847.01 | 1031.15 | PERFORATOR-11.2 | 11.2 | 15.61 | 11.00 |
| 2015 | 2256043.35 | 6862846.60 | 1031.21 | PERFORATOR-10.2 | 10.2 | 15.12 | 9.43 |
| 2016 | 2256042.65 | 6862847.78 | 1031.26 | PERFORATOR-15.5 | 15.5 | 16.19 | 6.28 |
| 2017 | 2256042.50 | 6862848.58 | 1031.25 | PERFORATOR-5.8 | 5.8 | 16.97 | 5.48 |
| 2018 | 2256041.17 | 6862848.13 | 1031.21 | PERFORATOR-7.6 | 7.6 | 16.44 | 1.03 |
| 2019 | 2256046.44 | 6862852.88 | 1031.22 | CARRIER-TUBE-5.0 | 5 | 21.91 | 14.70 |
| 2020 | 2256062.48 | 6862854.64 | 1031.51 | PERFORATOR-5.5 | 5.5 | 31.52 | 43.26 |
| 2021 | 2256063.67 | 6862861.76 | 1031.61 | PERFORATOR-8.8 | 8.8 | 37.74 | 37.16 |
| 2022 | 2256060.05 | 6862864.42 | 1031.59 | PERFORATOR-7.7 | 7.7 | 37.93 | 30.37 |
| 2023 | 2256056.54 | 6862868.57 | 1031.62 | PERFORATOR-8.3 | 8.3 | 40.07 | 23.01 |
| 2024 | 2256083.84 | 6862870.02 | 1031.84 | PERFORATOR-15.6 | 15.6 | 57.57 | 48.26 |
| 2025 | 2256055.46 | 6862881.57 | 1031.70 | PERFORATOR-8.0 | 8 | 51.97 | 16.29 |
| 2027 | 2256058.89 | 6862926.48 | 1032.27 | PERFORATOR-5.9 | 5.9 | 96.49 | 10.76 |
| 2028 | 2256066.10 | 6863045.19 | 1033.29 | PERFORATOR-5.1 | 5.1 | 214.98 | 6.74 |
| 2029 | 2256073.93 | 6863028.24 | 1033.34 | PERFORATOR-16.3 | 16.3 | 199.31 | 9.55 |
| 2030 | 2256089.50 | 6863023.52 | 1033.37 | CARRIER-TUBE-115.1 | 115.1 | 197.90 | 14.22 |
| 2032 | 2256051.89 | 6863036.88 | 1033.15 | CARRIER-TUBE-131 | 131 | 205.49 | 3.07 |
| 2033 | 2256051.60 | 6863023.33 | 1033.03 | PERFORATOR-8.0 | 8 | 191.94 | 3.20 |
| 2034 | 2256057.26 | 6862979.98 | 1032.75 | PERFORATOR-7.2 | 7.2 | 149.19 | 6.30 |
| 2035 | 2256056.18 | 6862978.50 | 1032.86 | PERFORATOR-5.8 | 5.8 | 147.61 | 5.95 |
| 2036 | 2256053.84 | 6862956.31 | 1032.48 | PERFORATOR-7.5 | 7.5 | 125.29 | 5.94 |
| 2037 | 2256061.33 | 6862951.14 | 1032.61 | PERFORATOR-7.5 | 7.5 | 121.19 | 9.72 |
| 2038 | 2256064.79 | 6862941.42 | 1032.46 | PERFORATOR-5.5 | 5.5 | 112.31 | 12.29 |
| 2039 | 2256072.22 | 6862943.02 | 1032.48 | PERFORATOR-7.4 | 7.4 | 115.66 | 15.72 |
| 2040 | 2256082.98 | 6862942.74 | 1032.66 | PERFORATOR-5.7 | 5.7 | 118.76 | 20.76 |
| 2044 | 2256059.93 | 6862741.83 | 1030.35 | PERFORATOR-6.1 | 6.1 | 91.85 | 168.03 |
| 2045 | 2256056.29 | 6862914.49 | 1032.15 | PERFORATOR-12.4 | 12.4 | 84.22 | 10.55 |
| 2046 | 2256026.28 | 6862945.76 | 1032.00 | PERFORATOR-12.2 | 12.2 | 115.00 | 352.71 |

| | | | | | | | |
|---|---|---|---|---|---|---|---|
| 2047 | 2256048.89 | 6863001.01 | 1032.66 | PERFORATOR-15.2 | 15.2 | 169.51 | 2.71 |
| 2048 | 2256041.98 | 6863106.91 | 1033.65 | PERFORATOR-5.1 | 5.1 | 275.23 | 0.23 |
| 3030 | 2256193.50 | 6863129.55 | 1035.53 | CARRIER-TUBE-6.6 | 6.6 | 334.69 | 27.13 |

## Test 5

| PT_ID | East | North | Elev | Description | Mass (g) | Distance (ft) | Azimuth (°) |
|---|---|---|---|---|---|---|---|
| 3001 | 2256075.07 | 6862863.96 | 1031.60 | PERFORATOR-7.1 | 7.1 | 47.02 | 46.65 |
| 3002 | 2256072.47 | 6862861.77 | 1031.54 | PERFORATOR-6.2 | 6.2 | 43.62 | 46.40 |
| 3003 | 2256075.57 | 6862863.54 | 1031.65 | CARRIER-TUBE-172.3 | 172.3 | 47.10 | 47.45 |
| 3004 | 2256082.12 | 6862875.79 | 1031.83 | PERFORATOR-7.5 | 7.5 | 60.38 | 43.08 |
| 3005 | 2256064.89 | 6862881.26 | 1031.97 | PERFORATOR-7.8 | 7.8 | 55.08 | 25.85 |
| 3006 | 2256060.30 | 6862873.32 | 1031.74 | PERFORATOR-7.8 | 7.8 | 45.94 | 25.01 |
| 3007 | 2256067.42 | 6862889.96 | 1031.91 | PERFORATOR-8.9 | 8.9 | 64.03 | 24.49 |
| 3008 | 2256066.57 | 6862892.43 | 1031.92 | PERFORATOR-9.3 | 9.3 | 65.95 | 22.92 |
| 3009 | 2256052.66 | 6862893.26 | 1031.86 | PERFORATOR-7.2 | 7.2 | 62.68 | 10.83 |
| 3010 | 2256051.59 | 6862893.35 | 1031.88 | PERFORATOR-7.2 | 7.2 | 62.59 | 9.85 |
| 3011 | 2256053.47 | 6862901.34 | 1031.95 | PERFORATOR-8.1 | 8.1 | 70.78 | 10.25 |
| 3012 | 2256059.90 | 6862920.07 | 1032.25 | PERFORATOR-7.2 | 7.2 | 90.41 | 12.15 |
| 3013 | 2256048.20 | 6862915.35 | 1031.99 | PERFORATOR-5.9 | 5.9 | 83.98 | 5.00 |
| 3014 | 2256033.76 | 6862920.07 | 1031.93 | PERFORATOR-16 | 16 | 88.66 | 355.39 |
| 3015 | 2256075.64 | 6862814.26 | 1031.29 | PERFORATOR-10.4 | 10.4 | 38.88 | 116.63 |
| 3016 | 2256076.52 | 6862812.43 | 1031.24 | PERFORATOR-8.4 | 8.4 | 40.51 | 118.39 |
| 3017 | 2256082.38 | 6862798.14 | 1031.13 | PERFORATOR-15.1 | 15.1 | 53.36 | 128.96 |
| 3018 | 2256071.90 | 6862795.15 | 1031.06 | PERFORATOR-7.8 | 7.8 | 47.93 | 139.67 |
| 3019 | 2256072.59 | 6862783.79 | 1030.90 | PERFORATOR-5.4 | 5.4 | 57.45 | 146.49 |
| 3020 | 2256069.46 | 6862783.09 | 1030.93 | PERFORATOR-5.6 | 5.6 | 56.37 | 149.54 |
| 3021 | 2256069.30 | 6862781.14 | 1030.91 | PERFORATOR-5.2 | 5.2 | 57.99 | 150.65 |
| 3022 | 2256065.46 | 6862786.79 | 1030.95 | PERFORATOR-7.6 | 7.6 | 51.19 | 151.29 |
| 3024 | 2256058.53 | 6862776.48 | 1030.63 | PERFORATOR-5.0 | 5 | 57.96 | 162.27 |
| 3025 | 2256061.90 | 6862771.76 | 1030.61 | PERFORATOR-7.5 | 7.5 | 63.50 | 160.67 |
| 3026 | 2256066.70 | 6862770.44 | 1030.70 | PERFORATOR-8.5 | 8.5 | 66.47 | 157.14 |
| 3027 | 2256064.69 | 6862756.85 | 1030.52 | PERFORATOR-6.5 | 6.5 | 78.54 | 162.35 |
| 3028 | 2256053.71 | 6862750.97 | 1030.30 | CARRIER-TUBE-29.9 | 29.9 | 81.73 | 170.97 |
| 3029 | 2256027.79 | 6862672.67 | 1029.15 | GUN_BODY | 8090 | 159.56 | 184.71 |
| 3031 | 2256117.51 | 6863109.01 | 1034.51 | PERFORATOR-8.2 | 8.2 | 287.71 | 15.45 |
| 3032 | 2256105.40 | 6863070.99 | 1034.25 | PERFORATOR-5.0 | 5 | 247.85 | 15.09 |
| 3033 | 2256053.51 | 6863060.37 | 1033.32 | PERFORATOR-8.2 | 8.2 | 229.03 | 3.16 |
| 3034 | 2256059.77 | 6863031.57 | 1033.09 | PERFORATOR-6.3 | 6.3 | 200.77 | 5.40 |
| 3035 | 2256067.00 | 6862979.65 | 1032.83 | CARRIER-TUBE-111 | 111 | 150.25 | 10.01 |
| 3036 | 2256091.76 | 6862937.35 | 1032.62 | PERFORATOR-8.8 | 8.8 | 117.27 | 25.71 |
| 3037 | 2256051.82 | 6862868.84 | 1031.43 | PERFORATOR-5.0 | 5 | 38.73 | 16.41 |
| 3038 | 2256064.20 | 6862875.75 | 1031.87 | PERFORATOR-5.2 | 5.2 | 49.85 | 27.89 |
| 3039 | 2256081.12 | 6862905.03 | 1032.14 | PERFORATOR-7.0 | 7 | 83.66 | 28.75 |
| 3040 | 2256059.79 | 6862928.56 | 1032.26 | PERFORATOR-6.9 | 6.9 | 98.70 | 11.05 |
| 3041 | 2256049.48 | 6862977.28 | 1032.56 | PERFORATOR-8.3 | 8.3 | 145.85 | 3.38 |
| 3042 | 2256052.47 | 6862982.13 | 1032.65 | PERFORATOR-5.2 | 5.2 | 150.89 | 4.40 |
| 3043 | 2256046.99 | 6862997.53 | 1032.77 | CARRIER-TUBE-15.2 | 15.2 | 165.96 | 2.11 |

| | | | | | | | |
|---|---|---|---|---|---|---|---|
| 3044 | 2256060.92 | 6863077.28 | 1033.65 | PERFORATOR-12.1 | 12.1 | 246.41 | 4.66 |
| 3045 | 2256035.56 | 6862999.29 | 1032.70 | PERFORATOR-7.4 | 7.4 | 167.69 | 358.18 |
| 3046 | 2256042.40 | 6862987.06 | 1032.48 | PERFORATOR-8.3 | 8.3 | 155.38 | 0.56 |
| 3047 | 2256037.08 | 6862980.53 | 1032.54 | PERFORATOR-8.3 | 8.3 | 148.89 | 358.54 |
| 3048 | 2256010.94 | 6862974.74 | 1032.21 | CARRIER-TUBE-49.4 | 49.4 | 146.15 | 348.18 |
| 3049 | 2256032.48 | 6862662.39 | 1028.99 | PERFORATOR-5.1 | 5.1 | 169.50 | 182.84 |
| 3050 | 2256029.67 | 6862874.84 | 1031.37 | PERFORATOR-7.7 | 7.7 | 44.58 | 345.44 |
| 2001 | 2256067.22 | 6862830.81 | 1031.22 | PERFORATOR-8.3 | 8.3 | 26.36 | 91.91 |
| 2002 | 2256065.55 | 6862842.81 | 1031.34 | PERFORATOR-6.5 | 6.5 | 27.06 | 65.74 |
| 2003 | 2256069.14 | 6862846.41 | 1031.37 | PERFORATOR-5.1 | 5.1 | 31.86 | 62.48 |
| 2004 | 2256069.61 | 6862851.93 | 1031.46 | PERFORATOR-8.3 | 8.3 | 35.15 | 54.83 |
| 2005 | 2256070.82 | 6862852.90 | 1031.53 | PERFORATOR-5.2 | 5.2 | 36.69 | 54.69 |
| 2006 | 2256073.12 | 6862854.26 | 1031.42 | PERFORATOR-8.8 | 8.8 | 39.36 | 55.00 |
| 2007 | 2256079.39 | 6862848.29 | 1031.66 | PERFORATOR-6.6 | 6.6 | 41.94 | 66.68 |
| 2008 | 2256079.63 | 6862855.84 | 1031.64 | PERFORATOR-5.1 | 5.1 | 45.67 | 58.06 |
| 2009 | 2256072.70 | 6862862.67 | 1031.55 | PERFORATOR-7.2 | 7.2 | 44.42 | 45.77 |

## Test 6

| PT_ID | East | North | Elev | Description | Mass (g) | Distance (ft) | Azimuth (°) |
|---|---|---|---|---|---|---|---|
| 2001 | 2256044.93 | 6862829.16 | 1031.03 | PERFORATOR-9.3 | 9.3 | 4.78 | 122.00 |
| 2002 | 2256045.45 | 6862829.85 | 1031.04 | PERFORATOR-18.9 | 18.9 | 4.93 | 111.85 |
| 2003 | 2256049.76 | 6862841.00 | 1031.18 | PERFORATOR-8.1 | 8.1 | 12.87 | 43.67 |
| 2004 | 2256085.51 | 6862843.30 | 1031.66 | PERFORATOR-15.2 | 15.2 | 46.12 | 75.42 |
| 2005 | 2256101.02 | 6862831.99 | 1031.67 | PERFORATOR-5.7 | 5.7 | 60.15 | 89.71 |
| 2006 | 2256069.13 | 6862792.78 | 1031.05 | PERFORATOR-5.1 | 5.1 | 48.08 | 144.02 |
| 2007 | 2256104.62 | 6862766.59 | 1030.90 | PERFORATOR-5.0 | 5 | 91.11 | 135.60 |
| 2008 | 2256083.15 | 6862769.89 | 1030.80 | GUN_BODY-2 | 1638 | 74.87 | 145.63 |
| 2009 | 2256081.17 | 6862739.65 | 1030.54 | GUN_BODY-3 | 3640 | 100.48 | 156.36 |
| 2010 | 2256063.03 | 6862742.26 | 1030.40 | PERFORATOR-39.1 | 39.1 | 92.13 | 166.09 |
| 2011 | 2256048.83 | 6862734.49 | 1030.12 | PERFORATOR-5.2 | 5.2 | 97.52 | 175.32 |
| 2012 | 2256036.74 | 6862786.38 | 1030.50 | PERFORATOR-22.1 | 22.1 | 45.50 | 185.22 |
| 2013 | 2256038.13 | 6862791.02 | 1030.56 | PERFORATOR-9.3 | 9.3 | 40.76 | 183.86 |
| 2014 | 2256050.74 | 6862816.07 | 1031.02 | PERFORATOR-16.0 | 16 | 18.47 | 147.73 |
| 2015 | 2256036.98 | 6862831.40 | 1031.06 | PERFORATOR-13.8 | 13.8 | 3.91 | 265.76 |
| 2016 | 2256038.33 | 6862852.10 | 1031.28 | PERFORATOR-5.1 | 5.1 | 20.57 | 352.87 |
| 2017 | 2256036.41 | 6862856.65 | 1031.28 | PERFORATOR-12.9 | 12.9 | 25.36 | 349.84 |
| 2018 | 2256025.74 | 6862863.00 | 1031.29 | PERFORATOR-6.3 | 6.3 | 34.78 | 334.19 |
| 2019 | 2256028.26 | 6862871.95 | 1031.34 | PERFORATOR-7.7 | 7.7 | 42.19 | 342.61 |
| 2020 | 2256042.49 | 6862883.49 | 1031.67 | PERFORATOR-16.9 | 16.9 | 51.82 | 1.78 |
| 2021 | 2256068.60 | 6862888.69 | 1031.89 | PERFORATOR-5.8 | 5.8 | 63.38 | 25.93 |
| 2022 | 2256073.64 | 6862868.11 | 1031.58 | PERFORATOR-8.4 | 8.4 | 48.99 | 41.97 |
| 2023 | 2256020.81 | 6862825.05 | 1030.79 | PERFORATOR-5.2 | 5.2 | 21.14 | 251.70 |
| 2024 | 2256014.05 | 6862848.38 | 1031.04 | GUN_BODY-9.5 | 3907 | 31.60 | 301.89 |
| 2025 | 2256003.35 | 6862868.91 | 1031.03 | PERFORATOR-12.1 | 12.1 | 52.86 | 314.77 |
| 2026 | 2255989.61 | 6862846.65 | 1030.70 | PERFORATOR-6.8 | 6.8 | 53.41 | 286.27 |
| 2027 | 2255985.73 | 6862845.58 | 1030.65 | PERFORATOR-5.4 | 5.4 | 56.87 | 284.13 |
| 2028 | 2255959.15 | 6862827.77 | 1030.03 | PERFORATOR-21.2 | 21.2 | 81.82 | 267.26 |
| 2029 | 2255957.59 | 6862838.61 | 1030.19 | PERFORATOR-8.6 | 8.6 | 83.57 | 274.75 |
| 2030 | 2255956.65 | 6862867.07 | 1030.50 | PERFORATOR-16.8 | 16.8 | 91.36 | 292.78 |
| 2031 | 2256045.68 | 6862951.60 | 1032.34 | PERFORATOR-14.4 | 14.4 | 120.01 | 2.29 |
| 2032 | 2256064.09 | 6862955.88 | 1032.54 | PERFORATOR-5.7 | 5.7 | 126.34 | 10.59 |
| 2033 | 2256085.28 | 6863027.24 | 1033.37 | PERFORATOR-9.8 | 9.8 | 200.53 | 12.79 |
| 2034 | 2256089.45 | 6862957.11 | 1032.77 | PERFORATOR-6.7 | 6.7 | 134.50 | 21.17 |
| 2036 | 2255895.49 | 6862792.08 | 1029.24 | PERFORATOR-10.9 | 10.9 | 150.68 | 254.76 |
| 2037 | 2255857.29 | 6862639.01 | 1026.93 | PERFORATOR-19.6 | 19.6 | 266.14 | 223.62 |
| 2038 | 2255775.74 | 6862602.34 | 1025.62 | PERFORATOR-9.4 | 9.4 | 350.57 | 229.14 |
| 2039 | 2255752.95 | 6862810.76 | 1027.00 | PERFORATOR-5.0 | 5 | 288.69 | 265.84 |
| 2040 | 2255817.38 | 6862837.45 | 1028.61 | PERFORATOR-38.3 | 38.3 | 223.58 | 271.48 |
| 2041 | 2255848.59 | 6862847.71 | 1029.31 | PERFORATOR-18.6 | 18.6 | 192.95 | 274.76 |
| 2042 | 2255811.32 | 6862872.80 | 1028.90 | PERFORATOR-23.6 | 23.6 | 233.21 | 280.15 |

| | | | | | | | |
|---|---|---|---|---|---|---|---|
| 2043 | 2255875.93 | 6862828.06 | 1029.50 | PERFORATOR-14.7 | 14.7 | 164.99 | 268.74 |
| 2044 | 2255918.07 | 6862811.50 | 1029.47 | PERFORATOR-21.5 | 21.5 | 124.46 | 260.66 |
| 2045 | 2255931.94 | 6862837.03 | 1030.00 | PERFORATOR-41.2 | 41.2 | 109.07 | 272.81 |
| 2046 | 2255918.21 | 6862884.88 | 1030.49 | PERFORATOR-17.3 | 17.3 | 133.70 | 293.44 |
| 2047 | 2255918.94 | 6862895.59 | 1030.66 | PERFORATOR-6.0 | 6 | 137.67 | 297.66 |
| 2048 | 2255928.37 | 6862946.87 | 1031.34 | PERFORATOR-13.7 | 13.7 | 161.01 | 315.67 |
| 2049 | 2255967.42 | 6862948.35 | 1031.29 | PERFORATOR-10.7 | 10.7 | 137.87 | 327.80 |
| 2050 | 2256143.70 | 6862787.10 | 1031.59 | PERFORATOR-18.4 | 18.4 | 112.08 | 113.44 |
| 2051 | 2256139.13 | 6862764.61 | 1031.38 | PERFORATOR-23.6 | 23.6 | 118.97 | 124.32 |
| 2052 | 2256229.79 | 6862729.21 | 1031.94 | PERFORATOR-36.4 | 36.4 | 214.92 | 118.48 |
| 2053 | 2256110.45 | 6862738.84 | 1030.87 | PERFORATOR-18.7 | 18.7 | 116.02 | 143.16 |
| 2054 | 2256166.06 | 6862581.77 | 1029.73 | PERFORATOR-16.7 | 16.7 | 279.51 | 153.39 |
| 2056 | 2256033.67 | 6862707.22 | 1029.50 | PERFORATOR-6.9 | 6.9 | 124.68 | 183.31 |
| 2057 | 2256042.69 | 6862719.12 | 1029.90 | PERFORATOR-5.0 | 5 | 112.58 | 179.08 |
| 2059 | 2255987.78 | 6863195.73 | 1034.43 | PERFORATOR-9.0 | 9 | 367.89 | 351.70 |
| 2061 | 2256052.67 | 6862997.06 | 1032.76 | DET-ASSEM-2.5 | 2.5 | 165.79 | 4.08 |
| 2062 | 2256043.24 | 6862974.33 | 1032.37 | PERFORATOR-9.9 | 9.9 | 142.66 | 0.95 |
| 2063 | 2256070.37 | 6862869.91 | 1031.64 | PERFORATOR-5.1 | 5.1 | 48.28 | 37.65 |
| 2064 | 2256120.41 | 6862889.54 | 1032.37 | PERFORATOR-15.3 | 15.3 | 98.35 | 53.97 |
| 2065 | 2256071.64 | 6862761.34 | 1030.57 | PERFORATOR-5.0 | 5 | 76.78 | 156.38 |
| 2066 | 2256039.86 | 6862749.34 | 1030.17 | PERFORATOR-13.0 | 13 | 82.35 | 180.71 |
| 2067 | 2256045.06 | 6862824.75 | 1030.99 | PERFORATOR-7.4 | 7.4 | 8.10 | 148.91 |

## Test 7

| PT_ID | East | North | Elev | Description | Mass (g) | Distance (ft) | Azimuth (°) |
|---|---|---|---|---|---|---|---|
| 2001 | 2256044.32 | 6862810.24 | 1030.86 | PERFORATOR-15.2 | 15.2 | 21.72 | 170.87 |
| 2002 | 2256048.66 | 6862799.72 | 1030.76 | PERFORATOR-5.1 | 5.1 | 32.91 | 166.32 |
| 2003 | 2256058.76 | 6862792.29 | 1030.82 | PERFORATOR-9.9 | 9.9 | 43.27 | 155.59 |
| 2004 | 2256068.13 | 6862781.20 | 1030.83 | PERFORATOR-5.0 | 5 | 57.38 | 151.64 |
| 2005 | 2256049.44 | 6862784.69 | 1030.60 | PERFORATOR-5.0 | 5 | 47.77 | 169.67 |
| 2006 | 2256049.78 | 6862775.20 | 1030.54 | PERFORATOR-5.5 | 5.5 | 57.18 | 171.04 |
| 2008 | 2256063.71 | 6862757.71 | 1030.53 | PERFORATOR-8.6 | 8.6 | 77.42 | 162.85 |
| 2009 | 2256070.87 | 6862749.42 | 1030.50 | PERFORATOR-11.9 | 11.9 | 87.57 | 159.97 |
| 2010 | 2256055.29 | 6862745.04 | 1030.30 | PERFORATOR-5.5 | 5.5 | 87.84 | 170.56 |
| 2011 | 2256046.89 | 6862742.65 | 1030.05 | PERFORATOR-8.3 | 8.3 | 89.24 | 176.14 |
| 2012 | 2256020.63 | 6862731.89 | 1029.64 | PERFORATOR-10.1 | 10.1 | 101.83 | 191.47 |
| 2013 | 2256038.78 | 6862834.25 | 1031.01 | PERFORATOR-8.6 | 8.6 | 3.32 | 320.68 |
| 2014 | 2256038.42 | 6862835.46 | 1031.04 | PERFORATOR-7.3 | 7.3 | 4.50 | 326.92 |
| 2016 | 2256023.99 | 6862866.44 | 1031.22 | PERFORATOR-6.0 | 6 | 38.64 | 334.08 |
| 2017 | 2256063.87 | 6862968.83 | 1032.70 | PERFORATOR-5.8 | 5.8 | 139.05 | 9.52 |
| 2018 | 2256039.20 | 6862831.90 | 1031.59 | GUN_BODY | 8451 | 1.69 | 277.26 |
| 2019 | 2256056.20 | 6862759.84 | 1030.48 | PERFORATOR-8.8 | 8.8 | 73.47 | 167.96 |
| 2020 | 2256057.38 | 6862763.49 | 1030.58 | PERFORATOR-8.3 | 8.3 | 70.17 | 166.40 |
| 2021 | 2256075.21 | 6862775.36 | 1030.81 | PERFORATOR-6.6 | 6.6 | 65.96 | 148.64 |
| 2022 | 2256041.77 | 6862789.18 | 1030.60 | PERFORATOR-5.4 | 5.4 | 42.51 | 178.79 |
| 2023 | 2256037.56 | 6862744.15 | 1030.11 | PERFORATOR-7.8 | 7.8 | 87.60 | 182.17 |
| 2024 | 2255935.57 | 6862862.18 | 1030.36 | PERFORATOR-5.4 | 5.4 | 109.64 | 286.15 |
| 2025 | 2255788.22 | 6862914.83 | 1028.58 | PERFORATOR-15.8 | 15.8 | 265.99 | 288.21 |
| 2026 | 2255819.33 | 6863030.92 | 1030.47 | PERFORATOR-14.4 | 14.4 | 297.96 | 311.96 |
| 2027 | 2256145.35 | 6862772.31 | 1031.44 | PERFORATOR-8.3 | 8.3 | 120.17 | 119.61 |
| 2028 | 2256191.78 | 6862697.42 | 1031.42 | CARRIER-TUBE-52 | 52 | 201.99 | 131.66 |
| 2029 | 2256097.31 | 6862725.21 | 1030.57 | PERFORATOR-7.2 | 7.2 | 120.51 | 152.08 |
| 2030 | 2256100.37 | 6862731.82 | 1030.82 | CARRIER-TUBE-140.4 | 140.4 | 116.25 | 149.22 |
| 2031 | 2256037.19 | 6863015.31 | 1032.66 | PERFORATOR-6.5 | 6.5 | 183.66 | 358.85 |
| 2032 | 2256060.79 | 6862757.48 | 1030.54 | PERFORATOR-6.5 | 6.5 | 76.83 | 164.98 |
| 2033 | 2256084.40 | 6862709.24 | 1030.27 | PERFORATOR-5.0 | 5 | 129.95 | 160.43 |
| 2034 | 2256141.10 | 6862612.79 | 1029.77 | CARRIER-TUBE-8.8 | 8.8 | 240.75 | 155.40 |
| 2035 | 2256052.88 | 6862719.23 | 1029.99 | PERFORATOR-12.5 | 12.5 | 113.10 | 173.91 |
| 2036 | 2256051.72 | 6862729.34 | 1030.14 | PERFORATOR-5.0 | 5 | 102.92 | 173.95 |
| 2037 | 2256047.40 | 6862929.39 | 1032.14 | PERFORATOR-8.3 | 8.3 | 97.92 | 3.82 |

## Test 8

| PT_ID | East | North | Elev | Description | Mass (g) | Distance (ft) | Azimuth (°) |
|---|---|---|---|---|---|---|---|
| 2001 | 2256040.07 | 6862840.25 | 1031.08 | PERFORATOR-5.1 | 5.1 | 8.60 | 354.59 |
| 2002 | 2256041.96 | 6862838.71 | 1031.03 | PERFORATOR-5.2 | 5.2 | 7.11 | 8.79 |
| 2003 | 2256041.23 | 6862836.40 | 1031.03 | PERFORATOR-9.6 | 9.6 | 4.73 | 4.28 |
| 2006 | 2256039.80 | 6862834.93 | 1030.97 | PERFORATOR-5.1 | 5.1 | 3.41 | 341.62 |
| 2007 | 2256039.10 | 6862835.74 | 1031.00 | PERFORATOR-6.3 | 6.3 | 4.43 | 336.26 |
| 2008 | 2256040.99 | 6862833.04 | 1030.91 | PERFORATOR-5.0 | 5 | 1.36 | 4.82 |
| 2009 | 2256041.55 | 6862831.50 | 1030.85 | PERFORATOR-8.8 | 8.8 | 0.70 | 105.59 |
| 2010 | 2256040.36 | 6862832.68 | 1030.93 | PERFORATOR-7.3 | 7.3 | 1.12 | 332.45 |
| 2011 | 2256040.09 | 6862833.32 | 1030.92 | PERFORATOR-5.0 | 5 | 1.82 | 334.31 |
| 2012 | 2256038.09 | 6862830.64 | 1030.95 | PERFORATOR-5.0 | 5 | 2.98 | 249.42 |
| 2013 | 2256035.46 | 6862828.35 | 1031.61 | PERFORATOR-5.3 | 5.3 | 6.37 | 238.38 |
| 2014 | 2256048.79 | 6862831.57 | 1031.08 | PERFORATOR-7.9 | 7.9 | 7.91 | 90.85 |
| 2015 | 2256059.02 | 6862827.33 | 1031.18 | PERFORATOR-8.1 | 8.1 | 18.66 | 103.52 |
| 2016 | 2256044.88 | 6862841.16 | 1031.08 | BUCKLE-53 | 53 | 10.28 | 22.89 |
| 2017 | 2256051.45 | 6862834.45 | 1031.12 | BUCKLE-53.2 | 53.2 | 10.92 | 75.33 |
| 2018 | 2256041.32 | 6862828.40 | 1030.98 | PERFORATOR-7.2 | 7.2 | 3.32 | 172.36 |
| 2019 | 2256035.04 | 6862829.83 | 1031.11 | PERFORATOR-7.6 | 7.6 | 6.13 | 252.34 |
| 2021 | 2256034.13 | 6862851.95 | 1031.24 | PERFORATOR-6.2 | 6.2 | 21.35 | 341.58 |
| 2022 | 2256040.79 | 6862857.91 | 1031.34 | PERFORATOR-5.8 | 5.8 | 26.23 | 359.81 |
| 2023 | 2256042.43 | 6862858.73 | 1031.42 | PERFORATOR-9.3 | 9.3 | 27.08 | 3.28 |
| 2024 | 2256044.45 | 6862850.95 | 1031.26 | CARRIER-TUBE-56 | 56 | 19.59 | 10.51 |
| 2025 | 2256050.06 | 6862850.19 | 1031.27 | CARRIER-TUBE-142.1 | 142.1 | 20.65 | 26.38 |
| 2026 | 2256053.00 | 6862851.60 | 1031.37 | PERFORATOR-5.5 | 5.5 | 23.31 | 31.32 |
| 2027 | 2256054.01 | 6862856.55 | 1031.42 | PERFORATOR-9.4 | 9.4 | 28.11 | 27.85 |
| 2028 | 2256057.93 | 6862854.02 | 1031.37 | PERFORATOR-5.3 | 5.3 | 28.10 | 37.35 |
| 2029 | 2256070.13 | 6862856.02 | 1031.51 | PERFORATOR-5.2 | 5.2 | 38.05 | 50.24 |
| 2030 | 2256071.60 | 6862869.03 | 1031.69 | PERFORATOR-11.2 | 11.2 | 48.36 | 39.45 |
| 2031 | 2256067.69 | 6862874.57 | 1031.80 | PERFORATOR-7.1 | 7.1 | 50.58 | 32.02 |
| 2032 | 2256074.28 | 6862878.82 | 1031.75 | PERFORATOR-7.2 | 7.2 | 57.77 | 35.32 |
| 2033 | 2256076.09 | 6862889.34 | 1032.00 | PERFORATOR-5.0 | 5 | 67.55 | 31.41 |
| 2034 | 2256081.45 | 6862894.41 | 1032.08 | PERFORATOR-13.3 | 13.3 | 74.70 | 32.90 |
| 2035 | 2256091.08 | 6862903.37 | 1032.14 | PERFORATOR-6.3 | 6.3 | 87.51 | 35.01 |
| 2036 | 2256094.12 | 6862899.77 | 1032.21 | PERFORATOR-6.1 | 6.1 | 86.43 | 38.03 |
| 2037 | 2256102.74 | 6862907.65 | 1032.38 | PERFORATOR-7.7 | 7.7 | 97.96 | 39.16 |
| 2038 | 2256081.21 | 6862917.82 | 1032.41 | PERFORATOR-8.4 | 8.4 | 95.11 | 25.09 |
| 2039 | 2256043.46 | 6862914.84 | 1031.90 | PERFORATOR-9.1 | 9.1 | 83.19 | 1.78 |
| 2040 | 2256045.95 | 6862913.69 | 1032.09 | PERFORATOR-5.5 | 5.5 | 82.16 | 3.54 |
| 2041 | 2256046.68 | 6862901.69 | 1031.95 | PERFORATOR-9.8 | 9.8 | 70.25 | 4.74 |
| 2042 | 2256041.58 | 6862924.48 | 1032.06 | PERFORATOR-8.0 | 8 | 92.80 | 0.43 |
| 2043 | 2256049.51 | 6862890.52 | 1031.84 | PERFORATOR-5.1 | 5.1 | 59.46 | 8.34 |
| 2044 | 2256050.74 | 6862884.26 | 1031.69 | PERFORATOR-5.6 | 5.6 | 53.49 | 10.62 |

| | | | | | | | |
|---|---|---|---|---|---|---|---|
| 2045 | 2256058.53 | 6862868.37 | 1031.65 | PERFORATOR-5.0 | 5 | 40.71 | 25.70 |
| 2046 | 2256053.14 | 6862867.39 | 1031.51 | PERFORATOR-15.5 | 15.5 | 37.75 | 18.95 |
| 2047 | 2256049.40 | 6862873.51 | 1031.51 | CARRIER-TUBE-15.6 | 15.6 | 42.68 | 11.52 |
| 2048 | 2256036.03 | 6862871.32 | 1031.44 | PERFORATOR-9.0 | 9 | 39.93 | 353.03 |
| 2049 | 2256037.46 | 6862871.92 | 1031.49 | PERFORATOR-11.0 | 11 | 40.37 | 355.14 |
| 2050 | 2256034.95 | 6862873.26 | 1031.35 | PERFORATOR-6.3 | 6.3 | 42.00 | 351.88 |
| 2051 | 2256035.28 | 6862875.54 | 1031.48 | PERFORATOR-5.2 | 5.2 | 44.20 | 352.72 |
| 2052 | 2256043.64 | 6862876.49 | 1031.58 | PERFORATOR-7.7 | 7.7 | 44.88 | 3.53 |
| 2053 | 2256043.00 | 6862878.53 | 1031.68 | CARRIER-TUBE-48.1 | 48.1 | 46.89 | 2.59 |
| 2054 | 2256038.01 | 6862887.79 | 1031.64 | PERFORATOR-6.5 | 6.5 | 56.18 | 357.08 |
| 2055 | 2256009.81 | 6862900.37 | 1031.47 | PERFORATOR-10.3 | 10.3 | 75.38 | 335.66 |
| 2056 | 2255980.80 | 6862905.54 | 1031.11 | CARRIER-TUBE-24.3 | 24.3 | 95.20 | 320.87 |
| 2057 | 2256000.89 | 6862867.15 | 1031.07 | PERFORATOR-8.0 | 8 | 53.45 | 311.57 |
| 2058 | 2255971.50 | 6862813.11 | 1030.02 | PERFORATOR-5.3 | 5.3 | 71.82 | 255.01 |
| 2059 | 2255967.21 | 6862809.47 | 1029.94 | PERFORATOR-5.2 | 5.2 | 76.95 | 253.22 |
| 2060 | 2255967.92 | 6862804.19 | 1029.90 | PERFORATOR-5.0 | 5 | 77.97 | 249.35 |
| 2061 | 2255960.73 | 6862805.29 | 1029.79 | CARRIER-TUBE-138.4 | 138.4 | 84.39 | 251.77 |
| 2062 | 2255959.54 | 6862814.32 | 1029.95 | PERFORATOR-6.8 | 6.8 | 83.17 | 257.95 |
| 2064 | 2255942.92 | 6862819.93 | 1029.88 | PERFORATOR-5.0 | 5 | 98.67 | 263.16 |
| 2065 | 2255948.01 | 6862802.98 | 1029.71 | PERFORATOR-9.3 | 9.3 | 97.20 | 252.82 |
| 2066 | 2255944.58 | 6862797.96 | 1029.60 | PERFORATOR-7.1 | 7.1 | 102.03 | 250.70 |
| 2067 | 2255983.18 | 6862802.77 | 1030.15 | PERFORATOR-5.4 | 5.4 | 64.54 | 243.38 |
| 2068 | 2256005.15 | 6862804.93 | 1030.47 | PERFORATOR-6.2 | 6.2 | 44.64 | 233.17 |
| 2069 | 2256055.40 | 6862932.80 | 1032.28 | PERFORATOR-6.9 | 6.9 | 102.15 | 8.18 |
| 2070 | 2256066.46 | 6862931.03 | 1032.37 | PERFORATOR-5.6 | 5.6 | 102.58 | 14.44 |
| 2071 | 2256045.19 | 6862942.26 | 1032.26 | PERFORATOR-5.4 | 5.4 | 110.65 | 2.23 |
| 2072 | 2256035.02 | 6862948.80 | 1032.25 | CARRIER-TUBE-114.5 | 114.5 | 117.25 | 357.13 |
| 2073 | 2256052.94 | 6862959.99 | 1032.51 | PERFORATOR-7.0 | 7 | 128.86 | 5.37 |
| 2074 | 2256049.86 | 6862965.59 | 1032.59 | PERFORATOR-6.9 | 6.9 | 134.20 | 3.84 |
| 2075 | 2256071.17 | 6862956.86 | 1032.57 | PERFORATOR-5.8 | 5.8 | 128.79 | 13.60 |
| 2076 | 2256064.49 | 6862949.58 | 1032.51 | PERFORATOR-5.0 | 5 | 120.24 | 11.32 |
| 2077 | 2256064.17 | 6862969.60 | 1032.75 | PERFORATOR-8.9 | 8.9 | 139.87 | 9.59 |
| 2078 | 2256060.55 | 6862982.32 | 1032.84 | PERFORATOR-12.6 | 12.6 | 151.91 | 7.44 |
| 2079 | 2256051.23 | 6862996.98 | 1032.77 | PERFORATOR-5.0 | 5 | 165.61 | 3.58 |
| 2080 | 2256061.33 | 6863012.46 | 1033.16 | PERFORATOR-7.6 | 7.6 | 181.92 | 6.45 |
| 2081 | 2256075.71 | 6862990.40 | 1032.97 | PERFORATOR-8.6 | 8.6 | 162.49 | 12.38 |
| 2082 | 2256081.39 | 6863016.49 | 1033.33 | PERFORATOR-6.5 | 6.5 | 189.19 | 12.37 |
| 2083 | 2256077.18 | 6863020.56 | 1033.24 | PERFORATOR-6.8 | 6.8 | 192.32 | 10.88 |
| 2084 | 2256071.32 | 6863019.34 | 1033.18 | PERFORATOR-8.7 | 8.7 | 190.10 | 9.21 |
| 2085 | 2256057.88 | 6863037.27 | 1033.19 | PERFORATOR-5.4 | 5.4 | 206.28 | 4.73 |
| 2086 | 2256083.82 | 6863058.15 | 1033.52 | PERFORATOR-6.0 | 6 | 230.50 | 10.74 |
| 2087 | 2256083.13 | 6863051.93 | 1033.55 | PERFORATOR-7.6 | 7.6 | 224.26 | 10.86 |
| 2088 | 2256072.06 | 6863065.42 | 1033.60 | PERFORATOR-5.0 | 5 | 235.80 | 7.60 |
| 2089 | 2256059.82 | 6863120.89 | 1034.01 | CARRIER-TUBE-50.4 | 50.4 | 289.82 | 3.75 |
| 2090 | 2256056.88 | 6863101.54 | 1033.82 | PERFORATOR-5.0 | 5 | 270.33 | 3.39 |

| | | | | | | | |
|---|---|---|---|---|---|---|---|
| 2091 | 2256080.93 | 6863136.04 | 1034.47 | PERFORATOR-5.2 | 5.2 | 306.97 | 7.50 |
| 2092 | 2256082.72 | 6863158.72 | 1034.69 | PERFORATOR-6.7 | 6.7 | 329.69 | 7.29 |
| 2093 | 2256099.05 | 6863166.39 | 1035.13 | PERFORATOR-7.3 | 7.3 | 339.72 | 9.86 |
| 2094 | 2256096.23 | 6863068.21 | 1033.91 | PERFORATOR-9.1 | 9.1 | 242.91 | 13.17 |
| 2095 | 2256128.88 | 6863033.73 | 1033.86 | CARRIER-TUBE-48.3 | 48.3 | 220.38 | 23.53 |
| 2096 | 2256143.75 | 6863003.48 | 1033.59 | PERFORATOR-5.4 | 5.4 | 200.24 | 30.91 |
| 2097 | 2256150.48 | 6862998.71 | 1033.59 | CARRIER-TUBE-27 | 27 | 199.77 | 33.27 |
| 2098 | 2256143.92 | 6862993.15 | 1033.48 | PERFORATOR-6.8 | 6.8 | 191.54 | 32.55 |
| 2099 | 2256110.96 | 6862952.19 | 1032.90 | PERFORATOR-5.0 | 5 | 139.40 | 30.18 |
| 2100 | 2256118.14 | 6862942.81 | 1032.73 | PERFORATOR-5.0 | 5 | 135.34 | 34.81 |
| 2101 | 2256096.74 | 6862921.85 | 1032.46 | PERFORATOR-9.2 | 9.2 | 106.06 | 31.78 |
| 2102 | 2256096.75 | 6862921.85 | 1032.46 | CARRIER-TUBE-17O | 170 | 106.07 | 31.78 |
| 2103 | 2256096.74 | 6862921.85 | 1032.46 | CARRIER-TUBE-90.4 | 90.4 | 106.06 | 31.78 |
| 2104 | 2256096.73 | 6862921.86 | 1032.47 | CARRIER-TUBE-33.3 | 33.3 | 106.07 | 31.77 |
| 2105 | 2256096.53 | 6862921.81 | 1032.46 | PERFORATOR-8.2 | 8.2 | 105.92 | 31.70 |
| 2106 | 2256096.35 | 6862921.72 | 1032.45 | PERFORATOR-5.0 | 5 | 105.75 | 31.64 |
| 2107 | 2256096.75 | 6862921.85 | 1032.46 | PERFORATOR-5.9 | 5.9 | 106.07 | 31.78 |
| 2108 | 2256096.76 | 6862921.83 | 1032.47 | PERFORATOR-5.8 | 5.8 | 106.06 | 31.79 |
| 2109 | 2256096.67 | 6862921.88 | 1032.46 | PERFORATOR-6.5 | 6.5 | 106.05 | 31.74 |
| 2110 | 2256096.74 | 6862921.85 | 1032.45 | PERFORATOR-5.0 | 5 | 106.07 | 31.78 |
| 2111 | 2256002.12 | 6862575.89 | 1027.66 | PERFORATOR-6.7 | 6.7 | 258.71 | 188.62 |
| 2113 | 2256033.96 | 6862558.00 | 1027.75 | GUN_BODY-6 | 8121 | 273.77 | 181.45 |
| 2114 | 2255941.72 | 6862778.89 | 1029.38 | PERFORATOR-6.8 | 6.8 | 112.34 | 241.96 |
| 2115 | 2255939.71 | 6862797.48 | 1029.51 | PERFORATOR-8.6 | 8.6 | 106.80 | 251.32 |
| 2116 | 2255924.20 | 6862785.03 | 1029.33 | PERFORATOR-15.4 | 15.4 | 125.66 | 248.21 |
| 2117 | 2255927.33 | 6862767.92 | 1029.13 | PERFORATOR-12.0 | 12 | 130.23 | 240.68 |
| 2118 | 2255933.20 | 6862820.38 | 1029.85 | PERFORATOR-5.1 | 5.1 | 108.27 | 264.01 |
| 2119 | 2255895.29 | 6862815.93 | 1029.42 | PERFORATOR-5.0 | 5 | 146.44 | 263.82 |
| 2121 | 2255892.36 | 6862830.13 | 1029.63 | PERFORATOR-7.0 | 7 | 148.53 | 269.40 |
| 2122 | 2255931.26 | 6862856.78 | 1030.31 | PERFORATOR-5.4 | 5.4 | 112.45 | 282.89 |
| 2123 | 2255961.98 | 6862910.10 | 1030.95 | PERFORATOR-15.2 | 15.2 | 111.24 | 314.82 |
| 2124 | 2255982.38 | 6862924.64 | 1031.35 | PERFORATOR-5.7 | 5.7 | 109.82 | 327.82 |
| 2125 | 2255972.79 | 6862934.02 | 1031.28 | CARRIER-TUBE-32.1 | 32.1 | 122.91 | 326.36 |
| 2126 | 2255958.74 | 6862947.60 | 1031.66 | PERFORATOR-5.3 | 5.3 | 142.07 | 324.68 |
| 2127 | 2255936.62 | 6862989.81 | 1031.68 | PERFORATOR-12.1 | 12.1 | 189.40 | 326.60 |
| 2128 | 2255947.90 | 6863007.67 | 1031.94 | PERFORATOR-6.4 | 6.4 | 199.04 | 332.15 |
| 2129 | 2255950.56 | 6863009.80 | 1032.08 | PERFORATOR-7.5 | 7.5 | 199.70 | 333.11 |
| 2130 | 2255955.22 | 6863010.18 | 1032.08 | PERFORATOR-6.1 | 6.1 | 197.98 | 334.36 |
| 2131 | 2255938.25 | 6863018.23 | 1032.02 | PERFORATOR-6.9 | 6.9 | 212.91 | 331.18 |
| 2132 | 2255946.28 | 6863036.75 | 1032.27 | CARRIER-TUBE-49.1 | 49.1 | 225.83 | 335.24 |
| 2133 | 2255971.90 | 6862987.79 | 1031.86 | PERFORATOR-5.0 | 5 | 170.66 | 336.16 |
| 2134 | 2255988.40 | 6863005.25 | 1032.44 | PERFORATOR-8.5 | 8.5 | 181.32 | 343.18 |
| 2135 | 2255980.90 | 6863050.02 | 1032.70 | CARRIER-TUBE-17.7 | 17.7 | 226.42 | 344.64 |
| 2136 | 2255998.68 | 6862951.88 | 1031.82 | PERFORATOR-5.3 | 5.3 | 127.38 | 340.66 |
| 2137 | 2255997.50 | 6862939.37 | 1031.66 | PERFORATOR-8.5 | 8.5 | 116.09 | 338.06 |

| | | | | | | | |
|---|---|---|---|---|---|---|---|
| 2138 | 2255994.19 | 6862993.70 | 1032.21 | PERFORATOR-5.0 | 5 | 168.61 | 343.92 |
| 2139 | 2256032.53 | 6862966.60 | 1032.31 | CARRIER-TUBE-55.9 | 55.9 | 135.17 | 356.46 |
| 2140 | 2256035.35 | 6862936.57 | 1032.24 | PERFORATOR-6.7 | 6.7 | 105.03 | 356.98 |
| 2141 | 2256036.83 | 6862932.02 | 1032.07 | PERFORATOR-6.9 | 6.9 | 100.42 | 357.69 |
| 2142 | 2256115.44 | 6862888.89 | 1032.40 | PERFORATOR-8.4 | 8.4 | 93.97 | 52.51 |
| 2143 | 2256050.55 | 6862852.70 | 1031.34 | PERFORATOR-10.2 | 10.2 | 23.13 | 24.71 |
| 2144 | 2256053.98 | 6862827.94 | 1031.10 | PERFORATOR-5.0 | 5 | 13.62 | 105.97 |
| 2145 | 2256078.90 | 6862735.94 | 1030.45 | PERFORATOR-5.0 | 5 | 103.02 | 158.34 |
| 2146 | 2256140.03 | 6862687.51 | 1030.50 | PERFORATOR-8.8 | 8.8 | 174.98 | 145.48 |
| 2147 | 2256249.64 | 6862678.26 | 1031.82 | PERFORATOR-8.6 | 8.6 | 259.08 | 126.31 |
| 2148 | 2256268.62 | 6862712.02 | 1032.21 | PERFORATOR-16.8 | 16.8 | 257.27 | 117.72 |
| 2149 | 2256203.84 | 6862649.42 | 1031.08 | GUN_BODY-5 | 8256 | 244.49 | 138.20 |
| 3001 | 2256060.30 | 6862827.93 | 1031.35 | PERFORATOR - 8.7 | 8.7 | 19.78 | 100.94 |
| 3002 | 2256060.17 | 6862824.86 | 1031.25 | PERFORATOR - 8.2 | 8.2 | 20.46 | 109.48 |
| 3003 | 2256063.22 | 6862824.49 | 1031.33 | PERFORATOR - 5.3 | 5.3 | 23.47 | 107.85 |
| 3004 | 2256064.89 | 6862824.45 | 1031.36 | PERFORATOR -6.6 | 6.6 | 25.08 | 106.77 |
| 3005 | 2256065.80 | 6862824.70 | 1031.20 | CARRIER-TUBE - 55.9 | 55.9 | 25.88 | 105.67 |
| 3006 | 2256070.43 | 6862824.87 | 1031.34 | PERFORATOR - 5.9 | 5.9 | 30.33 | 103.00 |
| 3007 | 2256071.57 | 6862823.66 | 1031.30 | PERFORATOR - 5.5 | 5.5 | 31.73 | 104.66 |
| 3008 | 2256089.31 | 6862814.88 | 1031.42 | PERFORATOR - 5.0 | 5 | 51.27 | 109.14 |
| 3009 | 2256104.43 | 6862798.06 | 1031.45 | PERFORATOR - 8.6 | 8.6 | 71.90 | 117.88 |
| 3010 | 2256100.39 | 6862796.62 | 1031.43 | PERFORATOR -9.1 | 9.1 | 69.07 | 120.51 |
| 3011 | 2256084.59 | 6862801.99 | 1031.25 | PERFORATOR - 8.1 | 8.1 | 52.84 | 124.20 |
| 3012 | 2256083.03 | 6862802.25 | 1031.29 | PERFORATOR -5.8 | 5.8 | 51.42 | 124.93 |
| 3013 | 2256078.62 | 6862797.58 | 1031.17 | CARRIER-TUBE - 29.3 | 29.3 | 50.87 | 132.10 |
| 3014 | 2256078.50 | 6862809.28 | 1031.28 | PERFORATOR - 8.8 | 8.8 | 43.79 | 120.78 |
| 3015 | 2256060.17 | 6862779.35 | 1030.90 | PERFORATOR - 7.0 | 7 | 55.78 | 159.77 |
| 3016 | 2256054.10 | 6862781.34 | 1030.74 | PERFORATOR - 5.2 | 5.2 | 52.05 | 165.29 |
| 3017 | 2256074.27 | 6862764.74 | 1030.72 | CARRIER-TUBE - 27.8 | 27.8 | 74.82 | 153.49 |
| 3018 | 2256105.86 | 6862763.92 | 1031.12 | GUN_BODY - 3 | 8095 | 93.89 | 136.20 |
| 3019 | 2256036.92 | 6862748.79 | 1030.26 | CARRIER-TUBE - 28.3 | 28.3 | 82.99 | 182.73 |
| 3020 | 2256034.83 | 6862749.28 | 1030.25 | PERFORATOR - 7.4 | 7.4 | 82.63 | 184.19 |
| 3021 | 2256029.69 | 6862747.55 | 1030.18 | PERFORATOR - 7.7 | 7.7 | 84.88 | 187.57 |
| 3022 | 2256035.47 | 6862738.37 | 1030.20 | PERFORATOR - 8.6 | 8.6 | 93.48 | 183.32 |
| 3023 | 2256032.98 | 6862733.98 | 1030.19 | GUN_BODY - 2 | 8144 | 98.02 | 184.62 |
| 3024 | 2256034.43 | 6862731.69 | 1030.16 | PERFORATOR - 7.3 | 7.3 | 100.21 | 183.69 |
| 3025 | 2256024.19 | 6862737.04 | 1030.02 | PERFORATOR - 5.0 | 5 | 96.10 | 190.00 |
| 3026 | 2256025.77 | 6862755.20 | 1030.15 | PERFORATOR - 8.2 | 8.2 | 77.97 | 191.18 |
| 3027 | 2256035.50 | 6862759.15 | 1030.26 | PERFORATOR - 5.5 | 5.5 | 72.74 | 184.24 |
| 3028 | 2256036.94 | 6862759.18 | 1030.45 | PERFORATOR -5.1 | 5.1 | 72.61 | 183.11 |
| 3029 | 2256042.31 | 6862772.22 | 1030.69 | PERFORATOR - 5.0 | 5 | 59.49 | 178.62 |
| 3030 | 2256048.26 | 6862788.19 | 1030.80 | PERFORATOR - 6.7 | 6.7 | 44.12 | 170.37 |
| 3031 | 2256048.86 | 6862792.23 | 1030.82 | PERFORATOR - 8.0 | 8 | 40.26 | 168.57 |
| 3032 | 2256044.57 | 6862805.19 | 1030.91 | PERFORATOR - 5.6 | 5.6 | 26.75 | 172.08 |
| 3033 | 2256034.53 | 6862793.12 | 1030.63 | PERFORATOR - 8.7 | 8.7 | 39.09 | 189.34 |

| | | | | | | | |
|---|---|---|---|---|---|---|---|
| 3034 | 2256026.03 | 6862783.79 | 1030.64 | PERFORATOR - 8.2 | 8.2 | 50.15 | 197.22 |
| 3035 | 2256026.93 | 6862776.82 | 1030.51 | PERFORATOR - 9.3 | 9.3 | 56.61 | 194.26 |
| 3036 | 2256021.40 | 6862769.22 | 1030.38 | PERFORATOR - 5.4 | 5.4 | 65.44 | 197.32 |
| 3037 | 2256015.57 | 6862804.82 | 1030.68 | PERFORATOR - 16.0 | 16 | 36.91 | 223.29 |
| 3038 | 2256025.70 | 6862804.89 | 1030.80 | PERFORATOR - 9.1 | 9.1 | 30.80 | 209.53 |
| 3039 | 2256040.86 | 6862812.05 | 1030.88 | PERFORATOR - 6.4 | 6.4 | 19.64 | 180.06 |
| 3040 | 2256038.22 | 6862816.39 | 1030.93 | CARRIER-TUBE - 26.2 | 26.2 | 15.52 | 189.84 |
| 3041 | 2256048.25 | 6862822.56 | 1031.17 | PERFORATOR - 9.0 | 9 | 11.73 | 141.05 |
| 3042 | 2256055.89 | 6862824.26 | 1031.30 | PERFORATOR- 14.7 | 14.7 | 16.75 | 116.32 |
| 3043 | 2256059.72 | 6862820.57 | 1031.24 | PERFORATOR - 5.1 | 5.1 | 21.88 | 120.55 |
| 3044 | 2256083.44 | 6862930.05 | 1032.56 | PERFORATOR - 8.4 | 8.4 | 107.18 | 23.40 |
| 3045 | 2256091.28 | 6862939.81 | 1032.68 | PERFORATOR - 9.0 | 9 | 119.29 | 24.99 |
| 3046 | 2256087.25 | 6862961.47 | 1032.83 | PERFORATOR - 6.6 | 6.6 | 137.82 | 19.66 |
| 3047 | 2256078.59 | 6862969.77 | 1033.10 | PERFORATOR - 5.3 | 5.3 | 143.14 | 15.28 |
| 3048 | 2256083.17 | 6862982.82 | 1033.10 | PERFORATOR -5.7 | 5.7 | 156.94 | 15.63 |
| 3049 | 2256091.65 | 6862990.56 | 1033.32 | PERFORATOR - 7.9 | 7.9 | 166.78 | 17.72 |
| 3050 | 2256106.59 | 6863059.24 | 1034.08 | PERFORATOR - 6.5 | 6.5 | 236.85 | 16.11 |
| 3051 | 2256158.65 | 6863205.45 | 1036.36 | PERFORATOR - 9.0 | 9 | 391.88 | 17.49 |
| 3052 | 2256140.84 | 6863197.26 | 1036.01 | PERFORATOR - 5.0 | 5 | 378.99 | 15.29 |
| 3053 | 2256091.62 | 6863056.92 | 1031.98 | PERFORATOR - 12.7 | 12.7 | 230.88 | 12.70 |
| 3054 | 2256209.14 | 6863064.37 | 1035.04 | PERFORATOR - 16.1 | 16.1 | 287.14 | 35.87 |
| 3055 | 2256194.45 | 6863067.43 | 1034.85 | PERFORATOR - 7.3 | 7.3 | 281.35 | 33.08 |
| 3056 | 2256169.74 | 6863081.13 | 1034.60 | PERFORATOR - 5.3 | 5.3 | 280.76 | 27.32 |
| 3057 | 2256149.09 | 6863061.05 | 1034.43 | PERFORATOR - 9.1 | 9.1 | 253.61 | 25.26 |
| 3058 | 2256169.91 | 6863057.23 | 1034.49 | PERFORATOR - 6.1 | 6.1 | 259.84 | 29.77 |
| 3059 | 2256188.02 | 6863023.29 | 1034.25 | PERFORATOR - 8.1 | 8.1 | 241.58 | 37.52 |
| 3060 | 2256164.88 | 6863021.50 | 1034.24 | PERFORATOR - 9.4 | 9.4 | 226.73 | 33.16 |
| 3061 | 2256201.00 | 6863029.86 | 1034.51 | PERFORATOR - 8.4 | 8.4 | 254.78 | 38.94 |
| 3062 | 2256327.80 | 6863056.24 | 1035.50 | PERFORATOR - 5.9 | 5.9 | 364.34 | 51.95 |
| 3063 | 2256241.50 | 6862900.71 | 1033.50 | CARRIER-TUBE -18.7 | 18.7 | 212.17 | 71.02 |
| 3064 | 2256238.93 | 6862842.11 | 1032.90 | PERFORATOR - 8.6 | 8.6 | 198.33 | 86.99 |
| 3065 | 2256227.94 | 6862838.52 | 1032.94 | PERFORATOR - 13.3 | 13.3 | 187.18 | 87.91 |
| 3066 | 2256215.94 | 6862841.79 | 1032.82 | PERFORATOR - 9.0 | 9 | 175.35 | 86.70 |
| 3067 | 2256212.62 | 6862830.54 | 1032.70 | PERFORATOR - 6.4 | 6.4 | 171.74 | 90.38 |
| 3068 | 2256204.09 | 6862810.07 | 1032.40 | CARRIER-TUBE - 93.0 | 93 | 164.63 | 97.54 |
| 3069 | 2256255.08 | 6862784.65 | 1032.66 | PERFORATOR - 20.2 | 20.2 | 219.30 | 102.39 |
| 3070 | 2255994.99 | 6862742.45 | 1029.74 | PERFORATOR - 8.6 | 8.6 | 100.35 | 207.21 |
| 3071 | 2255999.85 | 6862731.46 | 1029.61 | PERFORATOR - 5.1 | 5.1 | 108.30 | 202.26 |
| 3072 | 2255981.69 | 6862728.37 | 1029.33 | GUN_BODY -1 | 8094 | 119.07 | 209.81 |
| 3073 | 2255980.96 | 6862718.45 | 1029.27 | PERFORATOR- 9.1 | 9.1 | 128.11 | 207.89 |
| 3074 | 2255974.23 | 6862724.71 | 1029.37 | PERFORATOR - 8.5 | 8.5 | 126.04 | 211.92 |
| 3075 | 2255855.31 | 6862561.52 | 1026.25 | GUN_BODY - 4 | 8013 | 327.76 | 214.48 |
| 3076 | 2255893.14 | 6862663.07 | 1027.72 | CARRIER-TUBE - 29.7 | 29.7 | 224.18 | 221.22 |
| 3077 | 2255940.64 | 6862755.35 | 1029.37 | PERFORATOR -5.6 | 5.6 | 126.00 | 232.71 |
| 3078 | 2255964.85 | 6862761.96 | 1029.57 | HARDWARE -CAP - 94.7 | 94.7 | 103.17 | 227.48 |

| | | | | | | | |
|---|---|---|---|---|---|---|---|
| 3079 | 2255927.16 | 6862756.41 | 1029.04 | HARDWARE - CAP -78.5 | 78.5 | 136.37 | 236.49 |
| 3080 | 2255906.41 | 6862748.51 | 1028.85 | CARRIER-TUBE - 34.8 | 34.8 | 158.11 | 238.26 |
| 3081 | 2255902.38 | 6862753.47 | 1028.84 | PERFORATOR - 8.5 | 8.5 | 159.06 | 240.54 |
| 3082 | 2255887.91 | 6862764.69 | 1028.91 | PERFORATOR - 8.3 | 8.3 | 166.99 | 246.35 |
| 3083 | 2255886.68 | 6862785.53 | 1029.09 | PERFORATOR - 8.5 | 8.5 | 160.96 | 253.34 |
| 3084 | 2255889.64 | 6862786.66 | 1029.08 | PERFORATOR - 8.2 | 8.2 | 157.80 | 253.42 |
| 3085 | 2255874.74 | 6862826.74 | 1029.64 | PERFORATOR - 11.5 | 11.5 | 166.21 | 268.29 |
| 3086 | 2255889.13 | 6862856.47 | 1030.07 | PERFORATOR - 7.2 | 7.2 | 153.76 | 279.27 |
| 3087 | 2255792.24 | 6862840.79 | 1028.39 | PERFORATOR - 5.6 | 5.6 | 248.80 | 272.10 |
| 3088 | 2255904.21 | 6863000.68 | 1031.50 | PERFORATOR - 13.7 | 137 | 217.34 | 321.04 |
| 3089 | 2255906.02 | 6863008.95 | 1031.71 | CARRIER-TUBE -82.5 | 82.5 | 222.74 | 322.74 |
| 3090 | 2255897.75 | 6863068.94 | 1032.36 | CARRIER-TUBE - 49.5 | 49.5 | 277.08 | 328.90 |
| 3091 | 2255917.69 | 6863068.61 | 1032.54 | CARRIER-TUBE -49.5 | 49.5 | 267.04 | 332.53 |
| 3092 | 2255930.73 | 6863046.00 | 1032.41 | CARRIER-TUBE - 16.0 | 16 | 240.96 | 332.80 |
| 3093 | 2255941.30 | 6863077.58 | 1032.68 | PERFORATOR - 5.7 | 5.7 | 265.28 | 337.95 |
| 3094 | 2255944.60 | 6863174.17 | 1033.96 | PERFORATOR - 7.0 | 7 | 355.75 | 344.30 |
| 3095 | 2255957.34 | 6863178.31 | 1034.14 | PERFORATOR - 17.4 | 17.4 | 356.55 | 346.45 |
| 3096 | 2255984.05 | 6863221.51 | 1034.76 | PERFORATOR - 7.2 | 7.2 | 393.94 | 351.71 |
| 3097 | 2256029.56 | 6863192.90 | 1034.98 | CARRIER-TUBE - 15 | 15 | 361.39 | 358.21 |
| 3098 | 2256018.15 | 6863014.35 | 1030.36 | PERFORATOR - 5.7 | 5.7 | 184.07 | 352.91 |
| 3099 | 2256018.16 | 6863014.36 | 1030.37 | CARRIER-TUBE - 15.8 | 15.8 | 184.08 | 352.91 |
| 3100 | 2255997.36 | 6863042.49 | 1032.99 | CARRIER-TUBE - 14.0 | 14 | 215.25 | 348.33 |
| 3101 | 2255982.36 | 6863151.84 | 1033.90 | CARRIER-TUBE - 52.9 | 52.9 | 325.46 | 349.64 |
| 3102 | 2255989.49 | 6863137.27 | 1033.85 | CARRIER-TUBE - 48.7 | 48.7 | 309.87 | 350.45 |
| 3103 | 2256009.58 | 6863136.28 | 1033.93 | PERFORATOR - 5.0 | 5 | 306.20 | 354.13 |
| 3104 | 2256044.52 | 6863095.56 | 1033.97 | PERFORATOR - 6.3 | 6.3 | 263.90 | 0.79 |
| 3105 | 2256036.93 | 6863061.62 | 1033.30 | PERFORATOR - 8.0 | 8 | 229.96 | 359.02 |
| 3106 | 2256024.27 | 6863032.41 | 1033.05 | PERFORATOR - 12.8 | 12.8 | 201.40 | 355.27 |
| 3107 | 2256039.29 | 6863007.90 | 1032.86 | PERFORATOR - 6.8 | 6.8 | 176.22 | 359.48 |
| 3108 | 2256051.37 | 6862992.12 | 1032.86 | PERFORATOR - 7.1 | 7.1 | 160.77 | 3.74 |
| 3109 | 2256040.00 | 6862983.94 | 1032.70 | CARRIER-TUBE - 49.5 | 49.5 | 152.25 | 359.67 |
| 3110 | 2256029.99 | 6862959.51 | 1032.33 | PERFORATOR - 8.2 | 8.2 | 128.28 | 355.13 |
| 3111 | 2256053.31 | 6862931.10 | 1032.29 | PERFORATOR - 5.3 | 5.3 | 100.19 | 7.13 |
| 3112 | 2256030.86 | 6862956.10 | 1032.41 | PERFORATOR - 5.0 | 5 | 124.81 | 355.39 |
| 3113 | 2256058.26 | 6862874.51 | 1031.82 | PERFORATOR - 5.0 | 5 | 46.21 | 22.09 |
| 3114 | 2256046.99 | 6862878.77 | 1031.74 | PERFORATOR - 8.9 | 8.9 | 47.47 | 7.39 |
| 3115 | 2256058.72 | 6862831.58 | 1031.28 | PERFORATOR - 7.1 | 7.1 | 17.84 | 90.36 |
| 3116 | 2256066.94 | 6862814.34 | 1031.15 | PERFORATOR - 7.6 | 7.6 | 31.31 | 123.65 |
| 3117 | 2256036.21 | 6862811.57 | 1030.85 | PERFORATOR - 7.5 | 7.5 | 20.65 | 193.06 |
| 3118 | 2256012.46 | 6862742.83 | 1029.90 | PERFORATOR - 7.9 | 7.9 | 93.29 | 197.74 |
| 3119 | 2256062.72 | 6862688.15 | 1029.85 | PERFORATOR - 14.0 | 14 | 145.19 | 171.35 |
| 3120 | 2256086.34 | 6862660.03 | 1029.87 | PERFORATOR - 13.3 | 13.3 | 177.58 | 165.17 |
| 3121 | 2256032.64 | 6862607.38 | 1028.58 | PERFORATOR - 11.1 | 11.1 | 224.46 | 182.10 |
| 3131 | 2255964.52 | 6862816.06 | 1029.98 | PERFORATOR - 5.5 | 5.5 | 77.94 | 258.43 |
| 3133 | 2255988.34 | 6862889.02 | 1031.03 | PERFORATOR - 5.0 | 5 | 77.77 | 317.50 |